PhD Dissertation

Energy-efficient Wireless Communication Schemes and Real-Time Middleware for Machine-to-Machine Networks

Author

Tatjana Predojev

PhD Advisors

Dr Jesús Alonso-Zárate

Dr Mischa Dohler

Centre Tecnològic de Telecomunicacions de Catalunya (CTTC)

Department of Signal Theory and Communications (TSC)

Universitat Politècnica de Catalunya (UPC)

Barcelona, June 2014

Abstract

This thesis studies emerging Machine-to-Machine (M2M) systems that execute automated tasks without, or with minimum human intervention. M2M systems consist of devices deployed in the field to collect task-related information and send it to remote applications for processing. The applications optimise the tasks and issue control commands back to the devices. Ideally, after configuring the task policies, humans are excluded from the control loop. A prominent and urgent M2M use case concentrates on the automation of the electric power grid, also known as Smart Grid, that is considered in the thesis.

Many M2M scenarios require devices that are low-rate, low-cost and can be easily deployed and maintained. A fitting solution are wireless, battery-powered and resource-constrained devices (with limited processing power and memory). Low-maintenance requires years of lifetime, that can only be achieved with unprecedented energy efficiency of communication protocols. Specifically, we focus on the MAC and link layers in this thesis (especially on the Cooperative Automatic Repeat Request schemes) to improve the energy efficiency of the devices. Cooperative MAC extensions to the various standard technologies such as IEEE 802.11, IEEE 802.15.4 and its MAC amendments are proposed and evaluated. The radio transceiver of a device can be put to sleep state when inactive, yielding very low duty-cycles for low-rate devices, and thus achieving significant energy savings. Since the MAC layer controls the radio transceiver sleep states, duty-cycled MAC schemes are the cornerstone of the energy-efficient communication schemes. To that end, Cooperative and Duty-Cycled ARQ (CDC-ARQ) scheme has been designed, analysed and evaluated in this thesis. CDC-ARQ is based on dynamic packet forwarding depending on the current state of the wireless channel. The benefits are quantified by considering realistic wireless low-power links that experience shadowing and multipath fading channel effects. The conditions under which CDC-ARQ outperforms the standard forwarding techniques are presented. Finally, optimal link selection and retransmission strategies are determined for direct, multi-hop or CDC-ARQ forwarding. The studied energy-efficient wireless schemes are suitable e.g. for home and building automation which can contribute to the efficient use of the electric power in homes and buildings.

After considering the device domain, the focus of this thesis turns to the applications at the other end of the M2M system. The applications typically exchange data over wide areas with

many remote devices. Distributed computing techniques facilitate this data exchange, standardised and implemented in the middleware platform for M2M systems. The communication requirements of these applications are diverse in terms of data latency, update rate, number of associated devices etc. While the existing middleware solutions such as ETSI M2M fully support communication requirements of some applications, the solution is inadequate when it comes to the real-time latency constraint. Some suitable upgrades that improve the real-time performance of data exchange in ETSI M2M middleware are analysed in the thesis. The analysis is exemplified with three Smart Grid applications, one related to the home and building automation and the other two concerned with monitoring and control of the power flow in the electric grid.

Resumen

Esta tesis estudia sistemas Machine-to-Machine (M2M) en los que se ejecutan tareas de manera autónoma sin, o con mínima intervención humana. Los sistemas M2M están formados por dispositivos desplegados en un entorno que recolectan información relacionada con una tarea y la envían a aplicaciones para su proceso. Las aplicaciones optimizan estas tareas y responden a los dispositivos con comandos de control. Idealmente, después de configurar las políticas de tareas, los humanos son excluidos del lazo de control. Un importante caso de uso en M2M es la automatización de la red eléctrica, también conocido como Smart Grid, que se trata en esta tesis.

Muchos escenarios M2M requieren dispositivos de bajo bitrate, bajo coste y que puedan ser fácilmente desplegables y mantenidos. Una solución adecuada son los dispositivos inalámbricos, alimentados por batería y de capacidades limitadas (con reducida potencia de procesado y memoria). Un bajo mantenimiento requiere años de vida, que sólo pueden conseguirse con protocolos de comunicación altamente eficientes energéticamente. En esta tesis nos centramos principalmente en las capas MAC y de enlace (especialmente en esquemas Cooperative Automatic Repeat Request) para mejorar la eficiencia energética de los dispositivos. Proponemos y evaluamos extensiones de Cooperative MAC para varios estándares como IEEE 802.11, IEEE 802.15.4 y sus revisiones MAC. El transmisor radio de los dispositivos puede ponerse en estado de reposo cuando está inactivo, llevando a cortos periodos de activación (duty-cycle) en dispositivos de bajo bitrate, consiguiendo así un ahorro energético considerable. Dado que la capa MAC controla los estados de reposo de los transmisores radio, los esquemas de Duty-Cycle MAC son el pilar de las comunicaciones energéticamente eficientes. Por ello, en esta tesis diseñamos, analizamos y evaluamos esquemas Cooperative and Duty-Cycled ARQ (CDC-ARQ). CDC-ARQ se basa en la (re)transmisión dinámica de paquetes (dynamic packet forwarding) dependiendo del estado del canal inalámbrico. Cuantificamos las ganancias considerando enlaces inalámbricos de baja potencia con modelos realistas, que sufren efectos de apantallamiento (shadowing) desvanecimientos (fading) de canal, y presentamos las condiciones bajo las cuales CDC-ARQ consiguen mejores resultados que las técnicas estándar de forwarding. Finalmente, determinamos estrategias óptimas de selección de enlace y retransmisión para direct, multi-hop y CDC-ARQ forwarding. Los esquemas de comunicación inalámbricos energéticamente

eficientes son adecuados, por ejemplo, para automatización de edificios y hogar, contribuyendo a un buen uso de la energía eléctrica en dichos escenarios.

Después de considerar el entorno de dispositivos, la tesis se centra en las aplicaciones, al otro lado de los sistemas M2M. Las aplicaciones típicamente intercambian datos sobre amplias zonas con varios dispositivos remotos. Las técnicas de computación distribuida, estandarizadas e implementadas en plataformas middleware para sistemas M2M, facilitan este intercambio de datos. Los requisitos de comunicación de estas aplicaciones son diversos en términos de latencia, número de actualizaciones, número de dispositivos asociados, etc. Mientras que las soluciones middleware existentes tales como ETSI M2M satisfacen los requisitos de ciertas aplicaciones, dichas soluciones son inadecuadas para los requisitos de latencia de transmisión en tiempo real. Esta tesis propone y analiza modificaciones del ETSI M2M que mejoran el rendimiento en tiempo real. El análisis se ejemplifica con tres aplicaciones Smart Grid, una relacionada con la automatización del hogar y edificios, y las otras dos con la monitorización y control del flujo de potencia de la red eléctrica.

Contents

List of Acronyms

M2M	Machine-to-Machine
IoT	Internet-of-Things
SCADA	Supervisory Control And Data Acquisition
HVAC	Heating, Ventilation and Air Conditioning
WAMS	Wide Area Measurement System
PMU	Phasor Measurement Unit
GPS	Global Positioning System
MAC	Medium Access Control
PHY	Physical (layer)
QoS	Quality-of-Service
C-ARQ	Cooperative Automatic Repeat reQuest
CORBA	Common Object Request Broker Architecture
WLAN	Wireless Local Area Network
ETX	Expected Transmission Count
IETF	Internet Engineering Task Force
ROLL	Routing over Low-Power and Lossy networks
WPAN	Wireless Personal Area Network
CSMA/CA	Carrier Sensing Multiple Access (with) Collision Avoidance
CAP	Contention Access Period
CFP	Contention Free Period
CCA	Clear Channel Assessment
GTS	Guaranteed Time Slot
DCF	Distributed Coordination Function
TSCH	Time Synchronised Channel Hopping

TDMA	Time Division Multiple Access
SNR	Signal-to-Noise Ratio
NSCL	Network Service Capability Layer
GSCL	Gateway Service Capability Layer
DSCL	Device Service Capability Layer
RPL	Routing Protocol for Low-Power and Lossy Networks
PRCSMA	Persistent Relay Carrier Sensing Multiple Access
AP	Access Point
CSI	Channel State Information
QPSK	Quadrature Phase Shift Keying
O-QPSK	Offset Quadrature Phase Shift Keying
AWGN	Additive White Gaussian Noise
DSSS	Direct Sequence Spread Spectrum
pdf	probability density function
CDC-ARQ	Cooperative and Duty-Cycled ARQ
HTTP	Hyper Text Transfer Protocol
REST	Representational State Transfer
CoAP	Constrained Application Protocol
CRUD	Create, Retrieve, Update and Delete (methods)
URI	Uniform Resource Identifier
SCL	Service Capability Layer
RTT	Round Trip Time
TCP	Transmission Control Protocol
UDP	User Datagram Protocol
WS	Websocket

List of Figures and Tables

Chapter 1

Introduction

1.1 Motivation

The term Machine-to-Machine (M2M) communications, one of the enablers of Internet-of-Things (IoT), refers to communications between devices and (usually) *remote* control applications without any (or with very limited) human intervention. The devices are either resource-constrained, low-power, low-cost sensors and actuators - or - smart phones and alike (which are more powerful both in terms of processing power and regular battery recharging feasibility). In addition to the battery-powered devices, mains-powered devices can be expected in some use cases. On the other end, applications collect data from dispersed devices in order to offer real-time monitoring of the covered environments, or to perform various control tasks by issuing commands to actuators. Therefore, devices and applications exchange information (sometimes over great distances) in order to jointly execute automated, intelligent operations. The environments enhanced with M2M systems have been termed *Smart Environments*.

The name Machine-to-Machine was chosen to stress the absence of human involvement in the communication chain. The origins of M2M systems can be traced back to Supervisory Control And Data Acquisition (SCADA) industrial control systems. Modern M2M systems cover a vast range of use cases and no single technology can address them all. Some of these use cases are: utility metering, industrial automation, personal health monitoring, automated

heating, ventilation and air conditioning (HVAC) in homes and buildings, intelligent tracking and tracing in the supply chain, fleet management, urban monitoring, etc. [1]. An emerging use case of great importance is the automation of the electric power grid leading to the *Smart Grid*. Smart Grid blends modern communication networks with the power grid infrastructure to enable automated control. Smart Grid encompasses a large set of use cases, each focusing on the specific part of the power grid, from generation to consumer. All of them act together to achieve a common goal: make the energy supply sustainable and the grid more energy-efficient.

The Smart Grid initiative is still in its infancy. Use cases of the envisioned Smart Grid are so extensive and diverse, that one is obliged to focus on a specific problem, without pretending to address the Smart Grid as a whole. As the specific solutions evolve, they will interact and eventually blend into one complex system. In this thesis, we focus on two use cases:

1. Home and Building Automation
2. Wide Area Measurement System (WAMS)

The goal of ***Home and Building Automation*** is to improve the energy efficiency of homes and buildings. Devices that enable such automation are located at the consumer premises and can be used for the purposes of Demand Response combined with dynamic pricing. Demand Response aims to adapt power consumption to the available supply in the grid, opposed to the current practice of adapting supply to demand. A group of techniques, also known as peak shaving, aim to shift, rearrange and equalise consumption throughout the day while respecting user-defined constraints. Fitting examples include heating, air-conditioning, deep freezers, etc. The incentive to the consumer to consent to Demand Response is the variable price that becomes lower as the peak demand declines. Consider a simple example of the smart heating system that consumes most during the off-peak hours while maintaining the temperature within a range set by user. Such system consists of a control device connected to the power grid's price feed, a network of temperature sensors which provide ambient info to the control device and a network of actuators receiving commands from the control device in order to regulate the operation of heaters. To avoid cabling and the related inconveniences (such as high installation cost), a *wireless* solution is preferred to connect the control device with the sensors and actuators throughout the home or building. These sensor devices are low-power, short-range, low-cost and (mostly) battery-operated. Given the minimal maintenance requirement, they are expected to perform autonomously with a lifetime of at least *several years*. A critical optimisation parameter to enable years of lifetime is the *energy efficiency* of the communication scheme. Extreme energy efficiency fulfilling the lifetime requirement can only be achieved by heavy duty-cycling of the devices. When a device is duty-cycled, its radio transceiver (which is the greatest source of energy consumption [2]) is switched off at all times, except when the device is actively transmitting or receiving data. The communication scheme that instructs the radio to go to sleep or wake up needs to consider rate and latency constraints of the control application.

For most monitoring applications, duty-cycles of 1% are viable (the device is active only during 1% of its lifetime, otherwise it is sleeping). This thesis contributes to the body of state-of-the-art protocols concerned with the energy efficiency of the wireless communications schemes.

The goals of the ***Wide Area Measurement System*** are to make the electric power grid more reliable, stable, resilient and less prone to outages (especially the cascading outages leading to major blackouts). The large scale blackouts in the previous decades were the motivation for the deployment of SCADA systems to monitor the state of the power grid. These communication systems, based on the decades-old technology, have changed little over the years. At present, increasing energy demand brings the existing power grid to the stability limits, unable to be supervised with the heavily outdated SCADA. Data rates on communication links remain low, up to a few kilobits per second, and the latency is in the range of several seconds or more. As a consequence, the currently deployed SCADA communication systems limit the protection and control operations that the modern power applications and devices are capable of achieving [3]. For example, Phasor Measurement Unit (PMU) is a device that can provide time-synchronised measurements of voltage, current and phase across wide areas by synchronising with Global Positioning System (GPS) clocks. However, SCADA communication system cannot support latency and data rate requirements of control and monitoring applications that process PMU measurements. Therefore, greater reliability and resilience will only be achieved by introducing modern communication networks into the power grid infrastructure, in order to meet the stringent control application communication requirements. A real-time, wide-area situational awareness will lead to the robust and energy-efficient Smart Grid that is dynamic and capable of self-healing. This Smart Grid will then be able to safely incorporate the renewable energy sources such as solar and wind energy [4].

The electric power grid is one of the most complex men-made infrastructures. In order to allow different system components to exchange information, there is a need for a uniform communication framework. Among other tasks, this framework encompasses *distributed computing* techniques to connect remote applications to the measurement and protection devices deployed in the power grid. A communication framework for Smart Grids needs to support heterogeneous underlying network technologies, operating systems, applications written in different programming languages, a variety of traffic and Quality-of-Service (QoS) requirements, etc. Therefore, an introduction of a common layer between applications and network interfaces greatly facilitates application development and maintenance. This layer has been termed *middleware* and is the focus of the second use case. A middleware platform tailored for the Smart Grid that is proposed in the thesis is ubiquitous, scalable, interoperable and caters for the critical real-time requirement.

In summary, within the two prominent **Smart Grid** use cases, two main challenges have been identified and addressed in this thesis:

Home and Building Automation

Energy-efficient wireless communication protocols for resource-constrained, low-power devices

Wide Area Measurement System (WAMS)

Ubiquitous middleware framework for distributed computing in real-time between remote devices and control applications

The major part of this thesis is concerned with the first challenge (Chapters 3, 4 and 5). The second challenge is addressed in Chapter 6 of this thesis.

1.2 Contributions

To address the first challenge, we rely on the physical (PHY) and Medium Access Control (MAC) protocols as defined in IEEE 802.11 [5] and IEEE 802.15.4 [6] family of standards (especially IEEE 802.15.4e MAC amendments [7]). Optimal operating regimes of networks running these protocols have been studied, when the optimisation criterion is the energy efficiency. The standard IEEE 802.11 has been chosen as a starting point due to its wide-spread use. It has been enhanced using device cooperation to improve the energy efficiency. We employ a Cooperative Automatic Repeat reQuest (C-ARQ) scheme to take advantage of overhearing that is a consequence of the non-duty-cycled IEEE 802.11 MAC protocol. The first contribution of this thesis therefore states:

- Improve the energy efficiency of a **non-duty-cycled** MAC using C-ARQ

Duty-cycling was introduced in IEEE 802.15.4 standard. This standard for low-power, low-rate networks is considered to be more appropriate than IEEE 802.11 for resource-constrained, battery-powered devices with the expected lifetime measured in years. Therefore, we next focus on IEEE 802.15.4 MAC that specifies a duty-cycled scheme for the star topology. In particular, the effects of low-power, unreliable wireless links are considered. Link quality changes in space and time and is strongly dependent on the current state of the wireless channel between devices that form a link. Shadowing and multipath fading on such links cause outages whose impact on packet delivery is significant. Again, C-ARQ techniques have been applied, this time with the goal of combating link outages. In summary, the next contribution of this thesis is:

- Improve the energy efficiency of a **duty-cycled** MAC for the **star** topology by applying C-ARQ to combat link outages

The MAC layer amendments in IEEE 802.15.4e propose a functional multi-hop duty-cycling scheme. Multi-hop communication removes the range limitations of star topology. Resulting combination of the original PHY in IEEE 802.15.4 with the MAC in IEEE 802.15.4e is considered to be a winning solution for the resource-constrained devices that facilitate automation tasks [8]. We therefore examine the configuration of devices running the said protocols. In particular, we focus on link selection, given the described volatility of low-power links. Optimal link selection and retransmission strategies in duty-cycled networks have been proposed. The choice between direct or multi-hop forwarding, or the cooperative version of the two was examined. It results that cooperative retransmission which dynamically combines direct and multi-hop forwarding is the optimal choice in many cases, provided that the links' energy consumption is carefully taken into account. This contribution therefore extends the previous contribution to the more general, multi-hop scenario and presents practical guidelines for the network configuration. The main contribution can be summarised as follows:

- Propose optimal wireless link selection and retransmission strategies in **duty-cycled**, **multi-hop** networks

In all studied cases for the Home and Building Automation use case, cooperative ARQ schemes were designed and applied to minimise the total energy consumption by considering realistic wireless links.

The second challenge is concerned with closing the communication gap in the Smart Grid. Aside from a communication infrastructure capable of providing the stringent QoS application requirements, a middleware for distributed computing is needed to connect the dispersed measurement and actuation devices with remote control and monitoring applications. Without a common middleware, applications would have to support heterogeneous network interfaces resulting in expensive, monolithic and inflexible solutions. Some authors have chosen Common Object Request Broker Architecture (CORBA) middleware for this purpose [9]. We argue that *web services* are better suited for the distributed computing tasks in the Smart Grid. In particular, we found that ETSI M2M architecture [10] is a good fit for WAMS and other Smart Grid use cases. ETSI M2M uses the web service technology to provide standardised solutions to common problems shared by different applications and we show how it can be applied in and adapted to the Smart Grid. The last contribution of this thesis thus states:

- Devise a mapping of ETSI M2M architecture to the electric power grid and propose a **middleware** upgrade to support real-time communications

Finally, the proposed ubiquitous middleware addresses a wide set of Smart Grid use cases. We focus on the WAMS use case as the most representative (and most challenging) in order to propose the upgrade for real-time communications. However, ETSI M2M middleware as specified in [10] without any upgrade meets all the communication requirements of the Home and

Building Automation use case. The solutions presented in the first part of this thesis address the wireless communication network at the consumer, while relying on the control signals coming from the Smart Grid. The exchange of these control messages and the collected measurements is regulated by the middleware that is installed on the control device (i.e. gateway) at the consumer, as well as throughout the power grid communication network. The studied middleware therefore addresses applications at the gateway and reaches beyond the consumer in the M2M end-to-end communication system for the Home and Building Automation use case. As such, the middleware also defines how to connect each of the different wireless technologies studied in this thesis and enable them to interact.

In the following section, the contents of this PhD thesis are outlined in more detail. Next, the list of journal and conference papers that have resulted from this work is provided.

1.3 Outline

This PhD thesis covers two aspects of the Smart Grid: first it focuses on the energy-efficient communication protocols for Home and Building Automation; next, it addresses a middleware framework for the applications distributed over wide areas in the electric power grid. The thesis is organised as follows:

Chapter 2 provides the technical background for metrics, software techniques used in simulation and standard architectures and protocols that are the basis of this work. First, we introduce the background for analytical framework developed in this thesis which characterises empirical metrics for low-power wireless links. We describe and justify the adoption of those metrics. Next, standard communication protocols for low-power wireless networks, namely, IEEE 802.15.4 [6] and IEEE 802.15.4e [7] are presented. In the continuation, the principal simulation tool of this thesis (aside from Matlab), *ns-3* simulator, is described. Finally, ETSI M2M standard architecture [10], which provides the basis for the Smart Grid middleware, is introduced.

In Chapter 3, we present the energy efficiency analysis of a cooperation protocol for Wireless Local Area Networks (WLANs) based on IEEE 802.11 standard [5]. We consider devices whose default power management mode is active mode (no duty-cycling) and obtain the energy gain by exploiting overheard packets that would otherwise be discarded. To do so, C-ARQ algorithms are applied. In addition, we capitalise on the proximity of devices in LAN scenarios to employ adaptive rate retransmission. All analytical results, including the efficient operating regions, have been validated in Matlab simulations.

Chapter 4 focuses on a duty-cycled scheme for the star topology scenarios. This chapter covers the low-power algorithm presented in IEEE 802.15.4 standard. We elaborate on the cooperative

extensions of the standard protocol and show that significant energy gains can be obtained with our cooperative ARQ scheme. To perform the analysis, a realistic wireless channel model that considers shadow and multipath fading is adopted.

Chapter 5 examines another duty-cycled scheme as outlined in IEEE 802.15.4e standard. This chapter studies multi-hop scenarios and the optimal configuration of such network. Cooperative and Duty-Cycled ARQ (CDC-ARQ) scheme is proposed and applied to further improve the energy efficiency. Next, the standard and enhanced schemes are implemented in the ns-3 simulator to validate the analytical results. Simulation results allow us to extend the analytically tractable model to the multi-node scenarios and therefore demonstrate the practical applicability of our schemes.

Chapter 6 brings focus to the WAMS use case. We first detail the communication and traffic requirements of example Smart Grid applications. Second, we propose the mapping of ETSI M2M architecture to the electric power grid. A drawback of the current system which reflects on the time-critical applications is identified and a solution is proposed. Eventually, the resulting middleware is ubiquitous, scalable, flexible, interoperable and secure.

Chapter 7 concludes this PhD thesis with the summary of main results and contributions. Future research lines following from this work are outlined.

1.4 Publications

Chapter 3

Contributions of Chapter 3 have been published in 1 conference paper.

- T. Predojev, J. Alonso-Zarate, Luis Alonso, C. Verikoukis, *Energy Efficiency Analysis of a Cooperative Scheme for Wireless Local Area Networks*, in Proceedings of IEEE Global Communications Conference Exhibition & Industry Forum (GLOBECOM 2012), December 2012, Anaheim, California (USA)

Chapter 4

Contributions of Chapter 4 have been published in 2 conference papers.

- T. Predojev, J. Alonso-Zarate, M. Dohler, *Energy Efficiency of Cooperative ARQ Strategies in Shadowing Environments*, in Proceedings of IEEE INFOCOM 2012, Workshop on Communications and Control for Sustainable Energy Systems: Green Networking and Smart Grids, 25-30 March 2012, Orlando, Florida (USA)

- T. Predojev, J. Alonso-Zarate, M. Dohler, *Energy-Delay Tradeoff Analysis in Embedded M2M Networks with Channel Coding*, in Proceedings of IEEE International Symposium on Personal, Indoor and Mobile Radio Communications (PIMRC 2010), 26-29 Sept. 2010, Istanbul, Turkey

Chapter 5

Contributions of Chapter 5 have been published in 1 journal and 2 conference papers.

- T. Predojev, J. Alonso-Zarate, M. Dohler, L. Alonso, *Energy Consumption Optimisation for Duty-Cycled Schemes in Shadowed Environments*, published in International Journal of Distributed Sensor Networks, Hindawi, 2014
- T. Predojev, J. Alonso-Zarate, M. Dohler, *Energy Evaluation of a Cooperative and Duty-Cycled ARQ Scheme for Machine-to-Machine Communications with Shadowed Links*, in Proceedings of IEEE Symposium on Personal, Indoor and Mobile Radio Communications (PIMRC 2013), 8-11 September 2013, London, UK
- T. Predojev, J. Alonso-Zarate, M. Dohler, *Energy Analysis of Cooperative and Duty-Cycled Systems In Shadowed Environments*, in Proceedings of the IEEE International Workshop on Computer-Aided Modeling Analysis and Design of Communication Links and Networks (CAMAD), 17-19 September 2012

Chapter 6

Contributions of Chapter 6 have been submitted to 1 conference.

- T. Predojev, A. Al-Hezmi, J. Alonso-Zarate, M. Dohler, *A Real-Time Middleware Platform for the Smart Grid*, submitted to IEEE Online Conference on Green Communications

Bibliography

[1] (2014) ETSI M2M. [Online]. Available: http://www.etsi.org/technologies-clusters/technologies/m2m

[2] A. Bachir, M. Dohler, T. Watteyne, and K. Leung, "MAC Essentials for Wireless Sensor Networks," *IEEE Communications Surveys Tutorials*, vol. 12, no. 2, pp. 222–248, February 2010.

[3] C. Hauser, D. Bakken, and A. Bose, "A failure to communicate: next generation communication requirements, technologies, and architecture for the electric power grid," *IEEE Power and Energy Magazine*, vol. 3, no. 2, pp. 47–55, 2005.

[4] D. MacKay, *Without Hot Air*. UIT, 2008.

[5] *IEEE Standard 802.11-2012: Wireless Medium Access Control (MAC) and Physical Layer (PHY) Specifications for Wireless Local Area Networks (WLANs)*, IEEE Std., March 2012.

[6] *IEEE Standard 802.15.4-2011: Wireless Medium Access Control (MAC) and Physical Layer (PHY) Specifications for Low-Rate Wireless Personal Area Networks (WPANs)*, IEEE Std., September 2011.

[7] *IEEE Standard 802.15.4e-2012: Low-Rate Wireless Personal Area Networks (LR-WPANs) Amendment 1: MAC sublayer*, IEEE Std., April 2012.

[8] M. Palattella, N. Accettura, X. Vilajosana, T. Watteyne, L. Grieco, G. Boggia, and M. Dohler, "Standardized Protocol Stack for the Internet of (Important) Things," *IEEE Communications Surveys Tutorials*, vol. 15, no. 3, pp. 1389–1406, March 2013.

[9] H. Gjermundrod, D. Bakken, C. Hauser, and A. Bose, "GridStat: A Flexible QoS-Managed Data Dissemination Framework for the Power Grid," *IEEE Transactions on Power Delivery*, vol. 24, no. 1, pp. 136–143, 2009.

[10] ETSI M2M TR 102 690, "Machine-to-Machine communications (M2M); Functional architecture," ETSI, Tech. Rep., 2012.

Chapter 2

Background

This chapter presents a background for the original work presented in the subsequent chapters of this thesis. Main principles and techniques that were adopted and extended in the remainder of this thesis are summarised. Section 2.1 describes the metrics used in this thesis and justifies their adoption. Then, Section 2.2 outlines the protocols applied in Chapters 4 and 5 for the Home and Building Automation use case. Software tools used in the simulations are presented in Section 2.3. Finally, Section 2.4 describes the middleware architecture for the Wide Area Measurement System studied in Chapter 6.

2.1 Low-power Wireless Link Metrics

In this Section, we describe the evolution of metrics for low-power wireless links. In a network of low-power devices, total source-to-destination distance is often larger than a device's range. One of the promoted solutions to cover large distances without increasing the transmission power is multi-hop communication. In multi-hop communication, devices closer to the final destination act as relays to forward traffic from the source device. In order to choose a relay appropriately, link quality metrics need to be established.

2.1.1 Expected Transmission Count (ETX)

Low-power wireless links are known to be highly unreliable compared to their wireless predecessors (medium-power links, cellular links, etc.) [1]. Therefore, a need to characterise and understand those unreliable links has been present since the beginnings of low-power networks, given the links' profound influence on the design of communication protocols. The authors in [2] propose the Expected Transmission Count (ETX) as an empirical metric to account for unreliable wireless links in multi-hop networks. ETX of a link stands for the expected number of packet transmissions over that link, i.e. the original packet transmission and eventual retransmissions if previous attempts fail to deliver a packet. The goal in [2] was to find paths with highest throughput, since the energy conservation goal was not critical at the time. The authors demonstrated that adopting ETX as a routing metric produces paths with the lowest expected number of transmissions. In the experiments, they consider a wide range of link loss ratios, they study links with asymmetric gains, and take into account the interference between successive hops in multi-hop paths. ETX is measured on-site in real implementations by sending dedicated link probe packets and ensuring that each device calculates its local ETX value. The technique is called *link estimation*. Theoretical analysis of ETX is not given in [2] and all the conclusions of this work follow from experimental results. Over the years ETX became well known and wide spread metric for the link quality. Internet Engineering Task Force (IETF) adopted it as a suitable metric in the specifications for Routing over Low-Power and Lossy networks (ROLL) [3].

Following this line of work, the authors in [4] and [5] analyse the expected number of packet transmissions between a sender and a receiver device in a multi-hop network with low-power links in order to find an appropriate routing metric and demonstrate their findings analytically. When links are reliable, i.e. when retransmissions happen rarely, $ETX \rightarrow 1$, the routing metric would be obtained by simply counting the number of links (hops) on the possible route. If the influence of wireless channel is acknowledged, resulting in unreliable links with $ETX > 1$, the sum of the expected number of transmissions on each link in a multi-hop network produces the Expected Hop Count routing metric. Although ETX and Expected Hop Count describe the same effect - link unreliability - a different terminology is adopted to stress the distinction between them. Namely, while the former is an empirical metric, the latter relies on the analysis of packet success probability. Expected Hop Count is calculated analytically by averaging the packet success probability dependent on inter-device distance. To do this, log-normal shadowing model for the wireless channel is adopted in [4]. Next, an approximation of the dependence of packet success probability on distance is used in calculations. The results yield the optimal inter-device distance given the total route distance such that the Expected Hop Count is minimised.

Another study of the influence of realistic wireless channel on low-power links is presented in [6]. The authors adopt log-normal shadowing model, but stress that they consider static

and low-dynamic environments where the shadowing state does not change in time. They remind about the incorrectness of the perfect disk model and derive the theoretical bounds of the transitional region in which the packet success probability depends on the log-normal channel realisation. A comprehensive understanding of the wireless channel is certainly the first step in the design of efficient low-power networks and protocols.

In terms of efficiency, ETX represents a *cost* metric which increases with inter-device (hop) distance. In a multi-hop network, given a fixed source-to-destination distance, increasing inter-device distance leads to the smaller number of hops. Less hops represent an efficiency *gain*, but this also implies larger ETX and therefore larger cost. Therefore, there is a trade-off to be addressed.

2.1.2 Advancement Optimisation and Trade-off

Apart from defining the Expected Hop Count, the authors in [5] are also interested in a cost-gain trade-off. The gain consists in the packet progress towards the destination in a multi-hop network. The larger the hop distance, the higher the ETX and therefore, the higher the cost. The smaller the hop distance, $ETX \rightarrow 1$, but the packet advancement is also small with each hop, resulting in a higher number of hops. In another words, when inter-device distance increases $d \uparrow$, the expected number of transmissions increases $ETX \uparrow$ and the number of hops decreases $n \downarrow$. When inter-device distance decreases $d \downarrow$, ETX decreases $ETX \downarrow (ETX \geq 1)$, but the number of hops increases $n \uparrow$. The trade-off in [5] is defined as a ratio of cost over progress, $n \cdot \frac{ETX}{d}$ whose minimum is the optimal operational point.

Depending on the environment and obstacles, ETX will differ for links of the same distance. Therefore, the appropriate routing metric when wireless channel is taken into account is the shortest *weighted* path. In addition, when dynamic environments are considered, ETX experiences not only spatial, but also temporal variations. Temporal variations of ETX introduce new problem in the link estimation: if the probe packets are too far apart in time, a network ends up working with the inaccurate ETX; if the probe packets are sent too often, resources are wasted. We will address temporal variations of ETX in Chapters 4 and 5 of this thesis. However, our approach is analytical rather than empirical. Therefore, we denote the adopted metric Average Number of Transmissions per Packet to highlight its difference to the empirical ETX.

A trade-off formulation similar to the one above has been studied by many authors. Another example aiming to find optimum inter-device distance in a multi-hop packet radio network considering realistic wireless channel is presented in [7]. In this work, authors rely on the trade-off proposed in [8], which they further develop. Namely, the authors in [8] define the Expected Packet Progress as the product of the probability of successful packet transmission and the transmission range. Note that in this work the focus is on the packet transmission

probability following from a contention based MAC algorithm. They are solving a different set of problems in a different scenario compared to the one in [5]. Their goal is the throughput maximisation. However, the trade-off formulation follows the same idea used in [5] and explained above, although the exact formulation in these two examples is slightly different. The maximisation of the Expected Packet Progress leads to the optimal number of devices and thus to the optimal transmission range which maximises the network throughput. The authors in [7] rely on this trade-off formulation and introduce the unreliable wireless channel as a novelty. They improve the definition of the packet success probability as the product of successful transmission probability (which is a MAC parameter, the probability that packet will access the channel successfully and be transmitted collision-free) and the successful reception probability (which is a PHY parameter that depends on the channel, modulation, coding and the receiver thermal noise). The work in [7] is significant because of the channel model considered, which is static shadowing with superimposed multipath fading. The authors conclude that, compared to the deterministic propagation model that does not consider fading, the model that includes medium-scale shadowing and small-scale fading shows a significant degradation in performance that can reach even 40%. This result confirms the importance of including fading in the channel model in order to get realistic performance output.

The author of [7] later returns to this work and expands it for ad-hoc networks in [9]. In [9] the trade-off is denoted Advancement and represents the product of packet success probability and the progress in meters towards the final destination. If the final destination cannot be reached in a single hop, an optimal relay is sought such that the Advancement is maximised. The channel model in [9] considers Rayleigh multipath fading. Interference from neighbouring devices is also considered. A shadowing realisation is assumed to be known and static; it is expressed with the corresponding propagation exponent. Another contribution following from the formulation of Advancement trade-off is the concept of priority regions. Namely, if no relay is encountered in the optimal region closest to the final destination because of unfavourable channel conditions, the search for a relay continues in the region farther from the final destination and closer to the source device. The study in [9] opens a few interesting questions, such as the influence of a more dynamic channel propagation model, or the applicability of Advancement when studying energy consumption or delay. These topics are addressed in Chapter 5.

2.2 Medium Access Control Specifications for Low-Rate Wireless Personal Area Networks

This Section introduces the standard technologies used throughout this thesis. An overview of IEEE 802.15.4 specifications is given first. It was later realised by the community that Medium Access Control (MAC) layer as specified in [10] does not adequately meet the energy efficiency

requirements in many scenarios. For this reason, amendments to the MAC layer of the initial standard were proposed in IEEE 802.15.4e [11]. We therefore provide an overview of the IEEE 802.15.4e standard amendments as well.

In order to understand the importance of MAC layer for device's energy consumption, we first present different device power modes and their implications. Energy consumption of a device primarily depends on the power modes of its PHY radio transceiver [12]. The MAC layer controls the radio transceiver by issuing commands (service primitives) for transitions from one power mode to another. A transceiver can be in one of the following power modes [12]:

- switched off: *sleep* mode
- switched on: *active* mode, with the sub-modes:
  - transmit or actively receive data
  - idle listen to the wireless channel

A duty-cycled device will be in sleep state by default and will only wake up to actively transmit or receive data. By contrast, the radio transceiver of a non-duty-cycled device is never switched off (as required by the MAC protocol) and its default power mode is idle listen. Energy consumption in the sleep mode is negligible; power consumed while sleeping is in the order of magnitude of μW. Energy consumption in the active mode depends on the sub-mode a transceiver is in and varies across manufacturers. However, the order of magnitude of consumed power for *all* active sub-modes (when transmitting, actively receiving *or* idle listening) is mW, for all major manufacturers. Exact consumption measurements can be obtained from manufacturers' data sheets. In general, power is higher when a device is transmitting or actively receiving compared to idle listening [13]. However, non-duty-cycled MAC protocols proposed in the past rely on idle listening in order to function correctly (e.g. IEEE 802.11 Distributed Coordination Function (DCF) [14]). Therefore, even if the power in the idle listen mode is lower compared to transmission or reception, a device will be in this mode most of the time. Long time periods of idle listening then significantly contribute to the total energy consumption. Also, a device in idle listen mode will receive and decode all packets within its range, even those not intended for itself. Only after the destination address is read from the MAC header a packet is forwarded to the upper layer if the destination address matches the own address, or discarded if it does not. This effect is called *overhearing* and it additionally contributes to the device's energy consumption. Finally, putting the device to sleep mode results in a major energy efficiency improvement, at the cost of increased latency. It significantly reduces idle listening and overhearing. MAC protocols had to be redesigned for resource-constrained devices to allow duty-cycles of approximately 1% (or even lower) while maintaining the given data rate and latency requirements.

2.2.1 IEEE 802.15.4 Medium Access Control

The IEEE 802.15.4 standard [10] specifies the Physical (PHY) and Medium Access Control (MAC) layers for Wireless Personal Area Networks (WPANs). Main design criteria for the specifications presented in [10] are low-cost and low-energy consumption regime. Devices are simple, cheap, deployed in large numbers and mostly battery operated.

IEEE 802.15.4 MAC specifications outline a duty-cycled scheme which is required for energy efficiency (other schemes presented in [10] are not of interest for this study). The scheme assumes the existence of a coordinator device and is therefore most appropriate for star topologies. The coordinator is the only device which has to be active all the time when transmission from any associated device might occur. For this reason, its energy consumption is high, resulting in the requirement for it to be mains-powered. The traffic is mostly uplink from devices to the coordinator. The communication is slotted and packet transmissions may begin only in discrete time instants, at the beginning of the slot. Beaconing is used to maintain synchronisation; coordinators transmit periodic beacons to which other devices synchronise. Beaconing also imposes a superframe structure, defined as a time period between two beacons. The superframe consists of an active phase when devices wake up to transmit data and a sleep phase during which devices may switch off their radios. The active phase of the superframe further consists of the Contention Access Period (CAP) and the optional Contention Free Period (CFP). During CAP, devices contend for channel using Carrier Sensing Multiple Access with Collision Avoidance (CSMA/CA) algorithm. Before each transmission, device chooses a random number which determines the number of slots to backoff. When the discrete backoff time elapses, channel is sensed for activity, i.e. Clear Channel Assessment (CCA) procedure is executed. If CCA detects that other transmission is in progress, a device refrains from own transmission and performs random backoff procedure again. When the channel is sensed idle for two consecutive time slots, the device proceeds with the packet transmission to the coordinator. After the transmission is completed, an Acknowledgement (ACK) of correct reception is expected from the coordinator if acknowledgements are enabled. When ACK is not received, a device retransmits the packet by repeating the CSMA/CA procedure. For devices with strict delay constraints, scheduled transmission slots are preferred to avoid CSMA/CA and the related unpredictable delays. For this purpose, slots within CFP are introduced. These slots can be scheduled on device's request by the coordinator and announced in the beacon. Upon receiving the beacon, all devices are informed about the reserved slots when only the assigned device is allowed to transmit. CFP therefore guarantees channel access within the determined superframe. A diagram of the superframe is shown in Figure 2.1. The duration of sleep phase is determined by the delay requirements and the duty-cycle objective.

The main source of the improved energy efficiency in IEEE 802.15.4 beacon-enabled scheme compared to the IEEE 802.11 MAC protocol without power saving is the removal of idle listening. All devices except the coordinator are in the low-power, sleep mode unless they have

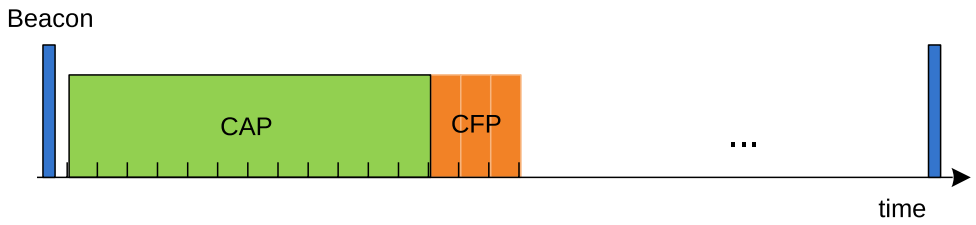

Figure 2.1: IEEE 802.15.4 superframe diagram: active phase consists of CAP and optional CFP, followed by sleep phase which lasts until the next beacon

data to transmit to the coordinator. The described beacon-enabled scheme belongs to the class of duty-cycled MAC schemes with common active periods, because all devices go to sleep and wake up within the same time intervals. The obligatory synchronisation for this type of schemes is maintained by beaconing.

IEEE 802.15.4 standard also defines a peer-to-peer, non beacon-enabled mode. In the non-beacon mode, all devices have to listen to the wireless channel all the time because there is no central coordinator. Devices apply unslotted CSMA/CA to access the wireless channel. Although this mode enables peer-to-peer communication which is difficult in the beacon-enabled mode, there is no duty-cycling. The energy consumption is therefore unacceptably high and cannot provide years of lifetime on a battery.

2.2.2 Motives for IEEE 802.15.4e Standard Amendments

As elaborated in the previous Section, the beacon-enabled mode with a coordinator is appropriate for star topologies. Given the limited range of devices with low transmission power (typically $10 - 20\ m$ achievable with $0\ dBm$), multi-hop communication is expected for most practical applications. IEEE 802.15.4 standard also outlines a multi-hop scheme compatible with the basic star-topology solution. This multi-hop scheme is known as cluster tree. In a cluster tree, more than one coordinator exists. Each coordinator forms its own cluster with the associated devices. Devices transmit to the local coordinator as described in Section 2.2.1 for the star topology. Coordinators are hierarchically organised with the main coordinator at the top. In other words, multiple coordinators form a tree rooted at the main coordinator. Local coordinator is a router of messages coming from associated cluster devices, or from other coordinators lower in hierarchy that are forwarding own cluster traffic. Each coordinator also dictates synchronisation within its own cluster, by periodically transmitting local beacons.

Multiple beacons within the same space may lead to the serious problem of beacon collisions. Collisions happen either with other beacons from different coordinators or with data packets from different clusters. Extensive research has addressed this problem. Time Division Beacon Frame Scheduling mechanism is presented in [15], where IEEE 802.15.4 superframes are scheduled according to a centralized algorithm run by the main coordinator. Time divi-

sion approach schedules beacon frames of a given coordinator during the inactive period of its neighbour clusters. This solution is extended in [16] where a beacon-enabled, multi-hop cluster tree is described that does not require all the coordinators to be in the radio range of the main coordinator. This is achieved with the introduction of special device denoted bridge. Bridge shares its time between the child cluster (where it acts as the coordinator) and the parent cluster (where it is just an ordinary device). It uses sleep period in one cluster to switch to another cluster. The presence of the sleep period in a superframe enables the creation of multi-cluster networks. Besides time division, frequency division is considered in [17] for beacon scheduling. Beacons are transmitted on different channels to prevent collisions. By doing so, more coordinators can be scheduled at the same time compared to pure time division solution.

However, all these solutions have proved to be dysfunctional in practice. Although star topologies are feasible, it is difficult to establish and maintain multi-hop communication in a cluster tree [18]. The main reason that IEEE 802.15.4 failed to provide functional multi-hop communication scheme is the high energy consumption of coordinators. As a consequence, they need to be mains-powered, which annuls the advantages of low installation costs of battery-powered devices. The concerns about powered routers and IEEE 802.15.4 MAC were summarised by Prof. David Culler, prominent figure in the worldwide TinyOS community [19], in a keynote for European TinyOS Technology Exchange back in 2009 [20], claiming that:

- "Beaconing doesn't work."
- "Low power mode is not defined for coordinators."

Nevertheless, numerous solutions for beacon collisions indicate steps in the right direction to derive operational MAC for resource-constrained, low-power, multi-hop networks. This new MAC cannot rely on powered routers i.e. powered tree roots. IEEE 802.15.4e standard MAC amendments present this new approach [11].

2.2.3 IEEE 802.15.4e Medium Access Control Amendments

The first novelty introduced in IEEE 802.15.4e Time Synchronised Channel Hopping (TSCH) mode is the reservation based approach opposed to contention based CSMA/CA [12]. For the contention based scheme to function, receivers have to be in the idle listen power mode for significant amounts of time. On the contrary, if a transmission is scheduled, the receiver knows exactly when to wake up to receive data addressed to it (if any). Scheduling thus significantly reduces idle listening and eliminates overhearing.

TSCH defines a fixed Time Division Multiple Access (TDMA) frame structure that is centrally scheduled. Each link formed by a pair of neighbour devices is assigned a unique time slot that repeats in a cyclical manner. The receiver wakes up only in the assigned slot and may enter

a sleep state (i.e. switch off its radio transceiver) for the rest of time. After it has woken up, it either receives a packet if the sender has one to send, or it goes quickly back to sleep if a packet preamble is not detected within a short, predefined time interval that is a fraction of the slot duration. The slot without a packet transmission is denoted as an *idle listen* slot. Links are normally dedicated, i.e. scheduled for each sender-receiver pair, or one sender and multiple receivers, to prevent packet collisions. Shared links with more than one sender are allowed in IEEE 802.15.4e TSCH, but they are not relevant for this thesis. Note that IEEE 802.15.4e only defines how the schedule is structured and executed, but not how the schedule is built.

Another novelty introduced in IEEE 802.15.4e is the absence of beacons. Synchronisation is maintained with acknowledgements or data packets; sender and receiver devices synchronise their clocks every time when they exchange data. Synchronisation is thus mostly data-driven. In the absence of data traffic (e.g. if senders have nothing to report), keep-alive messages are exchanged to maintain network-wide synchronisation. Although beacons are removed from the online mode of operation, they still play a role in the network formation. In the network formation phase, beacons are denoted as Advertise messages, to which devices wishing to join respond with Join messages. Join messages contain throughput and delay requirements and they are routed to the device that constructs the schedule. However, after the network formation phase is completed, Advertise/Join messaging is disabled.

Finally, TSCH proposes a channel hopping scheme. Aside from time division, frequency division is also applied. All 16 channels defined for 2.4 GHz band are used over the network lifetime. In each slot, both sender and receiver calculate the channel number (out of 16) that is going to be used for that slot; the procedure repeats for the subsequent slots. Channel number is calculated using channel offset and the total number of slots elapsed since the network formation. Channel hopping is applied to mitigate multipath fading and external interference. External interference in the overpopulated 2.4 GHz band is especially important to consider. The channels used in IEEE 802.11 networks partially overlap with the IEEE 802.15.4 channels. Hopping to different channel can alleviate strong interference coming from IEEE 802.11 devices and thus improve the probability of successful reception in the subsequent slot.

In summary, IEEE 802.15.4e TSCH [11] solves the problems in the original standard specifications using the following techniques and approaches:

- frame scheduling
- beacon dismissal
- channel hopping

2.3 Network Simulator ns-3

ns-3 is a discrete-event network simulator for the Internet and other networking systems [21]. It is open-source and primarily intended for research and education. ns-3 is developed in C++ programming language and built with Python-based Waf. We chose ns-3 as the principal simulation tool to validate the results of this thesis related to the Home and Building Automation use case. Besides ns-3, analytical and numerical calculations have been performed in Matlab.

ns-3 is modular in design; it is a set of libraries. User simulation scripts import these libraries to construct the network topology, install protocol stacks and test network algorithms. There are two types of libraries: core and technology libraries. **Core libraries** are normally used in every simulation, regardless of the concrete technology. They contain definitions for events, event schedulers, random variables, simulation log files, etc. Furthermore, network module contains abstractions for packets, headers, sockets, etc. **Technology libraries** implement protocol interfaces and packet formats (including the headers) by closely following the definitions of the corresponding standard technology. For instance, *lr-wpan* technology library [22] (partially) implements PHY and MAC as defined in [10]. This approach enables reliable simulations of real systems and facilitates the integration with a testbed. Service primitives and packet formats are the same as those of real devices. Each layer removes the layer-specific header, analyses it and performs next steps accordingly. The final goal of a fully supported technology model is to enable each simulated device to run an entire protocol stack and generate the output trace that is (almost) indistinguishable from the output of a real device.

A network creation begins with defining a channel that devices use to communicate. The channel abstraction is represented with the base class **Channel**, that has a propagation loss and propagation delay model. Some of the derived classes (subclasses) are e.g. WifiChannel for IEEE 802.11 networks or CsmaChannel for Ethernet LANs. Next, PHY and MAC are defined within the network device abstraction, represented with the class **NetDevice**. For example, LrWpanNetDevice for IEEE 802.15.4 contains LrWpanPhy and LrWpanMac objects. Network device contains both the simulated hardware and the software driver. Note that ns-3 is a *network* simulator and therefore no signal processing is done at the PHY layer. Instead, theoretically derived error functions are used to decide if a packet was successfully received, based on the current value of the Signal-to-Noise Ratio (SNR) determined by the channel model. In the next step, network layer is defined, e.g. TCP/IP protocol stack is installed. After the installation, IP addresses are assigned. Finally, user application is modelled with the base class **Application**. Classes derived from Application specify throughput and other traffic requirements. Application objects generate traffic and forward data packets to the lower layer. Traffic represents the events which start the simulation. With this design, simulated device runs the entire protocol stack from PHY to the application layer. This allows comprehensive and realistic simulations.

In Chapter 5 of this thesis, ns-3 was used to simulate networks of IEEE 802.15.4 PHY and

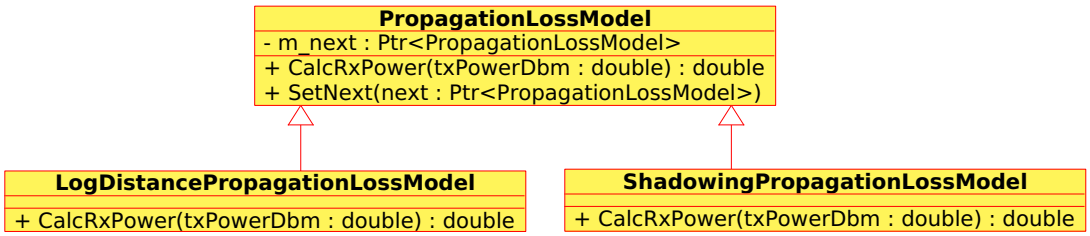

Figure 2.2: Class diagram for the propagation loss models

IEEE 802.15.4e MAC devices. The necessary code was implemented. Cooperative extensions of IEEE 802.15.4e MAC presented in this thesis have also been implemented.

In the next two Sections, we describe software design patterns defined in [23] and used in the simulations run to generate the results of this thesis.

2.3.1 Decorator Design Pattern for Wireless Channel Model

Decorator Pattern adds functionality to an object dynamically. Decorators provide a flexible alternative to subclassing. They have the same type (class) as the objects they decorate. One or more decorators can wrap an object. For all these reasons, they are an excellent design choice for modelling the communication channel propagation loss in ns-3. With decorators, channel model can be flexibly refined starting from large-scale path loss, (optionally) extended with medium-scale shadowing and (optionally) extended with small-scale multipath fading. All the available models can be combined dynamically (e.g. NakagamiPropagationLossModel is available, among many others).

Figure 2.2 shows a simplified class diagram for the propagation loss model, that is a member attribute of the Channel class. The base class is PropagationLossModel which contains a reference to itself according to decorator pattern. This reference is set with the function SetNext. Every time when function CalcRxPower is called, appropriate propagation loss is calculated and the result is delegated to the reference that is the next refinement of the model (if it was set). In the simulations for this thesis, LogDistancePropagationLoss object contains a reference to ShadowingPropagationLoss object which adds the studied shadowing effects. CalcRxPower therefore first calculates log-distance loss and then forwards the result for the random shadowing to be added. ShadowingPropagationLoss class was implemented for the purposes of this study.

2.3.2 Observer Design Pattern for Energy Model

Observer Pattern facilitates publish/subscribe relationships between objects. Observers subscribe at the publisher to receive updates about its state. Whenever the state of the publisher

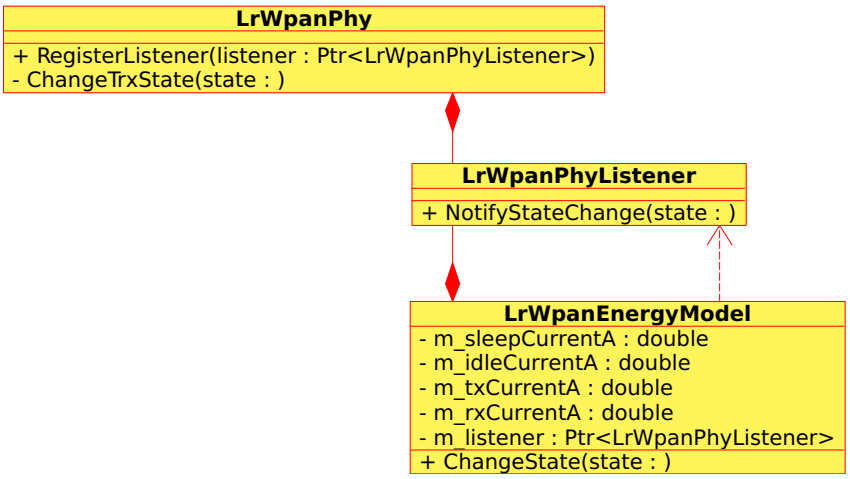

Figure 2.3: Class diagram for the energy consumption model

changes, updated values are automatically passed to the observers. Observer Pattern represents an elegant design choice for notifying the energy model about the changes in state of the radio transceiver. Energy model is loosely coupled with the PHY of the device, and receives state updates through the intermediate listener. Loose coupling also reinforces energy consumption calculation that is completely independent from MAC - all energy model knows about the device is when the radio transceiver changed its state and what that new state is.

Figure 2.3 shows a simplified class diagram for the energy model. LrWpanPhy is a publisher of the transceiver's state. It therefore maintains the list of listeners. When MAC requests a change in transceiver's state (e.g. from sleep to idle listen) or when PHY registers activity on the channel (which changes the transceiver's state from idle listen to receive), ChangeTrxState in LrWpanPhy object is called. This function then updates listeners with NotifyStateChange. LrWpanEnergyModel is next notified by LrWpanPhyListener through callback to ChangeState. After the state update is received by the energy model, energy consumed in the current state until that moment is calculated and state is updated. LrWpanPhyListener and LrWpanEnergyModel were implemented for the purposes of this study.

2.4 ETSI M2M Architecture

This Section presents ETSI M2M architecture for the middleware whose suitability for Wide Area Measurement System is examined in Chapter 6 of this thesis.

Over the course of previous years, different M2M use cases have been identified and have developed *vertically*, with implementations that target the specific needs of each use case. One of the principal objectives of ETSI M2M standard architecture is to define a common *horizontal* interface that would unite and replace verticals. To this aim, ETSI has deduced a set of common

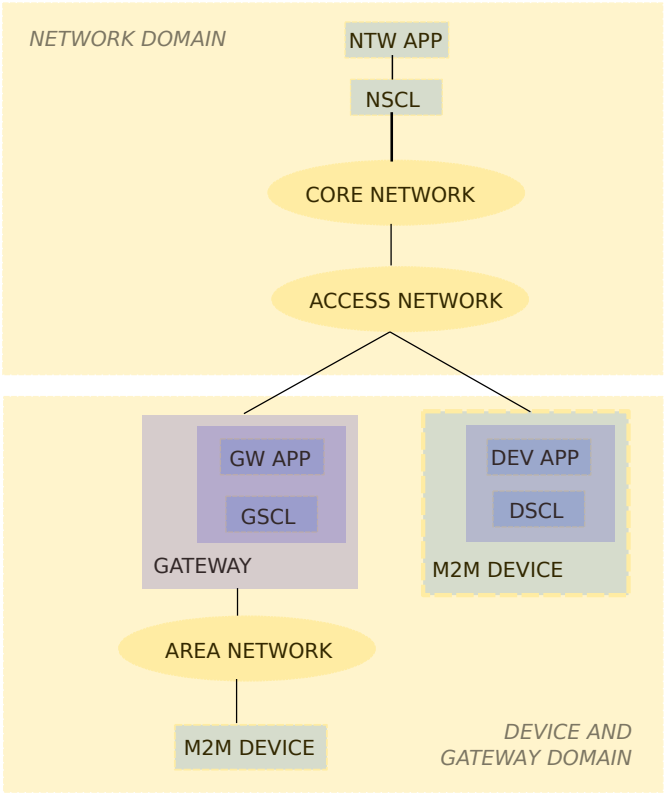

Figure 2.4: ETSI M2M Architecture

requirements shared by different M2M use cases. This set of requirements was next mapped to a well defined service logic whose purpose is to facilitate M2M application development under the common software framework [24].

ETSI M2M [25] defines a **middleware** for distributed M2M applications. Middleware is a software layer that lies between the operating system and applications on each side of the distributed computing system in a network. It supports heterogeneous network interfaces and provides common interface to the applications, regardless of the underlying network. In ETSI M2M architecture, a middleware is denoted *Service Capability Layer* (xSCL) to support the service logic, where x can stand for Network, Gateway or Device (therefore, we have NSCL, GSCL and DSCL modules).

Figure 2.4 shows ETSI M2M architecture. ETSI defines two principal domains in the M2M architecture:

1. **Network** domain
2. **Device** and **Gateway** domain

The Network domain consists of the access network and the core network that provide communication infrastructure to M2M network applications. The examples of these networks are

xDSL, UTRAN, WiMax, etc., in the access and 3GPP in the core network. NSCL is responsible for establishing a transport session for data transfer, security, address resolution, configuration, performance management etc. M2M network application collects and processes data from the devices in the field, stores them to a database and optionally issues commands to the actuators back in the device domain.

Within the device domain, there are two types of devices. Some have enough processing resources to run M2M device application with the required service logic in DSCL and they would connect directly to the access network in the network domain. However, most M2M devices are simple sensors or actuators with limited processing and memory resources, insufficient to execute M2M application services. For these devices, ETSI defines a **gateway** to perform the task of connecting to the access network, but also to speak the custom protocol of a device and do the necessary protocol translation. It is the task of gateway to translate the messages received from a device to the ETSI M2M standard interface. GSCL at the gateway also checks if a device is online, executes remote software updates, etc. A local network between the gateway and the devices is called M2M area network. Some examples of M2M area network are IEEE 802.15.4e [11] combined with RPL [26], then, power-saving WiFi or any other proprietary protocol. Area networks are studied in Chapters 3, 4 and 5 of this thesis.

The exchange of data happens as follows. An M2M device registers its data source at the gateway or directly at the network by using G/DSCL in order to publish the available data stream. In parallel, G/DSCL registers with the NSCL in order to be assigned an IP address and to become visible on the network. The security keys are exchanged for the secure transport session establishment. A new data source is next announced on the network and this announcement can be retrieved by the M2M network application. There are discovery procedures in xSCL that assist the application in finding the desired data. The application next subscribes to the selected data and the secure transport session is established. When new data is generated at the device, it is again announced to the network and the subscribed application is notified in order to retrieve the new data.

In summary, the purpose of xSCL is to hide the specific underlying network from the application and allow for the common service interface to be used across all application types. xSCL exposes network functionalities through a set of open interfaces, but does not dictate the concrete implementation of those interfaces.

Finally, ETSI M2M architecture is **distributed** rather than centralised. This is achieved with GSCL at the gateway, which is a lightweight server meant to serve as a network proxy. In effect, GSCL offloads the processing load from the NSCL, which is a fully-fledged server.

Bibliography

[1] N. Baccour, A. Koubaa, L. Motolla, M. Zuniga, H. Youssef, C. Boano, and M. Alves, "Radio Link Quality Estimation in Wireless Sensor Networks: a Survey," *ACM Transactions on Sensor Networks*, vol. 8, no. 4, November 2012.

[2] D. De Couto, D. Aguayo, J. Bicket, and R. Morris, "A High-Throughput Path Metric for Multi-Hop Wireless Routing," *ACM Mobicom*, September 2003.

[3] (2012) Routing Metrics Used for Path Calculation in Low-Power and Lossy Networks. [Online]. Available: http://tools.ietf.org/html/rfc6551

[4] J. Kuruvila, A. Nayak, and I. Stojmenovic, "Hop count optimal position-based packet routing algorithms for ad hoc wireless networks with a realistic physical layer," *IEEE Journal on Selected Areas in Communications*, vol. 23, no. 6, pp. 1267–1275, June 2005.

[5] I. Stojmenovic, A. Nayak, and J. Kuruvila, "Design guidelines for routing protocols in ad hoc and sensor networks with a realistic physical layer," *IEEE Communications Magazine*, vol. 43, no. 3, pp. 101 – 106, march 2005.

[6] M. Z. Zamalloa and B. Krishnamachari, "An Analysis of Unreliability and Asymmetry in Low-power Wireless Links," *ACM Transactions on Sensor Networks*, vol. 3, no. 2, June 2007. [Online]. Available: http://doi.acm.org/10.1145/1240226.1240227

[7] M. Zorzi and S. Pupolin, "Optimum transmission ranges in multihop packet radio networks in the presence of fading," *IEEE Transactions on Communications*, vol. 43, no. 7, pp. 2201–2205, 1995.

[8] H. Takagi and L. Kleinrock, "Optimal Transmission Ranges for Randomly Distributed Packet Radio Terminals," *IEEE Transactions on Communications*, vol. 32, no. 3, pp. 246–257, 1984.

[9] M. Zorzi and A. Armaroli, "Advancement optimization in multihop wireless networks," in *IEEE Vehicular Technology Conference*, vol. 5, 2003, pp. 2891–2894.

[10] *IEEE Standard 802.15.4-2011: Wireless Medium Access Control (MAC) and Physical Layer (PHY) Specifications for Low-Rate Wireless Personal Area Networks (WPANs)*, IEEE Std., September 2011.

[11] *IEEE Standard 802.15.4e-2012: Low-Rate Wireless Personal Area Networks (LR-WPANs) Amendment 1: MAC sublayer*, IEEE Std., April 2012.

[12] A. Bachir, M. Dohler, T. Watteyne, and K. Leung, "MAC Essentials for Wireless Sensor Networks," *IEEE Communications Surveys Tutorials*, vol. 12, no. 2, pp. 222–248, February 2010.

[13] (2010) CC2430 datasheet. [Online]. Available: http://www.ti.com/product/CC2430

[14] *IEEE Standard 802.11-2012: Wireless Medium Access Control (MAC) and Physical Layer (PHY) Specifications for Wireless Local Area Networks (WLANs)*, IEEE Std., March 2012.

[15] A. Koubaa, A. Cunha, and M. Alves, "A Time Division Beacon Scheduling Mechanism for IEEE 802.15.4/Zigbee Cluster-Tree Wireless Sensor Networks," in *Euromicro Conference on Real-Time Systems (ECRTS)*, July 2007, pp. 125–135.

[16] J. Misic and C. J. Fung, "The impact of master-slave bridge access mode on the performance of multi-cluster 802.15.4 network," *Elsevier Journal on Computer Networks*, vol. 51, no. 10, pp. 2411 – 2449, 2007.

[17] E. Toscano and L. Lo Bello, "Multichannel Superframe Scheduling for IEEE 802.15.4 Industrial Wireless Sensor Networks," *IEEE Transactions on Industrial Informatics*, vol. PP, no. 99, p. 1, 2011.

[18] M. Palattella, N. Accettura, X. Vilajosana, T. Watteyne, L. Grieco, G. Boggia, and M. Dohler, "Standardized Protocol Stack for the Internet of (Important) Things," *IEEE Communications Surveys Tutorials*, vol. 15, no. 3, pp. 1389–1406, March 2013.

[19] P. Levis, S. Madden, J. Polastre, R. Szewczyk, K. Whitehouse, A. Woo, D. Gay, J. Hill, M. Welsh, E. Brewer, and D. Culler, "TinyOS: An Operating System for Sensor Networks," in *Ambient Intelligence*, W. Weber, J. Rabaey, and E. Aarts, Eds. Springer Berlin Heidelberg, 2005, pp. 115–148. [Online]. Available: http://dx.doi.org/10.1007/3-540-27139-2_7

[20] (2009) Time to ROLL, Keynote by David Culler, 1st European TinyOS Technology Exchange. [Online]. Available: http://vimeo.com/3264574

[21] (2014) network simulator 3. [Online]. Available: http://www.nsnam.org/

[22] (2011) Low-rate, wireless personal area network (LR-WPAN) ns-3 model. [Online]. Available: http://code.nsnam.org/tomh/ns-3-lr-wpan/

[23] E. Gamma, R. Helm, R. Johnson, and J. Vlissides, *Design patterns: elements of reusable object-oriented software*. Boston, MA, USA: Addison-Wesley Longman Publishing Co., Inc., 1995.

[24] ETSI M2M TR 102 689, "Machine-to-Machine communications (M2M); M2M service requirements," ETSI, Tech. Rep., 2012.

[25] (2014) ETSI M2M. [Online]. Available: http://www.etsi.org/technologies-clusters/technologies/m2m

[26] (2012) RPL: IPv6 Routing Protocol for Low-Power and Lossy Networks. [Online]. Available: http://tools.ietf.org/html/rfc6550

Chapter 3

Energy Efficiency Analysis of a Cooperative Scheme for Wireless Local Area Networks

In this chapter, we analyse the energy efficiency of a C-ARQ protocol suitable for Wireless Local Area Networks (WLANs) to assess the protocol's applicability to the energy-constrained networks. Towards this aim, an energy model for the Persistent Relay Carrier Sensing Multiple Access (PRCSMA) protocol is derived. The model has been validated in Matlab simulations and shows that a C-ARQ based on PRCSMA can help improve the energy efficiency of wireless communications and thus increase the lifetime of devices.

3.1 Introduction

Over the last years we have witnessed a wide deployment of WLANs that apply the Distributed Coordination Function (DCF) defined in the IEEE 802.11 Standard [1] to enable access to a shared broadcast medium: the air. The main design goal of DCF was throughput maximization, without much emphasis on the energy consumption. Indeed, although the standard does define a power management mechanism, it is usually not commercially implemented. How-

ever, as mobility and the capability of autonomous operation (especially required in Machine-to-Machine networks) become relevant, energy efficiency is a must due to the fact that WLAN devices are equipped with a battery that provides a finite amount of energy. Unfortunately, the default operation of DCF leads to a solution whose power management mode is *active* mode. In this mode of operation, a device keeps its transceiver in idle listening also during intervals of inactivity, thus leading to a waste of the energy resources of the battery. In another words, DCF belongs to non-duty-cycled schemes. For this reason, the design and analysis of energy efficient solutions for WLANs have become a challenging research topic. Energy-aware MAC layer would increase the battery life and enable less frequent battery recharges.

In the past, the throughput and delay of the DCF (and its fine-tuning variants) have been extensively analysed in the literature using the seminal work of Bianchi in [2], based on the idea of modelling the backoff operation of devices with a Markov chain. Recently, the arising need for energy efficiency has triggered many research activities devoted to the energy analysis of DCF. An example can be found in [3], where the authors develop an energy model of DCF and suggest a suitable approximation in order to find the optimal size of the contention window, from the energy point of view, in idealistic channel conditions. To overcome this simplistic channel assumption, in [4], the energy efficiency with regard to the number of nodes has been evaluated by considering a Markov chain to model the channel errors. Another energy model concerning the number of devices in an IEEE 802.11 network is presented in [5]. In this work, the authors focus on the evaluation of different energy components and their ratio to the total energy consumption. A relevant observation for the analysis of the energy consumption of wireless communication devices was found in [5], stating that overhearing, i.e., receiving packets not intended for a device while it listens to the channel, takes a significant proportion of the total consumed energy. This is a consequence of the active power management mode of the device that receives all incoming packets and only filters them on the MAC layer to decide whether to process them further or to drop them.

The high energy cost of the active mode is wasted when the packets not addressed to the device are dropped after spending energy to decode them. However, active mode can be exploited to improve the energy efficiency of the communications. Indeed, this is what C-ARQ schemes do by letting overhearing stations act as spontaneous relays upon transmission error. A MAC protocol designed to coordinate the retransmissions from the relays in a C-ARQ scheme was proposed in [6]. It is called PRCSMA protocol and it is based on the DCF of the 802.11 standard. Previous works on the PRCSMA have shown that this protocol can boost the performance of wireless communications in terms of delay and throughput. As far as energy efficiency is concerned, only preliminary computer based performance evaluation has been presented in [7]. However, in order to be able to optimize the system parameters and find optimal operating points, it is necessary to formulate a theoretical model that allows evaluating the energy performance of the protocol. This is the main motivation for the work presented in this chapter.

3.1.1 Contribution

The main contribution of this chapter is the formulation of an energy model for PRCSMA. The model is used to compare the energy efficiency of PRCSMA with that of a traditional non-cooperative ARQ scheme where retransmissions are only performed by the source. The model is validated in Matlab simulations for a wide range of system parameters. The conditions under which PRCSMA outperforms non-cooperative ARQ are identified and discussed.

This chapter is organized as follows. The PRCSMA protocol is briefly described in Section 3.2. Section 3.3 defines the considered scenario and the energy model used for both the energy efficiency analysis of a non-cooperative ARQ scheme and PRCSMA. In Section 3.4, the proposed theoretical model is validated in computer simulations and the energy efficiency of the two schemes is compared. Finally, Section 3.5 concludes the chapter.

3.2 PRCSMA Overview

For completeness, a brief summary of PRCSMA is presented in this Section. The interested reader is referred to [6] for a complete description of the protocol.

PRCSMA is a novel MAC protocol that was specifically designed to coordinate retransmissions from the relays of a Cooperative-ARQ scheme. The rules of PRCSMA are based on the DCF of the IEEE 802.11 Standard, thus enabling backwards compatibility. The protocol works as follows. Consider a scenario formed by a source, a destination, and a group of devices within the transmission range of both the source and the destination. The source transmits packets to the destination following any MAC protocol rules, and it is assumed that the group of surrounding devices can overhear all ongoing transmissions. These are the devices in active mode running an application that requires constant monitoring of the channel. If a device receives and decodes without errors a data packet not addressed to its address, it does not discard it, but it buffers the packet for a certain time interval in a special queue denoted cooperative queue. When the destination receives a data packet with unrecoverable errors, instead of requesting a retransmission from the source, it broadcasts a Call for Cooperation (CFC) control packet and initiates a *cooperation phase*. Those devices that buffered the original packet from the source and receive this CFC packet become active relays and attempt to retransmit the original packet. In order to avoid a certain collision, the relays execute a backoff before the first transmission attempt. To do so, each relay selects a random value for the contention window within the range $CW = [0, W]$. For the randomly selected number of time slots with a constant duration of δ seconds, each relay senses the activity in the channel. If the channel is idle within a slot, the counter is decreased by one unit. If a transmission in the channel is detected, the counter is frozen until the ongoing transmission ends. The countdown is resumed when the channel be-

comes idle again. When the backoff counter value reaches zero, the relay attempts to transmit. There are three possible outcomes of this transmission attempt:

1. **More than one relay transmits.** This results in a collision and the packet cannot be decoded at the destination. Consequently, the destination takes no further action. Silence from the destination indicates to the relays that the cooperation phase continues.

2. **Only one relay transmits but the packet is erroneously received at the destination.** The destination receives and decodes the packet but takes no action since the packet was received erroneously. The cooperation phase continues.

3. **Only one relay transmits and the packet is successfully received at the destination.** The destination transmits an Acknowledgement (ACK) packet to notify the end of the cooperation phase.

Note that an ACK is transmitted only when the destination device is able to decode the original packet. If a relay transmits but does not receive the ACK packet, it resets the backoff counter and attempts a new transmission. From the perspective of each individual relay, cooperation might end because of own, but also other relay's successful retransmission.

According to this operation, the benefits of C-ARQ are drawn from the adaptive rate scheme that exploits favourable channel conditions between the relays and the destination. This allows relays to transmit at a higher rate than the one used in the main source-to-destination channel. When the channel conditions between the source and all the receiving devices are unfavourable, it might happen that none of the potential relays has an errorless copy of the original packet. In this case, the cooperation phase ends after the expiration of a predefined timeout period, after which retransmission is requested from the source.

3.3 Scenario and Energy model

We consider the scenario shown in Figure 3.1. It represents a remote Access Point (AP) as a data source and a number of devices in its communication range. We assume that the subset of all the devices run in active power management mode and thus monitor the channel continuously. Once a destination device is selected for transmission, the number of potential relays, i.e., active devices in the transmission range of both the source and the destination, is denoted by n. The scenario is thus formed by a number of $n + 2$ devices, i.e., source, destination, and n potential relays.

The average packet error rate from source to destination is denoted p_{SD}. The packet error rate from source to relay i, $i = \{1, ..., n\}$, is $p_{SR_1} \approx p_{SR_2} \approx p_{SR_i} \approx p_{SR_n} = p_{SR}$ and we

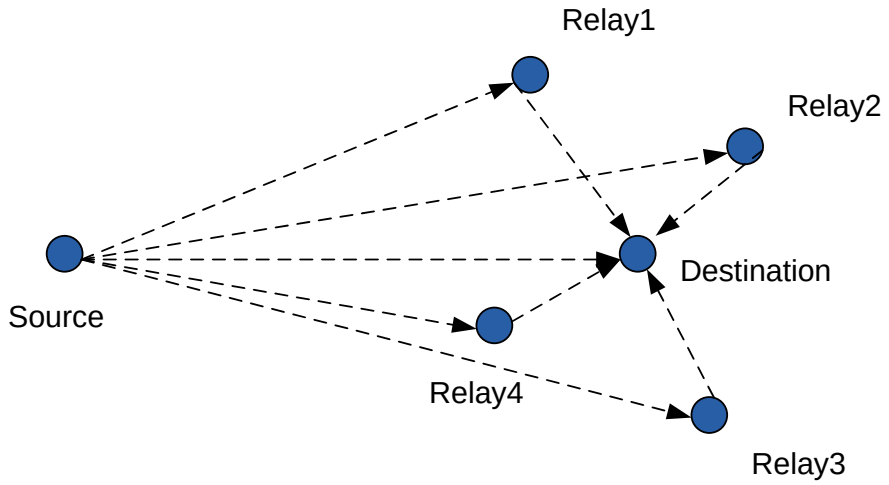

Figure 3.1: Network scenario showing remote AP and its associated devices

assume that $p_{SD} = p_{SR}$. We also assume that the packet error rate from relay i to destination is $p_{R_1D} \approx p_{R_2D} \approx p_{R_iD} \approx p_{R_nD} = p_{RD}$ because the channel conditions between any relay and the destination are i.i.d. (independent and identically distributed). Upon a transmission from the source, out of the n potential relays, only k will receive the packet from the source without errors and thus become actual active relays. Indeed, the average number of active relays can be calculated as

$$\mathrm{E}[k] = \lceil n(1 - p_{SD}) \rceil, \tag{3.1}$$

where $\lceil x \rceil$ indicates the closest greatest integer number to x, and it is taken to account for the worst-case collision probability.

We focus on the basic channel access of PRCSMA, i.e., without Request-to-Send and Clear-to-Send handshake between the relays and the destination.

We differentiate three transceiver states: transmit, receive and idle, with respective consumption powers P_{tx}, P_{rx} and P_{idle}. The energy consumed during a period of T_x seconds in each of these modes can be expressed as E_x^T, E_x^R, E_x^I, respectively:

$$E_x^T = P_{tx} \cdot T_x, \;\; E_x^R = P_{rx} \cdot T_x, \;\; E_x^I = P_{idle} \cdot T_x. \tag{3.2}$$

The different values that T_x can take are T_{SIFS} and T_{DIFS} for the duration of a SIFS a DIFS, respectively, and T_{ACK} and T_{CFC} for the duration of the transmission of an ACK and CFC packets, respectively. As far as data packet transmission is concerned, it is necessary to differentiate between the transmissions from the source and from a relay. We consider the packets of constant bit-length and we assume that, although the data transmission rates are adaptive, once they are established, they remain constant for the duration of the communication session. We denote the bit length of a data packet by L and we define R_{SD} and R_{RD} as the transmission rates from source to destination and from relays to destination, respectively. It is possible to

express

$$E_{SD}^{T} = P_{tx} \cdot \frac{L}{R_{SD}}, E_{SD}^{R} = P_{rx} \cdot \frac{L}{R_{SD}} \tag{3.3}$$

$$E_{RD}^{T} = P_{tx} \cdot \frac{L}{R_{RD}}, E_{RD}^{R} = P_{rx} \cdot \frac{L}{R_{RD}}, \tag{3.4}$$

where E_{SD}^{T}/E_{SD}^{R} correspond to the energy consumption in a transmission/reception between source and destination, and E_{RD}^{T}/E_{RD}^{R} to the energy consumption in a transmission/reception between a relay and the destination.

According to [8], the energy efficiency of the protocol can be defined as

$$\lambda = \frac{total\ amount\ of\ delivered\ data\ (bits)}{total\ energy\ consumed\ (Joule)}. \tag{3.5}$$

In the next Sections, we analyse the energy expenditure and energy efficiency of a traditional non-cooperative ARQ scheme, and that of a C-ARQ with PRCSMA.

3.3.1 Energy analysis for Non-cooperative ARQ

Recall the scenario in Figure 3.1. Every transmission from the source is received by the destination and by all the potential relays. We consider a non-cooperative ARQ. This means that, in the case of erroneous reception of a packet, it will not be acknowledged, thus triggering a retransmission from the source along the same transmission path.

The total energy spent in the network for a transmission from the source can be computed as

$$E_S = (n+2)E_{DIFS}^{I} + E_{SD}^{T} + (n+1)E_{SD}^{R} + (n+2)E_{SIFS}^{I}. \tag{3.6}$$

Note that this expression does not account for the energy spent in the acknowledgement process. Indeed, if the packet is received and acknowledged successfully by the destination, the energy consumption associated to a successful transmission from the source can be defined as

$$E_{SS} = E_S + E_{ACK}^{T} + (n+1)E_{ACK}^{R}. \tag{3.7}$$

Similarly, if the packet is received with errors, all the nodes of the scenario will listen to the channel for the duration of ACK timeout, here assumed to be equivalent to the duration of an ACK packet. The energy spent when a transmission from the source results in error can be computed as

$$E_{SE} = E_S + (n+2)E_{ACK}^{I}. \tag{3.8}$$

Finally, the energy efficiency of a Non-cooperative ARQ scheme can be calculated as

$$\begin{aligned}\lambda_{NC} &= \frac{L}{(1-p_{SD})E_{SS} + p_{SD}\left(E_{SS} + \frac{1}{1-p_{SD}}E_{SE}\right)} \\ &= \frac{L}{E_{SS} + \frac{p_{SD}}{1-p_{SD}}E_{SE}},\end{aligned} \tag{3.9}$$

where the first component of the sum in the denominator stands for successful receptions and the second component accounts for the average number of retransmissions from the source.

3.3.2 Energy analysis for PRCSMA

The embedded Markov chain proposed in [6] describes the counter state of a relay executing the PRCSMA protocol when a cooperation phase is running. This model is based on the work presented in [2] for the modeling of the DCF, and is used to model the sub-network formed by the active relays once a cooperation phase has been initiated. The probability that the counter of a relay reaches zero and, consequently, attempts to transmit a packet, is denoted by P_0. This parameter can be used to calculate the probabilities of different sub-network states that depend on the counter states of *all* the active relays for a given time slot. P_I is the probability that the whole sub-network formed by the active relays is idle. P_S is the probability that only one relay is transmitting and the transmission was successful and P_E is the probability that only one relay transmits and the transmission is received with errors. Finally, P_C is the probability that more than one relays transmit and thus collide [6]. These probabilities depend on the number of active relays k. However, all the n potential relays monitor the activity on the channel and account for the total energy expenditure.

We differentiate the following energy consumption states in the sub-network formed by the active relays:

1. **Idle.** All the relays remain in the idle state because none of the counters have expired. The total energy spent in the network in this case is

$$E_I = (n+2)E_\delta^I, \tag{3.10}$$

   where δ is the duration of the slot time.

2. **One transmission.** The counter of only one relay reaches zero. The total energy spent in the network in this case is

$$E_R = (n+2)E_{DIFS}^I + E_{RD}^T + (n+1)E_{RD}^R. \tag{3.11}$$

   With probability $(1-p_{RD})$ this transmission will be successful and will result in the end of the cooperation phase. With probability p_{RD}, it will be received with errors and the cooperation phase will continue.

3. **Collision.** The total energy consumption involved in a collision depends on the number of colliding relays. The energy spent when m relays collide can be computed as

$$E_C(m) = (n+2)E^I_{DIFS} + mE^T_{RD} \quad + \quad (n+2-m)E^R_{RD}. \tag{3.12}$$

We are next interested in the computation of the expected energy spent during the contention phase defined as the cooperation phase subtracting the actual time devoted to successful transmissions. Towards this end, the probability of successful transmission from a relay is denoted by P_S, and thus the expected number of slots in the contention phase is

$$E[X] = \frac{1}{P_S} - 1, \tag{3.13}$$

where the final successful slot has been subtracted. Consequently, the expected energy spent in the contention phase accounts for the energy spent in *i)* the idle state, *ii)* erroneous transmissions, and *iii)* collisions. The probabilities of being in each of these states are conditioned on the probability of not being successful $1 - P_S$. Therefore, the expected energy in the contention phase is obtained as

$$E_{cont} = E[X]\left(\frac{P_I}{1-P_S}E_I + \frac{P_E}{1-P_S}E_R + \frac{P_C}{1-P_S}E_C(m)\right), \tag{3.14}$$

where P_C is the probability of collision and can be computed as

$$P_C = \sum_{m=2}^{k} P_C(m). \tag{3.15}$$

$P_C(m)$ is the probability of having m relays colliding when there is a collision in the subnetwork formed by the active relays and can be expressed as

$$P_C(m) = \binom{k}{m} P_0^m (1-P_0)^{k-m},\ 2 \le m \le k. \tag{3.16}$$

Therefore, the total average energy spent in collisions can be computed as

$$\begin{aligned}\sum_{m=2}^{k} P_C(m)E_C(m) = (n+2)(E^I_{DIFS} + E^R_{RD}) \cdot \\ \cdot \left[1 - (1-P_0)^k\left(1 + \frac{kP_0}{1-P_0}\right)\right] + \\ +kP_0(1-(1-P_0)^{k-1})(E^T_{RD} - E^R_{RD}).\end{aligned} \tag{3.17}$$

To complete the energy model, it is necessary to consider the case when no potential relay has received the original packet without error (i.e., $k = 0$), and thus the cooperation fails, since there is no relay able to retransmit the original packet. In this case, all the nodes of the

network remain idle until a cooperation timeout expires. The destination then sends a negative ACK packet in order to inform the source that a new retransmission is required. In terms of energy consumption, this packet is equivalent to an ACK packet. The duration of the timeout is arbitrary, but we consider for this analysis that it can be computed as the duration of the maximum contention window, i.e., of duration $W \cdot \delta$. Therefore, the energy spent during a cooperation timeout can be computed as

$$E_{to} = (n+2)WE_{\delta}^{I}. \tag{3.18}$$

Finally, the total energy spent in a cooperation phase can be written as

$$\begin{aligned} E_{coop} &= E_{CFC}^{T} + (n+1)E_{CFC}^{R} + (n+2)E_{SIFS}^{I} + p_{SD}^{n}E_{to} + \\ &+ (1-p_{SD}^{n})\left[E_{cont} + E_{R} + (n+2)E_{SIFS}^{I}\right] + \\ &+ E_{ACK}^{T} + (n+1)E_{ACK}^{R}. \end{aligned} \tag{3.19}$$

If the cooperation fails, the source will retransmit the original packet. The average number of retransmissions is computed as

$$N = \frac{1}{1-p_{SD}^{n+1}}, \tag{3.20}$$

because it is sufficient that either the destination or any of the relays receives the packet correctly.

All the components can be summed up to compute the energy efficiency of PRCSMA as

$$\lambda_C = \frac{L}{\frac{1}{1-p_{SD}^{n+1}}\left[(1-p_{SD})E_{SS} + p_{SD}(E_S + E_{coop})\right]}. \tag{3.21}$$

The first component in brackets in the denominator stands for successful receptions from the source and the second is attributed to the entire cooperation process starting with the erroneous reception from the source and including all the different energy modes involved in the cooperation phase.

3.4 Energy Model Evaluation

The validation of the analysis presented in the previous section has been done through computer simulations executed in a custom MATLAB simulator. The system parameters are given in Table 3.1. It has been shown in the literature that the energy spent for receiving a packet is approximately the same as the energy spent for listening the channel [9] and therefore we adopt $P_{rx} = P_{idle}$.

Table 3.1: Simulation Parameters

Parameter	**Value**	**Parameter**	**Value**
DIFS	$50\ \mu s$	R_{SD}	24 Mbps
SIFS, δ	$10\ \mu s$	R_{RD}	54 Mbps
ACK, CFC	14 Bytes	R_C	6 Mbps
DATA	512 Bytes	P_{Tx}	1900 mW
W	16	P_{Rx}, P_{idle}	1340 mW

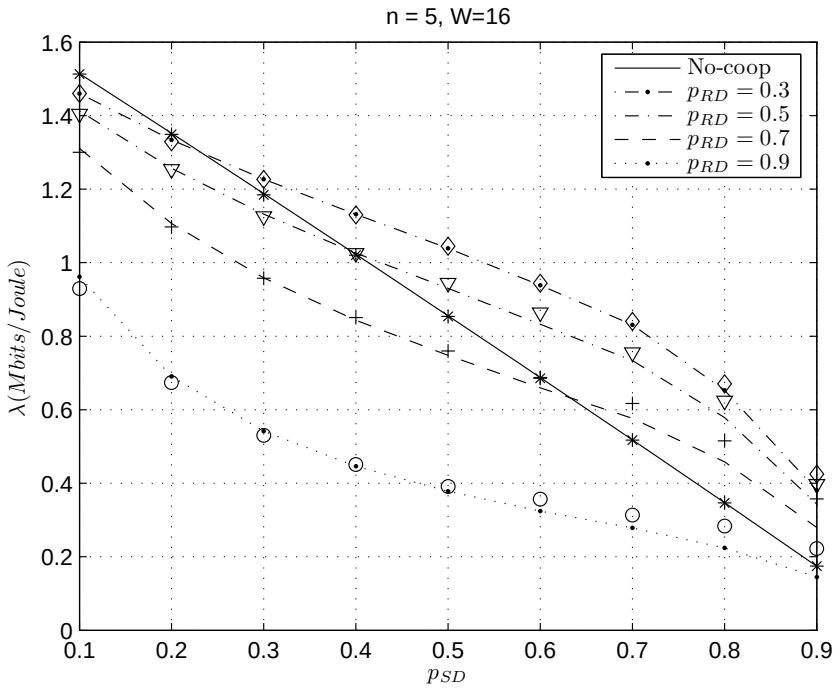

Figure 3.2: Energy efficiency of Non-cooperative and Cooperative-ARQ scheme for varying channel quality from source-to-destination p_{SD} and relay-to-destination p_{RD}.

In the simulation, devices execute the protocol rules and the energy expenditure is recorded for each of the system states. The network state depends on whether a packet from the source was received erroneously by the destination, thus inducing the cooperation phase regulated by randomly set backoff counters. To calculate the energy efficiency, the total data delivered to destination is divided by the total energy spent as defined in Eq. (3.5). None of the probabilities developed in the energy model to yield the expected energy spent in the different system states were used in the simulations. The results are plotted in Figure 3.2 and Figure 3.3.

Figure 3.2 shows a comparison between the energy efficiency of non-cooperative ARQ scheme and PRCSMA for varying values of p_{SD} and p_{RD}. Lines represent the values obtained with the theoretical model. The markers in the figure stand for simulation results and were omitted in the legend to avoid overloading it. We may first observe the good agreement between

the theoretical model and the simulation which confirms the validity of the analysis done in Section 3.3. It is worth seeing that PRCSMA performs best for the intermediate values of source-to-destination quality. When p_{SD} is small, the cooperation gain does not compensate the protocol overhead cost. As p_{SD} increases, the benefits of PRCSMA are clearly visible due to the increased number of successful cooperations whose energy cost is smaller than retransmissions from the source. However, we may observe that the energy efficiency of PRCSMA drops after p_{SD} becomes greater than a certain value ($p_{SD} > 0.7$ in Figure 3.2). This happens because the channel quality from the source is so low that often there are no active relays so the packet will be, eventually, retransmitted from the source. We are interested in finding this turning point. Because of the relative long duration of data packet transmissions, the energy spent for transmissions and overhearing is greater than energy spent on the transmission of control packets or idling until the timeout expires. Therefore, the most significant terms in Eq. (3.19) are E_{cont} and E_R. If we look at the energy efficiency expression Eq. (3.21), we see that the influence of channel on the contribution of these components is $p_{SD}(1 - p_{SD}^n)$. If we calculate $\frac{\partial p_{SD}(1-p_{SD}^n)}{\partial p_{SD}} = 0$, the turning point obtained from the above approximation is

$$p_{SD}^* = \left(\frac{1}{n+1}\right)^{\frac{1}{n}}. \tag{3.22}$$

For $n = 5$, $p_{SD}^* = 0.7$ as the Figure 3.2 confirms. For $p_{SD} > p_{SD}^*$, the cooperation gains are reduced.

Figure 3.2 also shows the energy efficiency for different values of p_{RD}. As expected, when the relay-to-destination packet error rate is high, cooperation does not produce any benefit. However, the proximity of relays implies small values of p_{RD} in practical scenarios. This enables using the higher transmission rate than in the original channel. Therefore, in many scenarios, C-ARQ is the most energy-efficient ARQ approach.

We next studied the dependence of energy efficiency on the contention window size, as shown in Figure 3.3. Collisions are costly, since for $W = 4$ the energy efficiency is greatly reduced. On the other hand, increased probability of the idle state in the cooperation phase, caused by the large value of W, does not have a major impact. For this reason, contention probability should always be kept low, by setting high values of W, even at the cost of longer idle periods.

3.5 Chapter Summary and Conclusions

An energy model based on Markov chain theory and applicable to the PRCSMA protocol has been presented in this chapter. This model has been used to assess the energy efficiency of the protocol and it has been compared to the efficiency of a traditional non-cooperative ARQ scheme. The validity of the model has been confirmed by computer-based simulations.

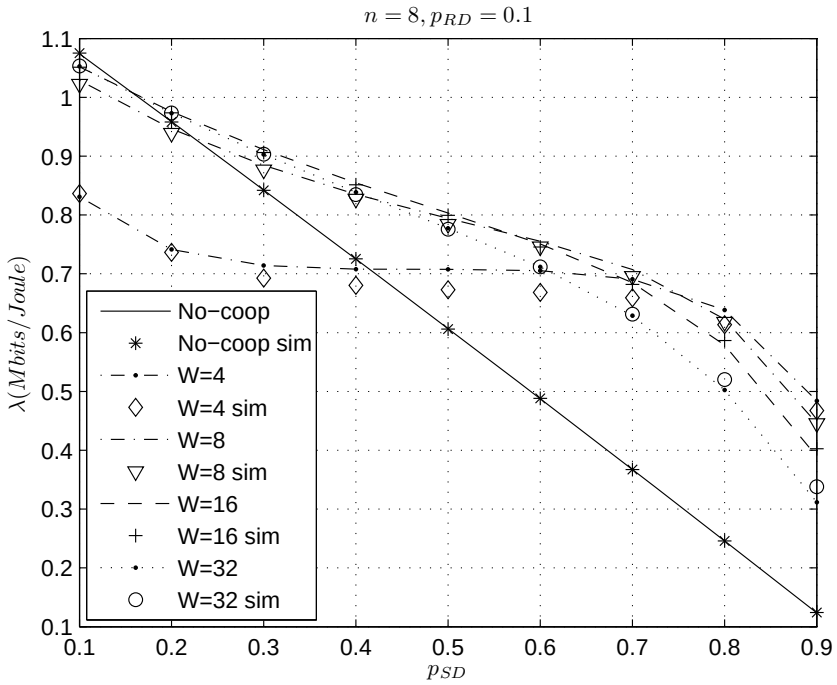

Figure 3.3: Energy efficiency of Non-cooperative and Cooperative-ARQ scheme for varying contention window size.

The results show that the PRCSMA outperforms non-cooperative ARQ for medium to high packet error rates in the source-to-destination channel. The results also demonstrate that, in the cooperation phase, collisions should be avoided even at the cost of more idle slots to achieve better energy efficiency.

This chapter studied the improvements that can be achieved with non duty-cycled devices. However, further significant improvements in energy efficiency can be achieved only by *duty-cycling* the devices. In the next chapter, duty-cycled devices are introduced and the related implications on C-ARQ are studied. In duty-cycled networks, there is no overhearing and consequently, the techniques presented in this chapter cannot be applied without undergoing significant changes. In addition, the base technology is changed from IEEE 802.11 to IEEE 802.15.4 that defines a duty-cycled scheme. IEEE 802.15.4 is more appropriate for resource-constrained devices. Also, exploring various technologies expands the applicability of results presented in this thesis.

Bibliography

[1] *IEEE Standard 802.11-2012: Wireless Medium Access Control (MAC) and Physical Layer (PHY) Specifications for Wireless Local Area Networks (WLANs)*, IEEE Std., March 2012.

[2] G. Bianchi, "Performance Analysis of the IEEE 802.11 Distributed Coordination Function," *IEEE Journal on Selected Areas in Communications*, vol. 18, no. 3, pp. 535–547, March 2000.

[3] P. Serrano, A. Garcia-Saavedra, M. Hollick, and A. Banchs, "On the energy efficiency of IEEE 802.11 WLANs," in *European Wireless Conference (EW)*, April 2010, pp. 932–939.

[4] J. Yin, X. Wang, and D. Agrawal, "Energy efficiency evaluation of wireless LAN over bursty error channel," in *IEEE Global Telecommunications Conference (GLOBECOM)*, vol. 6, December 2005, pp. 5 pp.–3632.

[5] M. Ergen and P. Varaiya, "Decomposition of Energy Consumption in IEEE 802.11," in *IEEE International Conference on Communications, (ICC)*, June 2007, pp. 403–408.

[6] J. Alonso-Zarate, L. Alonso, and C. Verikoukis, "Performance analysis of a persistent relay carrier sensing multiple access protocol," *IEEE Transactions on Wireless Communications*, vol. 8, no. 12, pp. 5827–5831, December 2009.

[7] J. Alonso-Zarate, E. Stavrou, A. Stamou, P. Angelidis, L. Alonso, and C. Verikoukis, "Energy-Efficiency Evaluation of a Medium Access Control Protocol for Cooperative ARQ," in *IEEE International Conference on Communications (ICC)*, June 2011, pp. 1–5.

[8] M. Zorzi and R. Rao, "Energy constrained error control for wireless channels," in *Global Telecommunications Conference, 1996. GLOBECOM '96.*, vol. 2, nov 1996, pp. 1411 – 1416 vol.2.

[9] L. Feeney and M. Nilsson, "Investigating the energy consumption of a wireless network interface in an ad hoc networking environment," in *Proceedings of the IEEE International Conference on Computer Communications (IEEE INFOCOM)*, vol. 3, 2001, pp. 1548 – 1557 vol.3.

Chapter 4

Energy Efficiency Analysis and Evaluation of Low-Power Networks

This chapter examines energy-efficient schemes suitable for Wireless Personal Area Networks (WPANs) based on IEEE 802.15.4 [1] standard protocol. The focus is on duty-cycled MAC as outlined in the standard. Opposed to Chapter 3 where adaptive rate and overhearing are exploited, Cooperative Automatic Repeat reQuest (C-ARQ) is tailored for duty-cycled networks and used to combat shadow fading in a direct link. In order to quantify the energy efficiency, we use a metric based on the average number of packet transmissions in a realistic wireless channel. Shadowing and multipath fading effects are considered. Next, the improvements in energy efficiency of the standard schemes using C-ARQ techniques are presented. The analytical results are validated in Matlab simulations.

4.1 Introduction

We consider C-ARQ to examine whether it can improve the energy efficiency and reliability of low-power devices. Traditional C-ARQ schemes consist in the following: due to broadcast nature of the wireless channel, in case of erroneous packet reception, a retransmission may be requested not only from the source, but also from the neighbour devices, denoted relays, which

overheard the original transmission and may experience better channel conditions to the destination than the source. The concept was presented in [3] for the single-relay case, where the effects of the wireless fading channel were modelled as a two-state Markovian process, which allowed to determine under what conditions cooperation can be beneficial. In order to extend the scheme to networks with more than one relay, two MAC protocols were proposed in [4] and [5]. In these works, the benefits of cooperation come from the adaptive data rates in the relay-to-destination channel. Namely, the spatial proximity of the relays to the destination and the related more favourable channel is used to transmit at higher data rates than the one applied in the original source-to-destination channel. The adaptive transmission rates rely on the PHY layer specification of IEEE 802.11 Standard [6]. Both CoopMAC and rDCF are proactive protocols and always exploit cooperation as a means of communication. A reactive cooperative protocol was proposed in [7], where the C-ARQ scheme that regulates channel access of the relays is activated only when a transmission fails. Therefore, the overhead associated to cooperation is only spent when really needed. None of these works about cooperation at the MAC layer studies the energy efficiency of the proposed cooperative schemes, but rather focus on improving the throughput and lowering the delay. We have analysed the energy efficiency of the protocol presented in [7] in Chapter 3. The performance analysis performed in that Chapter focuses mainly on large data payloads and the downlink from a remote network coordinator to a device. Therefore, this analysis is suitable for the Internet data traffic or multimedia streaming, but inappropriate for low-power M2M networks.

The suitability of executing C-ARQ schemes in low-power networks without data rate adaptation remains an open issue that has recently started to receive attention. A cooperation protocol for low-power networks was presented in [8]. It is based on preamble sampling algorithms used in low-traffic networks where devices duty-cycle, i.e., are put to sleep and woken up occasionally, in order to detect the activity in the channel. The key idea of preamble sampling is that every packet is preceded with a preamble long enough to be detected by all the devices in the communication range during a complete duty-cycle. The cooperative protocol presented in [8] uses the preamble sampling concept to wake up the potential relays. The performance was evaluated by computer simulation in Rayleigh fading channels. The performance metrics used were the consumed energy per packet and the data delivery ratio. Although results show that cooperation improves the reliability significantly, the consumed energy of the proposed algorithm is either close to the reference non-cooperative protocol, or even higher. This solution thus trades energy for reliability, which is not the optimal strategy for battery-operated devices.

4.1.1 Contribution

It is worth emphasising that while the energy efficiency was not the major concern when C-ARQ schemes were first proposed, it becomes the essential performance metric in low-power

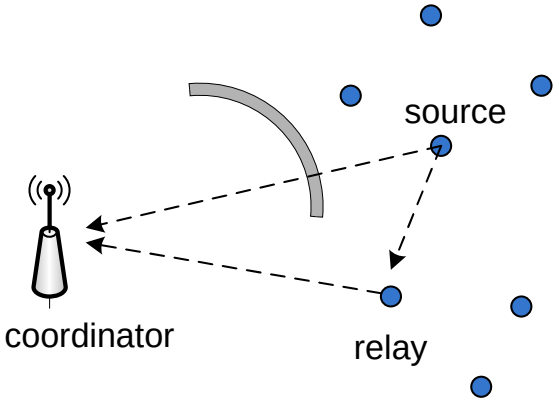

Figure 4.1: The studied scenario consisting of a coordinator, devices and moving obstacles

networks and, therefore, the benefits of C-ARQ schemes need to be re-examined. For example, considering the energy consumption associated to **overhearing** presents an additional cost that was irrelevant before, but has a key role in low-power networks. In this chapter we show that C-ARQ schemes can improve the energy efficiency in harsh shadowing environments even when a constant rate transmission is applied. We consider the widely spread IEEE 802.15.4 standard [1] for the **star topology** as a study case. This standard does not include data rate adaptation, but it defines a constant data rate of 250 Kbps for the 2.4 GHz band. In addition, the maximum size of data packets is defined to be of 127 bytes, i.e., significantly smaller than in Wireless Local Area Networks (WLANs) where C-ARQ schemes have been typically studied and whose maximum data packet size is 2312 bytes.

The contributions of this chapter present an initial study to test the applicability of C-ARQ in duty-cycled, low-power networks. The conditions under which a C-ARQ scheme proves beneficial in low-power networks without data rate adaptation in realistic wireless channel have been examined. To this end, we analyse the energy efficiency and reliability of a C-ARQ scheme suitable for low-power networks. We carefully consider the cost of overhearing at a relay device to model the energy consumption reliably.

The rest of the chapter is organized as follows: Section 4.2 introduces the system model including the scenario and the adopted channel model. The analysis of the energy efficiency is given in Section 4.3, including the analysis of the parameters needed to calculate the energy efficiency. Model parameters are validated in Section 4.4. The performance evaluation is presented in Section 4.5 and, finally, the chapter is concluded in Section 4.6.

4.2 System Model

4.2.1 Scenario

We consider the uplink transmission from a group of n devices to a single common coordinator, e.g. Access Point, Gateway, or Base Station. The scenario is shown in Figure 4.1. A sub-group of the n devices is currently shadowed by a large moving obstacle, while the rest of devices have a line-of-sight (LOS) path with the coordinator. Due to the blocking obstacle, the probability that all the transmissions from the shadowed devices to the coordinator fail is very high. We assume that an alternative path exists through a device acting as relay, which experiences more favourable channel conditions. This is a two-hop path expanding from the source to the relay and from the relay to the coordinator, which enables the execution of cooperative strategies.

We consider the beacon-enabled access mode described in [1] and summarised in Section 2.2.1 of this thesis. The coordinator is not energy-constrained and thus can listen to the channel constantly and periodically transmits a beacon. The devices are energy-constrained and remain in the sleep state unless they have data to transmit to the coordinator. Whenever a device has data to transmit, it executes a random backoff before waking up to perform Clear Channel Assessment (CCA), i.e., to assess whether the channel is idle or busy. A transmission is started if the channel is found idle. Otherwise, a new backoff is executed. In addition, all the devices need to periodically wake up in order to synchronize to the beacons. Therefore, it is essential that all the devices listen to the beacon even under unfavourable channel conditions. The devices typically set the transmission power to $P_t = 0\ dBm$ for data transmissions in order to save energy. The maximum power depends on the local regulation but it is generally limited to $10\ dBm$ [1]. Since the coordinator is not battery-powered we assume that the beacon is always transmitted at the maximum allowed power. The obstacle between the devices and the coordinator introduces additional partition loss. The loss varies depending on the type of material, e.g. a large obstacle like a concrete wall attenuates the signal by 13 dB [9]. Taking into account the additional power budget of the beacon and the fact that its length is smaller than the data packet length, we can safely assume that the beacon is received by all the devices and can thus be used to coordinate the cooperation process, as described in the next section.

4.2.2 Retransmission Strategies

In the case of transmission error, the coordinator can decide whether to adopt a non-cooperative retransmission scheme or to initiate a cooperation phase.

In the case of executing a non-cooperative retransmission scheme, the coordinator can request retransmission from the source. In order to save energy, the maximum number of transmission attempts denoted N_{max} is limited (e.g. [1] recommends maximum of 4 transmission attempts).

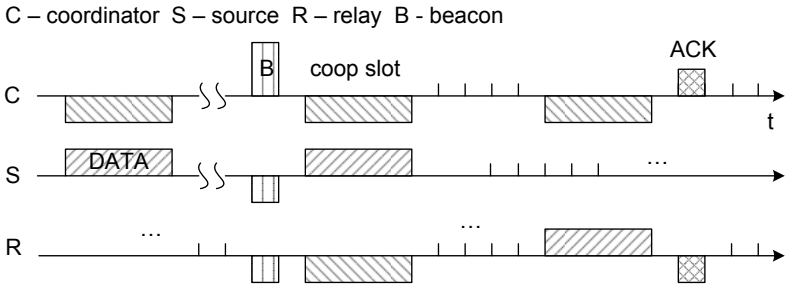

Figure 4.2: Cooperation diagram; packet is depicted above the time line when it is being transmitted, below the time line when it is being received

In the case that the coordinator opts for a cooperative retransmission scheme, then the cooperation algorithm works as follows. The cooperative process is depicted in Figure 4.2. The source transmits a packet that is received by the coordinator with unrecoverable errors. The coordinator then reserves a cooperation slot for a source-relay pair and announces it in the next beacon, thus initiating a cooperation phase. The cooperation slot is similar to the Guaranteed Time Slot (GTS) considered in IEEE 802.15.4 standard [1]. Since all devices listen to the beacon, the device acting as relay knows when it needs to wake up in order to receive the retransmitted packet from the source. The packet is then retransmitted in the cooperation slot by the source. The subsequent retransmissions continue from the relay up to the maximum number of allowed transmission attempts N_{max}. The system is considered to be in outage if the packet is still not successfully delivered after N_{max} number of attempts, in which case it will be discarded.

Two different cooperative strategies are considered:

1. Cooperation with relay selection, where the coordinator indicates in the beacon the selected relay candidate. This decision can be based on locally available Channel State Information (CSI) regarding all or some of the devices.

2. Cooperation without relay selection, where a relay with unknown shadowing state is chosen randomly by the coordinator.

4.2.3 Channel Model

We consider a realistic wireless channel model where a signal from the transmitter to the receiver experiences three effects: pathloss, shadowing, and multipath fading. Considering the effects of pathloss, the average received power is

$$P_r(dBm) = P_t - PL(d_0) - 10\alpha \log_{10} d, \tag{4.1}$$

where P_t is the transmission power, $PL(d_0)$ is the pathloss at reference distance d_0, α is the pathloss exponent and d is the distance from the transmitter.

We define μ as the mean Signal-to-Noise Ratio (SNR) at the receiver without considering shadowing or multipath fading effects, and it can be expressed as

$$\mu(dB) = P_r - P_n. \tag{4.2}$$

P_n is the average receiver thermal noise and it can be computed as [10]

$$P_n = (F + 1)kTB, \tag{4.3}$$

where F is the noise figure, k is Boltzmann constant, T is the temperature in Kelvin, and B is the signal bandwidth.

Apart from pathloss, the signal at the receiver experiences shadowing and multipath fading effects. The instantaneous SNR is denoted γ. We model the multipath effects of the wireless channel as a Rayleigh block fading process. Precisely, this multipath fading channel model is known as the frequency-flat block-fading Rayleigh channel. The transmission time of a packet is shorter than the inverse of the fading bandwidth. The fading state therefore remains constant for the duration of the transmission of an entire data packet but changes for each retransmission. The average value of γ, denoted $\overline{\gamma}$, represents the average SNR considering the effects of shadowing. We assume that the value of $\overline{\gamma}$ remains constant at least during the period of time between two beacons and, therefore, all the packet retransmissions from the same source experience the same shadowing state. Therefore, the probability density function (*pdf*) of γ has an exponential distribution (derived from the Rayleigh distribution of the amplitude) conditioned on $\overline{\gamma}$, i.e.,

$$p_\gamma(\gamma|\overline{\gamma}) = \frac{1}{\overline{\gamma}} e^{-\frac{\gamma}{\overline{\gamma}}}. \tag{4.4}$$

In its turn, the *pdf* of $\overline{\gamma}$ is lognormally distributed conditioned on μ and with standard deviation σ, both expressed in dBs, and can thus be expressed as

$$p_{\overline{\gamma}}(\overline{\gamma}|\mu) = \frac{10}{\ln 10\sqrt{2\pi}\sigma\overline{\gamma}} \exp\left[-\frac{(10\log_{10}\overline{\gamma} - \mu)^2}{2\sigma^2}\right]. \tag{4.5}$$

Figure 4.3 is generated by simulating the described channel and shows different channel realisations in time for each channel usage. Mean SNR is normalised to the value of μ. Because the values are in dB scale, shadowing state $\overline{\gamma}$ is normally distributed around the mean μ (normal distribution becomes lognormal on a linear scale). Rayleigh multipath fading γ is superimposed on the random value of $\overline{\gamma}$. Note that when a packet error occurs, shadowing state remains the same for all subsequent retransmission attempts. Multipath fading is constant for the duration of a packet.

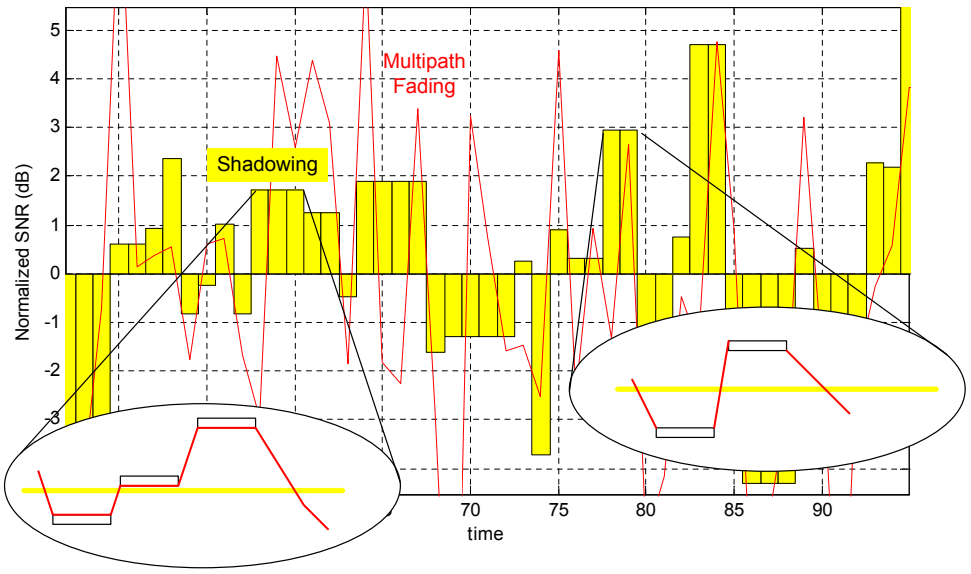

Figure 4.3: Shadowing state $\overline{\gamma}$ for each packet transmission with superimposed multipath fading γ

4.2.4 Modulation and Coding

The PHY of IEEE 802.15.4 is adopted in this study without modifications. Bit and packet error rates at the receiver can be computed as follows. Offset Quadrature Phase Shift Keying (O-QPSK) modulation is considered, as specified in IEEE 802.15.4 in the 2.4 GHz band [1]. If we assume perfect demodulation with coherent detection in the presence of Additive White Gaussian Noise (AWGN), O-QPSK has the same bit error rate as the Quadrature Phase Shift Keying (QPSK), and the bit error probability is expressed as [11]

$$P_b = Q(\sqrt{2\gamma}), \tag{4.6}$$

where Q function is defined as

$$Q(x) = 1 - Q(-x) = \frac{1}{\sqrt{2\pi}} \int_x^\infty e^{-y^2/2} dy. \tag{4.7}$$

The packet error rate assuming independent bit errors (which holds true for block fading channels and AWGN) is

$$P_p = 1 - (1 - P_b)^L, \tag{4.8}$$

where L is the packet length in bits. In the standard [1], Direct Sequence Spread Spectrum (DSSS) is used to combat interference in the license-free 2.4 GHz band. Each data symbol consisting of four bits is mapped into a 32-chip sequence and then sent over the wireless channel. To relate mean SNR μ and Energy-per-bit vs. Noise power spectral density $\frac{E_b}{N_0}$ we use the expression

$$\frac{E_b}{N_0} = \mu \frac{B_N}{R_b}, \tag{4.9}$$

where B_N is the noise bandwidth and R_b is the data bit rate, therefore $\frac{B_N}{R_b}$ characterizes the DSSS gain.

4.2.5 Energy Model

It is assumed that each device has three operating modes:

1. Transmitting, with associated power consumption P_{tx}.
2. Receiving, with associated power consumption P_{rx}.
3. Sleep, i.e., with the radio switched-off and associated power consumption $P_s \approx 0$.

We assume that $P_{tx} \approx P_{rx}$. This means that the energy spent for packet transmission is approximately the same as the energy spent for the reception. The focus is on the energy spent by the devices, because the coordinator is mains-powered. We consider the two following models:

- In the non-cooperative scheme, all the other devices of the network are in sleep mode when a device is transmitting to the coordinator.
- In the cooperative schemes, just one relay is woken up for the cooperation phase, while the others remain in sleep state.

4.3 Energy Efficiency Analysis

4.3.1 Definitions

The energy efficiency of the scheme is defined as the ratio of the total number of successfully received bits to the total energy spent by all the devices (excluding the coordinator) in delivering them. The coordinator is excluded because it is not battery powered and therefore its energy consumption is not critical. The energy efficiency λ was already defined in Chapter 3. We repeat the definition here

$$\lambda = \frac{total\ amount\ of\ delivered\ data\ (bits)}{total\ energy\ consumed\ (Joule)}. \tag{4.10}$$

In the non-cooperative case, the energy efficiency can be expressed as

$$\lambda_{NC} = \frac{(1 - p_{out})L}{\overline{\overline{N}}_{tx} P_{tx} \frac{L}{R_b}}, \tag{4.11}$$

where p_{out} is the outage probability, defined as the probability that a packet was not successfully delivered after reaching the maximum number of transmission attempts, $\overline{\overline{N}}_{tx}$ is the average number of transmissions per packet, averaged over multipath fading and shadowing, and R_b is the data transmission bit rate. Note that the energy is spent only by the source device to transmit the packet because the other devices are sleeping. Since the energy spent at the coordinator is not considered, this expression does not include the energy spent for the packet reception.

The expression for the energy efficiency of the cooperative scheme incorporates the energy cost associated to the active relay to receive the retransmitted packet from the source device. Therefore, the energy efficiency can be defined as

$$\lambda_C = \frac{(1 - p^c_{out})L}{\overline{\overline{N}}^c_{tx} P_{tx} \frac{L}{R_b} + P_p P_{rx} \frac{L}{R_b}}, \tag{4.12}$$

where p^c_{out} is the outage probability of the cooperative scheme, defined as the event that a packet cannot be successfully delivered to the coordinator after reaching the maximum number of transmission attempts from source and/or relay, and $\overline{\overline{N}}^c_{tx}$ is the average number of transmissions in the cooperation process including the original transmission, first retransmission from the source in case of error, and subsequent retransmissions from the relay. Since cooperation is initiated only when the original packet transmission results in error, the energy cost of packet reception by the relay is proportional to the packet error probability P_p. Finally, to get the total amount of delivered data in λ, average number of cooperation slots relative to the total number of packets is included.

Recall that since we consider a constant transmission rate without data rate adaptation, it is expected that the benefits of cooperation come from overcoming bad channel conditions, i.e. substituting a blocked path by a two-hop line-of-sight communication path, and thus reduce the number of required retransmissions. In the non-cooperative scheme when the ordinary ARQ is applied, all the retransmissions during the unfavourable shadowing state will fail until the outage limit is reached and the packet is discarded. In the cooperative scheme, the retransmissions from relay have better chances of success due to the independent channel conditions. Thus the data reliability of the system can be improved. Therefore we expect $p_{out} > p^c_{out}$ and $\overline{\overline{N}}_{tx} > \overline{\overline{N}}^c_{tx}$. These are the cooperation benefits. However, the cooperation cost represented by the energy consumed by the relay when receiving the packet requires the careful evaluation and comparison of λ_{NC} and λ_C.

From the parameters in Eq. (4.11), the average number of transmissions per packet $\overline{\overline{N}}_{tx}$ and the outage probability p_{out} are the only parameters that depend on the wireless channel. In the next sections, we compute the values of $\overline{\overline{N}}_{tx}$ and p_{out}, in order to obtain the value of the energy

efficiency. For the cooperative case, the values of $\overline{\overline{N}}_{tx}^{c}$ and p_{out}^{c} are evaluated by simulation, due to analytical complexity.

4.3.2 Average Number of Transmissions per Packet in Rayleigh Fading Environments

The average number of transmissions per packet required for successful delivery, for a fixed shadowing state, can be expressed as

$$\overline{N}_{tx}^{inf}(\overline{\gamma}) = \sum_{n=1}^{\infty} n \cdot P_p(\overline{\gamma})^{n-1} \cdot (1 - P_p(\overline{\gamma})) = \frac{1}{1 - P_p(\overline{\gamma})}, \tag{4.13}$$

where $\overline{\gamma}$ remains constant for all the retransmissions of a given packet. This expression is valid for infinite number of retransmissions until success. Therefore, when applied to the studied case where the upper limit on the number of attempts is imposed, Eq. (4.13) represents an approximation. However, as it will be shown briefly, this approximation is valid within certain limits.

In order to compute the packet error probability in block fading environment $P_p(\overline{\gamma})$, we start with the bit error probability given in Eq. (4.6) for QPSK modulation. Next, Eq. (4.8) is averaged over the fading distribution, and thus

$$1 - P_p(\overline{\gamma}) = \int_0^{\infty} (1 - Q(\sqrt{2\gamma}))^L p_\gamma(\gamma|\overline{\gamma}) d\gamma. \tag{4.14}$$

Using the binomial formula Eq. (4.14) can be rewritten as

$$1 - P_p(\overline{\gamma}) = \int_0^{\infty} \sum_{m=0}^{L} \binom{L}{m} (-1)^m \cdot Q^m(\sqrt{2\gamma}) p_\gamma(\gamma|\overline{\gamma}) d\gamma. \tag{4.15}$$

Now we exchange the order of summation and integration and use the exponential *pdf* given in Eq. (4.4) in place of a generic one

$$1 - P_p(\overline{\gamma}) = \sum_{m=0}^{L} \binom{L}{m} (-1)^m \cdot \mathcal{I}(m), \tag{4.16}$$

with

$$\mathcal{I}(m) = \frac{1}{\overline{\gamma}} \int_0^{\infty} Q^m(\sqrt{2\gamma}) e^{-\frac{\gamma}{\overline{\gamma}}} d\gamma. \tag{4.17}$$

Although the problem was formulated in the seventies [12], the closed-form solution for the

integral in Eq. (4.17) has been found quite recently in [13] and it states

$$\mathcal{I}(m) = \left(\frac{1}{2}\right)^m - \left(\frac{1}{2}\right)^m m\sqrt{\frac{2\overline{\gamma}}{2\overline{\gamma}+2}} - \left(\frac{1}{2}\right)^m \frac{m}{\sqrt{2\pi}} \times \sum_{n=1}^{m-1} \Gamma(\frac{n}{2}+\frac{1}{2})\binom{m-1}{n}(-1)^n \left(\frac{2}{\sqrt{2\pi}}\right)^n \times \left(\frac{4\overline{\gamma}}{(n+1)2\overline{\gamma}+2}\right)^{\frac{n+1}{2}} \times F_A^{(n)}\left(\frac{n}{2}+\frac{1}{2}, \underbrace{1,\ldots,1}_{n \text{ terms}}; \underbrace{\frac{3}{2},\ldots,\frac{3}{2}}_{n \text{ terms}}; \underbrace{\frac{2\overline{\gamma}}{(n+1)2\overline{\gamma}+2},\ldots,\frac{2\overline{\gamma}}{(n+1)2\overline{\gamma}+2}}_{n \text{ terms}}\right), \quad (4.18)$$

where $\Gamma(n)$ is the (complete) Gamma-function and $F_A^{(n)}$ is the A type Lauricella hypergeometric function of n variables.

4.3.3 Outage Probability in Shadowing Environments

Recall that the outage is defined as the event when the maximum number of transmission attempts N_{max} is reached and a given packet is still not successfully delivered and is therefore discarded. The average number of transmissions $\overline{N}_{tx}$ given in (4.13) can be viewed as the average number of errors $\overline{N}_{err}$, followed by the last successful transmission. From (4.13) we have

$$\overline{N}_{tx} = 1 + \overline{N}_{err} = 1 + \frac{P_p(\overline{\gamma})}{1 - P_p(\overline{\gamma})}. \quad (4.19)$$

The average number of errors is the function of $\overline{\gamma}$ and in the outage event it is greater or equal to the maximum number of transmissions $\overline{N}_{err} = \frac{P_p(\overline{\gamma})}{1-P_p(\overline{\gamma})} = f(\overline{\gamma}) \geq N_{max}$. Therefore, to find the threshold $\overline{\gamma}_{th}$ for which the outage occurs, we need the value of the inverse function of the average number of errors at $\overline{N}_{err} = N_{max}$, which is $\overline{\gamma}_{th} = f^{-1}(N_{max})$. Any value of $\overline{\gamma}$ realisation that satisfies $\overline{\gamma} \leq \overline{\gamma}_{th}$ causes the outage for the given packet. The value $\overline{\gamma}_{th}$ is obtained numerically from the inverse function. Then the outage probability can be computed as [14]

$$p_{out} = \int_0^{\overline{\gamma}_{th}} p_{\overline{\gamma}}(\overline{\gamma}|\mu)d\overline{\gamma} = Q\left(\frac{\mu - 10log_{10}(\overline{\gamma}_{th}(N_{max}))}{\sigma}\right), \quad (4.20)$$

where $p_{\overline{\gamma}}(\overline{\gamma}|\mu)$ is the lognormal distribution as given in Eq. (4.5).

The average number of transmissions per packet for a fixed shadowing state and with the outage probability given in (4.20) is thus

$$\overline{N}_{tx}(\overline{\gamma}) = \begin{cases} \frac{1}{\frac{1}{\overline{\gamma}}\int_0^{\infty}(1-Q(\sqrt{2\gamma}))^L e^{-\frac{\gamma}{\overline{\gamma}}}d\gamma}, & \overline{\gamma} > \overline{\gamma}_{th} \\ N_{max}, & 0 < \overline{\gamma} \leq \overline{\gamma}_{th}. \end{cases} \quad (4.21)$$

where the upper limit on the number of transmissions is imposed for the values of $\overline{\gamma}$ that fall within the outage constraint. For $\gamma > \overline{\gamma}_{th}$, the adopted approximation in Eq. (4.13) is valid.

Finally, the average number of transmissions over all shadowing states needed to calculate the energy efficiency of the non-cooperative scheme in Eq. (4.11) is obtained by averaging Eq. (4.21) over the lognormal distribution

$$\begin{aligned} \overline{\overline{N}}_{tx}(\mu) &= \int_0^{\infty} \overline{N}_{tx}(\overline{\gamma}) p_{\overline{\gamma}}(\overline{\gamma}|\mu) d\overline{\gamma} \qquad (4.22) \\ &= \int_0^{\overline{\gamma}_{th}} N_{max} \cdot p_{\overline{\gamma}}(\overline{\gamma}|\mu) d\overline{\gamma} + \int_{\overline{\gamma}_{th}}^{\infty} \frac{1}{\frac{1}{\overline{\gamma}} \int_0^{\infty} (1 - Q(\sqrt{2\gamma}))^L e^{-\frac{\gamma}{\overline{\gamma}}} d\gamma} \cdot p_{\overline{\gamma}}(\overline{\gamma}|\mu) d\overline{\gamma} \\ &= N_{max} \cdot p_{out} + \int_{\overline{\gamma}_{th}}^{\infty} \frac{1}{\frac{1}{\overline{\gamma}} \int_0^{\infty} (1 - Q(\sqrt{2\gamma}))^L e^{-\frac{\gamma}{\overline{\gamma}}} d\gamma} \cdot p_{\overline{\gamma}}(\overline{\gamma}|\mu) d\overline{\gamma} \end{aligned}$$

Recall that Eq. (4.22) represents the average number of transmissions per packet in shadowing environments when the upper limit on the maximum number of attempts is imposed. This upper limit causes packet loss that is characterised with the outage probability, calculated as per Eq. (4.20). Because of the analytical complexity, the integral in Eq. (4.22) is solved numerically.

4.4 Model Validation

To validate the analytical model for the energy efficiency, the wireless channel outlined in Section 4.2.3 was simulated in Matlab in order to obtain the derived parameters: $\overline{N}_{tx}(\overline{\gamma})$, p_{out} and $\overline{\overline{N}}_{tx}(\mu)$. The energy efficiency of the non-cooperative and cooperative scheme is then calculated and compared.

Figure 4.4 shows a histogram of simulated shadowed values for $\overline{\gamma}$ in comparison with analytical formulation in Eq. (4.5). Two exemplary cases are shown. The arrow in Figure 4.4 indicates a trend of the *pdf* shape as μ increases.

Figure 4.5 validates the analytical derivation of $\overline{N}_{tx}(\overline{\gamma})$ in Eqs. (4.13), (4.14), (4.15), (4.16), (4.17) and (4.18). Because of computing limitations (primarily the calculation of Lauricella hypergeometric function in Eq. (4.18)), unrealistic packet length of $L = 8$ is chosen to validate the results. We see in Figure 4.5 that analytical and numerical calculation of $\overline{N}_{tx}(\overline{\gamma})$ agree.

Figure 4.5 together with Figure 4.4 shows why outage probability has to be invoked. For realistic values of packet length and mean SNR, e.g. $L = 27bytes$ and $\mu \leq 10dB$, when $\overline{\gamma} \to 0$, the product $\overline{N}_{tx}(\overline{\gamma}) p_{\overline{\gamma}}(\overline{\gamma}|\mu)$ is not bounded and is therefore analytically intractable. For this reason we chose to limit $\overline{N}_{tx}(\overline{\gamma})$ for $\overline{\gamma} \to 0$ to N_{max}. This choice is also practical, as most systems impose an upper limit to the allowed number of packet transmission attempts to prevent a waste of system resources in channel outage conditions. For example, $N_{max} = 8$ in IEEE 802.11 and $N_{max} = 4$ in IEEE 802.15.4.

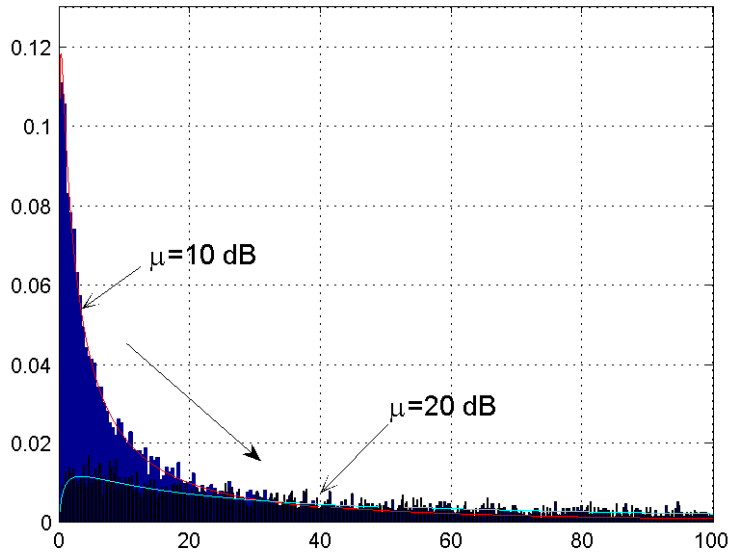

Figure 4.4: Lognormal distribution of $\overline{\gamma}$ conditioned on μ for two different values of μ; histogram of simulated $\overline{\gamma}$ (in blue and black) vs. theoretical *pdf* (in red and cyan)

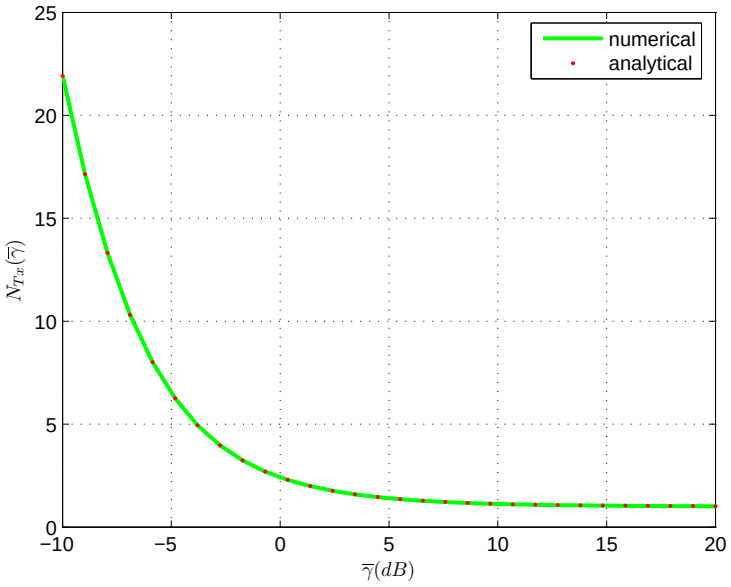

Figure 4.5: Average number of transmissions $\overline{N}_{tx}(\overline{\gamma})$ in Rayleigh block channel when multipath fading is averaged out, conditioned on shadowing state $\overline{\gamma}$; Numerical vs. analytical results

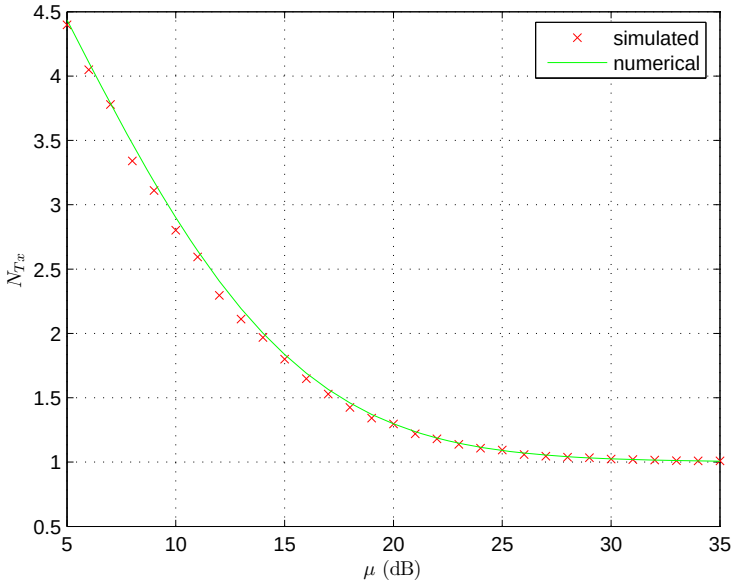

Figure 4.6: Average number of transmissions $\overline{\overline{N}}_{tx}(\mu)$ in shadowing environments, conditioned on mean SNR μ; Simulation vs. numerical results

Finally, Figure 4.6 shows the numerical solution of Eq. (4.22) for $\overline{\overline{N}}_{tx}(\mu)$ compared to simulation results. We see in the figure that the results agree. Therefore, Eq. (4.22) can be used to estimate the energy efficiency of the scheme. Recall that the average number of packet transmissions includes certain outage probability which depends on N_{max}. This outage probability is shown in Figure 4.7. To obtain the results, packet length was set to $L = 27bytes$ and $N_{max} = 8$. Also, observe in Figure 4.6 that the average number of transmissions asymptotically approaches one. This means that there exists mean SNR μ which achieves good performance and higher μ would only increase the cost without any performance gain. When system is designed, this should be taken into account.

4.5 Performance Evaluation

4.5.1 Scenario

Energy efficiency results were obtained numerically and in simulations in Matlab. The transmission power was set to $P_t = 0\ dBm$ and the distance to the coordinator was varied from 10 to 18 m in the steps of 2 m to get the different values of P_r at the receiver. The pathloss at reference distance is $PL(d_0) = 55\ dB$ and the pathloss exponent is set to $\alpha = 4$ as proposed in [10]. As per (4.3), at room temperature of $T = 300K$, adopting the noise figure $F = 7.3dB$ as measured in [15] and knowing that the signal bandwidth is $B = 2MHz$ we get the noise floor of $P_n = -103dBm$. DSSS gain is calculated by knowing that $B_N = B$ and data bit rate

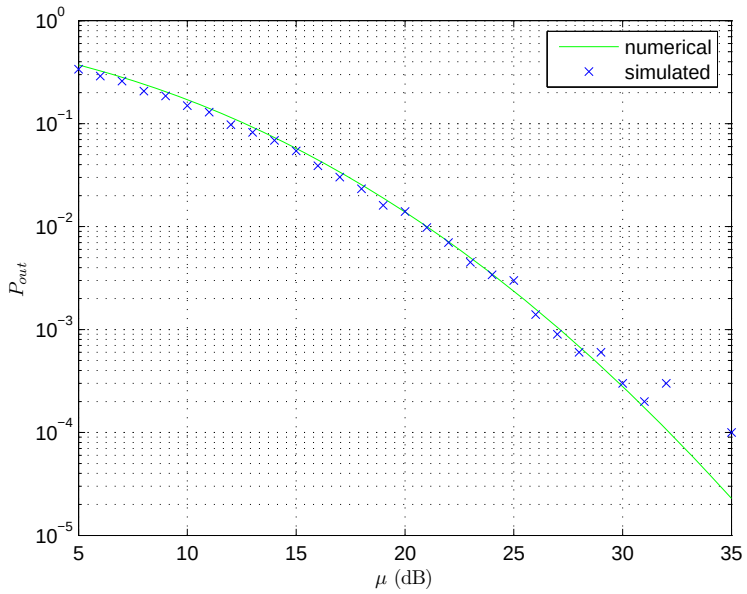

Figure 4.7: Outage probability p_{out} in shadowing environments; $N_{max} = 8$, $L = 27bytes$

$R_b = 250\ kbps$, leading to the relation $E_b/N_0 = 8 \cdot \mu$. The maximum number of transmissions was set to $N_{max} = 4$ and the shadowing standard deviation is $\sigma = 8\ dB$. The power levels for different operating modes P_{tx} and P_{rx} are taken from the CC2430 transceiver data sheet [16] and they are $P_{tx} = 80.7\ mW$ and $P_{rx} = 80.1\ mW$, respectively. The packet length is set to $L = 127bytes$.

For the non-cooperative case, a new realization of a log-normally distributed shadowed mean is generated for each new packet, while it remains constant for all the packet retransmissions. The signal amplitude of the packet was multiplied by the Rayleigh distributed variable and the AWGN was added. Finally, the errors at reception were counted as well as the number of discarded packets when the number of errors reaches N_{max} in order to estimate the outage probability.

The cooperative algorithm operates as follows. Since we can calculate the threshold $\overline{\gamma}_{th}$, after the first failed transmission the coordinator requests cooperation if the channel to the source is estimated to be in outage. In the next attempt, the packet is retransmitted by the source to be obtained by the relay, while the coordinator again tries to decode the packet. The repeated failure at the coordinator reinforces the assumption of the severely shadowed source-to-destination channel meaning that the failure is not due to the temporary multipath fading effect. The following retransmissions proceed from the relay. The relay is located at the same distance to the coordinator as the source resulting in the same μ, but with different shadowing state $\overline{\gamma}$. If the relay selection is applied, the favourable relay candidate is indicated whose current shadowing state satisfies $\overline{\gamma} > \mu$ and therefore has greater chances of success. To ensure fairness when comparing the cooperative and non-cooperative scheme, the total number of attempts from the

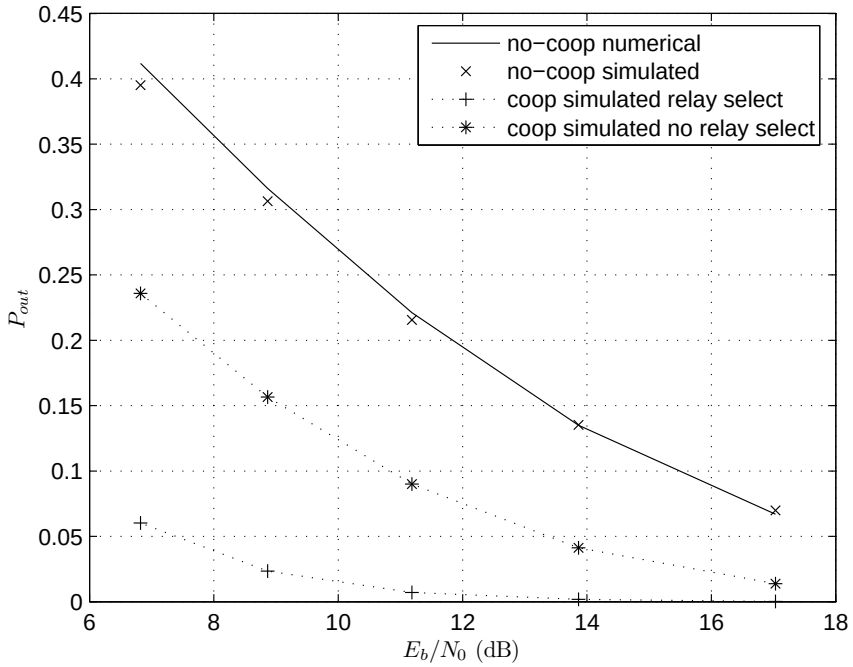

Figure 4.8: Outage probability of cooperative and non-cooperative scheme.

source and the relay together is limited to maximum N_{max} transmissions, the same as in the non-cooperative case. Finally, $\overline{\overline{N}}_{tx}^{c}$ is estimated, as well as the outage probability following from the number of discarded packets.

4.5.2 Results

The resulting outage probability is shown in Figure 4.8. We see that the reliability is significantly improved when using the cooperative scheme, especially with the relay selection. For the lower values of E_b/N_0 the outage probability of the non-cooperative scheme is not acceptable, while the cooperative scheme provides quite reliable data transmissions. Based on our evaluation, even if the cooperation has the additional energy cost consumed at the relay when receiving the packet, the benefits outweigh the cost and the energy efficiency results to be better for all the tested values of E_b/N_0 as shown in Figure 4.9. This is due to the fact that the cooperation is initiated only in unfavourable channel conditions. However, we may note that as the E_b/N_0 improves, the energy efficiency of cooperation approaches the non-cooperative case indicating that the cooperation should be used only when needed, i.e. when the probability of channel being in outage is high.

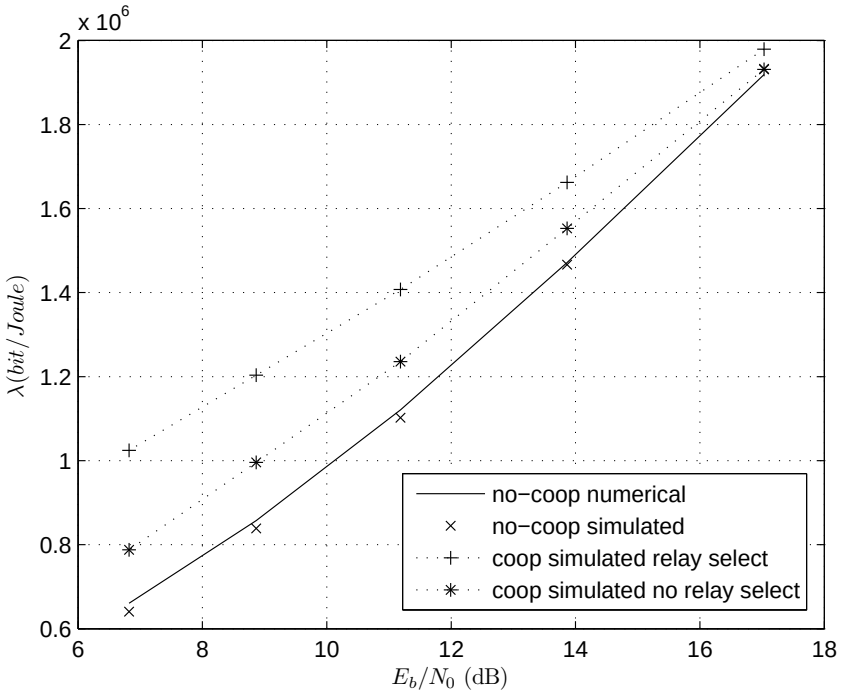

Figure 4.9: Energy efficiency of cooperative and non-cooperative scheme.

4.6 Chapter Summary and Conclusions

A notable improvement of energy efficiency and reliability can be attained in short-range low-power and constant bit-rate networks by executing a C-ARQ scheme at the MAC layer. Precisely, an improvement of up to 20% (without relay select) or 40% (with relay select) in terms of energy efficiency and 15% (without relay select) or 35% (with relay select) in terms of reliability has been demonstrated. The active relays can be woken up only when needed and thus the energy for overhearing is consumed only when the current channel realization between a source and the destination is unfavourable and likely to be in outage. The results presented in this chapter show that cooperation is especially suitable for networks with hard reliability constraints since it can significantly reduce the outage probability. C-ARQ enables communication between two remote devices in conditions when traditional non-cooperative schemes cannot operate. Therefore, C-ARQ can combat shadow fading with the cost of having a two-hop communication model instead of a single-hop communication.

A limitation of the scheme presented in this chapter is the communication range. Star topology in low-power networks limits the range to 10-20 meters, depending on the environment. There are many scenarios that require higher communication range, achieved with multi-hop communication in low-power networks. We therefore consider multi-hop communication in the next chapter. Since IEEE 802.15.4 does not specify a functional duty-cycled multi-hop MAC scheme, we turn to MAC amendments in IEEE 802.15.4e.

Bibliography

[1] *IEEE Standard 802.15.4-2011: Wireless Medium Access Control (MAC) and Physical Layer (PHY) Specifications for Low-Rate Wireless Personal Area Networks (WPANs)*, IEEE Std., September 2011.

[2] *IEEE Standard 802.15.4e-2012: Low-Rate Wireless Personal Area Networks (LR-WPANs) Amendment 1: MAC sublayer*, IEEE Std., April 2012.

[3] M. Dianati, X. Ling, K. Naik, and X. Shen, "A node-cooperative ARQ scheme for wireless ad hoc networks," *IEEE Transactions on Vehicular Technology*, vol. 55, no. 3, pp. 1032 –1044, May 2006.

[4] P. Liu, Z. Tao, and S. Panwar, "A cooperative MAC protocol for wireless local area networks," in *IEEE International Conference on Communications, (ICC)*, vol. 5, May 2005, pp. 2962 – 2968.

[5] H. Zhu and G. Cao, "rDCF: A Relay-Enabled Medium Access Control protocol for wireless ad hoc networks," *IEEE Transactions on Mobile Computing*, vol. 5, no. 9, pp. 1201 –1214, Sept. 2006.

[6] *IEEE Standard 802.11-2012: Wireless Medium Access Control (MAC) and Physical Layer (PHY) Specifications for Wireless Local Area Networks (WLANs)*, IEEE Std., March 2012.

[7] J. Alonso-Zarate, L. Alonso, and C. Verikoukis, "Performance Analysis of a Persistent Relay Carrier Sensing Multiple Access Protocol," *IEEE Transactions on Wireless Communications*, vol. 8, no. 12, pp. 5827–5831, December 2009.

[8] A. Ben Nacef, S.-M. Senouci, Y. Ghamri-Doudane, and A.-L. Beylot, "A Cooperative Low Power MAC Protocol for Wireless Sensor Networks," in *IEEE International Conference on Communications (ICC)*, June 2011, pp. 1 –6.

[9] A. Goldsmith, *Wireless Communications*, 1st ed. Cambridge University Press, 2005.

[10] M. Zuniga and B. Krishnamachari, "Analyzing the transitional region in low power wireless links," in *IEEE Communications Society Conference on Sensor and Ad Hoc Communications and Networks SECON*, October 2004, pp. 517–526.

[11] M. K. Simon and M.-S. Alouini, *Digital Communication over Fading Channels*, 2nd ed. Wiley, 2005.

[12] R. Eaves and A. Levesque, "Probability of block error for very slow rayleigh fading in gaussian noise," *IEEE Transactions on Communications*, vol. 25, no. 3, pp. 368 – 374, March 1977.

[13] R. Radaydeh and M. Matalgah, "Results for Infinite Integrals Involving Higher-Order Powers of the Gaussian Q-Function with Application to Average SEP Analysis of DE-QPSK," *IEEE Transactions on Wireless Communications*, vol. 7, no. 3, pp. 793 –798, March 2008.

[14] P. Mary, M. Dohler, J.-M. Gorce, G. Villemaud, and M. Arndt, "M-ary symbol error outage over Nakagami-m fading channels in shadowing environments," *IEEE Transactions on Communications*, vol. 57, no. 10, pp. 2876–2879, October 2009.

[15] T.-K. Nguyen, V. Krizhanovskii, J. Lee, S.-K. Han, S.-G. Lee, N.-S. Kim, and C.-S. Pyo, "A Low-Power RF Direct-Conversion Receiver/Transmitter for 2.4-GHz-Band IEEE 802.15.4 Standard in 0.18-micro CMOS Technology," *IEEE Transactions on Microwave Theory and Techniques*, vol. 54, no. 12, pp. 4062 –4071, Dec. 2006.

[16] (2011) CC2430 datasheet. [Online]. Available: http://www.ti.com/lit/ds/symlink/cc2430.pdf

Chapter 5

Energy Consumption Optimisation in Low-Power Networks

The focus of this chapter is the optimal configuration of a wireless low-power, short-range, multi-hop, duty-cycled network w.r.t. the minimal energy consumption. This chapter goes one step forward from Chapter 4 by removing the range limitation of star topology. Precisely, the energy consumption of a truncated-ARQ scheme in realistic shadowing environments is examined for the reference IEEE 802.15.4e standard protocol using Time Synchronised Channel Hopping (TSCH) and for its cooperative extension that is presented in the chapter. Opposed to IEEE 802.15.4 studied in Chapter 4, MAC amendments in IEEE 802.15.4e specify a duty-cycled *and* multi-hop MAC scheme. We show how to choose between the direct or multi-hop forwarding, or the cooperative version of the two. We determine the optimal forwarding strategy for both loose and strict reliability requirements. Low-power links are parametrised by the inter-device distance and the corresponding outage probability, for the fixed output transmission power. It is shown that significant amounts of energy can be saved when the most adequate scheme of the three is applied. All analytical results are validated in the network simulator ns-3.

5.1 Introduction

Following years of research and fine-tuning, viable technical solutions for resource-constrained devices in the low energy consumption regime have been devised and the standardised protocol stack has been put forward [1]. The lifetime of wireless M2M devices is measured in years or decades; extreme energy efficiency is thus a must and only achieved through aggressive duty-cycling [2]. A duty-cycled device keeps the radio transceiver in sleep state most of the time, except for the periodic wake-ups used to transmit the collected data. In this way, both overhearing and idle listening are evaded with the goal of conserving energy. The IEEE 802.15.4e standard amendments [3] define the required duty-cycled scheme. With the energy-efficient standardised protocol stack provided in [1], remaining work is to find the adequate device configuration which includes the optimal forwarding strategy, in realistic environments. These issues are addressed in this chapter.

Link (un)reliability is core to our study: it is known that short inter-device distances typically imply more reliable links, whilst reliability decreases with the increase in distance. Therefore, one of the key parameters in our work is the optimal inter-device distance under the typical (low) values of output transmission power. We characterise the resulting link (un)reliability with the link outage probability. Link outages result in discarded packets, therefore, outage probability provides the estimation of link quality. In addition, this approach enables network design under outage constraints specified in advance. The metrics are similar to the ones adopted in Chapter 4, but the results are more oriented towards practical use.

5.1.1 Contribution

In order to formulate the energy consumption model for the link layer of M2M low-power devices, we start by deducing a link metric that considers realistic operating conditions. Physical layer studies (e.g. [4]) typically focus on the physical phenomena of the wireless channel and related effects on the error probability. The channel is thus subject to large-, medium- and/or small-scale fading, the latter two in time being static, block or fast. On the other hand, the studies of upper layers experimentally measure the impact of wireless channel, such that the channel effects are reflected in bursty or independent link behaviour (e.g. [5]). We connect the two approaches into the link layer analytical model, while capitalising on the results and observations of previous works. Indeed, we analyse how wireless channel effects interact with higher layers, link layer in particular, and how this interaction affects the link quality. A metric we adopt in this thesis is dependent on two critical parameters under study: link distance and the related outage probability. This metric is the Average Number of Transmissions per Packet $\overline{N}_{tx}$. By considering outages at the link layer, we provide original approach in the analysis of low-power, unreliable links.

Accurate link characterisation offers insight in how to optimise the overall energy consumption. For example, dynamic forwarding is an effective way of combating link outages through path diversity. Using other available links when primary link is in outage eventually saves energy. Specifically, we focus on the Cooperative Automatic Repeat reQuest (C-ARQ) as a reactive form of dynamic forwarding. Traditionally, C-ARQ relies on overheard packets by the neighbouring devices which then become relays [6]. In a duty-cycled scheme, this is not possible. Therefore, we specifically adapt the C-ARQ technique to the multi-hop duty-cycled scheme without assuming overhearing at the relay and optimise it for the most energy-efficient operating regime. The resulting scheme is denoted Cooperative and Duty-Cycled ARQ (CDC-ARQ). Opposed to C-ARQ studied in Chapter 4, there is no coordinator device to regulate the cooperation process dynamically depending on channel conditions. The main idea of our CDC-ARQ scheme is to introduce path diversity in the scheduling functions. CDC-ARQ does not rely on overhearing, or the presence of coordinator, but rather on the analysis of wireless low power links. We consider realistic wireless channel with shadow fading. In the analysis, we focus on the specifics of low-power M2M networks in order to present customised results that are ready-applicable in practice. Nevertheless, our analytical model supports changes in the modulation or coding scheme, output transmission power, etc. One of the key features of CDC-ARQ technique is that it can be easily fitted into the standard, as no changes must be done to the physical (PHY) nor the Medium Access Control (MAC) layers, but just to the scheduling functions. All references to the standard in this chapter refer to IEEE 802.15.4e [3].

In Chapter 4, the star topology is examined and it is shown that benefits can be obtained by forwarding through a relay after the initial transmission failure. In the present chapter, we move from star to **multi-hop** topologies. We extend the analysis beyond cooperative scenario to offer a comprehensive overview of low-power wireless links. For a given outage probability constraint, we find the most energy-efficient forwarding strategy of the three available choices: direct, multi-hop or CDC-ARQ forwarding. CDC-ARQ for a duty-cycled device alternates between the direct and multi-hop forwarding depending on the channel conditions.

In summary, the main contributions of this chapter are:

1. A link energy consumption model is formulated to reflect the wireless channel effects.
2. Link selection guidelines are provided which strive to minimise the overall energy consumption, for either loose or strict reliability requirements. In particular, the bounds for the efficient direct, multi-hop or CDC-ARQ forwarding are derived and presented.

Finally, the analytical model provided in this chapter is validated in ns-3 network simulator [7]. The simulator is described in Chapter 2 of this thesis. An ns-3 simulation mimics the real world as close as possible, since the implementation closely follows the related standard technology. Therefore, aside from validating our analytical model, we show that the techniques presented here are suitable for real devices and can be easily integrated into IEEE 802.15.4e standard.

The remainder of the chapter is organised as follows: Section 5.2 lists some related works. Section 5.3 presents the system model. Section 5.4 contains the derived analytical energy model. The model validation is presented in Section 5.5 together with the results extended beyond the model in the simulations. Finally, the chapter is concluded in 5.6.

5.2 Related work

The optimal link distance that maximises energy efficiency has been previously investigated in [8] for different node densities and path loss exponents. The results obtained in [8] apply to a circular coverage area without considering the fading effects, which are acknowledged in this work. With the distance fixed, various cooperative schemes have been put forward in the literature in order to improve the reliability without trading it for higher energy consumption. Vardhe *et al.* study cooperation using distributed space time codes in [9], for equidistant relays on a direct path to destination. In [10], the energy efficiency of direct, multi-hop and cooperative transmission schemes is studied for fixed outage probability in order to find the optimal output transmission power; the results however span the range of output power values significantly above the typical setting for the M2M low-power networks. These works apply to non-duty-cycled schemes and thus assume overhearing as the basis for cooperation which makes them unsuitable for duty-cycled systems envisioned in [3].

To overcome the complexity of cooperative scheme implementation at the PHY layer (such as synchronisation issues etc.), cooperation at the link layer presents an alternative in the form of C-ARQ. In a C-ARQ scheme, a device seeks cooperation from neighbours to re-route data packets locally in the case of a temporary wireless channel outage on the primary link. C-ARQ for non-duty-cycled schemes was analytically studied in Chapter 3 of this thesis. Alizai *et al.* take an experimental approach in [11] to show that a re-routing technique decreases the total number of packet (re)transmissions in low-power networks. A detailed energy consumption analysis is still needed to quantify the actual benefits and, therefore, configure the links accordingly. Cooperation at the link layer is simpler to implement in duty-cycled systems compared to the more complex PHY cooperative schemes.

A cost metric similar to ours to characterise the link quality was previously investigated in [12]. However, in [12], infinite packet retransmissions until success were assumed, which results in significant energy cost in outage conditions, thus diverging from the optimal solution. The cost metric in [12] was verified experimentally, while we take an analytical approach that is validated by comprehensive simulations. Authors in [13] study the problem of dynamic data forwarding depending on the link quality from the routing perspective. Based on the results, they conclude that the dynamic forwarding provides highly robust and reliable systems.

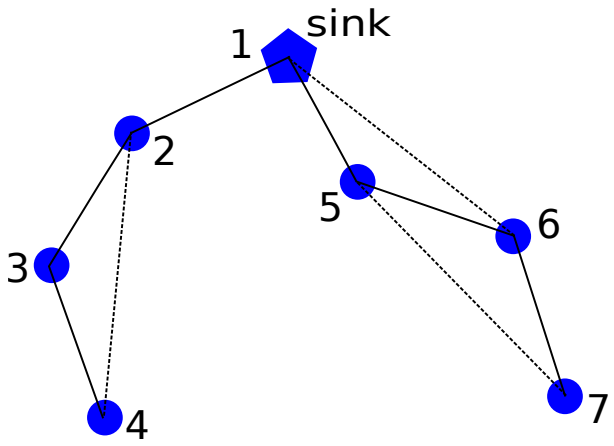

Figure 5.1: M2M device network scenario; solid line stands for a high-quality link, dashed line for a medium-quality link

5.3 System Model

5.3.1 Scenario

An M2M device network is considered, consisting of N devices and a data collector denoted sink. A traffic pattern is convergecast towards the sink and the devices may opt for a direct or a multi-hop transmission to the sink if a direct link cannot be established. The number of hops on a multi-hop path is denoted as k. Any link that can improve progress to the sink by decreasing k is denoted as a direct link. To transmit a packet to the sink, various combinations of links between a pair of devices can be formed, as shown in Figure 5.1. The links represented with solid lines are short-range and in average more reliable than the medium-range links represented with dashed lines. Therefore, we classify a short-range link with small probability of error as a high-quality link, distinguished from a medium-range link with greater probability of error denoted as a medium-quality link. The unreliability that is bound to the medium-range links is the main reason why they are usually discarded, even though they offer better progress to the sink.

5.3.2 Medium Access Control Layer

We consider TSCH mode of the MAC protocol in IEEE 802.15.4e [3], as presented in Chapter 2, Section 2.2.3. It defines a fixed Time Division Multiple Access (TDMA) frame structure that is centrally scheduled. Each *link* formed by a pair of neighbour devices is assigned a unique time slot that repeats in a cyclical manner. The receiver wakes up only in the assigned slot and may enter a sleep state (i.e. switch off its radio transceiver) for the rest of time. After it has woken up, it either receives a packet if the transmitter has one to send, or it goes quickly

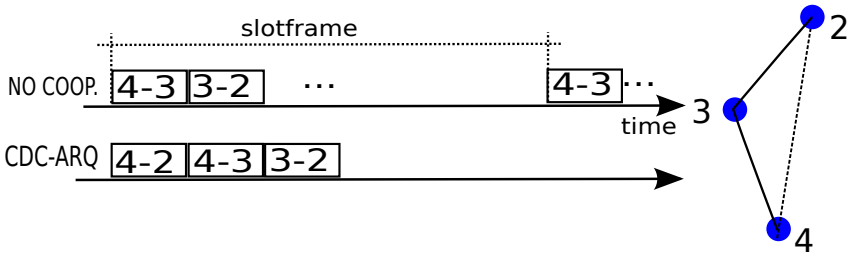

Figure 5.2: TDMA slot scheduling with and without cooperation

back to sleep if a packet preamble is not detected within a short, predefined time interval that is a fraction of the slot duration. The slot without a packet transmission is denoted as the *idle listen* slot. We consider dedicated links that are scheduled for each transmitter-receiver pair to prevent packet collisions.

5.3.3 CDC-ARQ Overview

CDC-ARQ technique enables the efficient use of medium-range links. CDC-ARQ operates as follows: each new transmission is first attempted over the direct, medium-quality link, e.g. over link 4-2 in Figure 5.1. If it fails, the packet is redirected to the multi-hop path that offers higher reliability (4-3-2). Time slots are assigned both for the medium-range, medium-quality links, as well as for the backup multi-hop path that consists of short-range equidistant links, as shown in Figure 5.2. If the initial attempt over medium quality link succeeds, the receivers on backup links only perform idle listen in the fraction of their slots. With CDC-ARQ, two forwarding options cooperate to provide a better service for the current channel realisation. Short-range links are approximated to be equidistant and k times shorter than the direct links. The goal is to find a link distance coupled with the appropriate forwarding scheme that results in minimum energy consumption.

5.3.4 Modulation and Coding

To exemplify the analysis, we focus on the transceiver of the IEEE 802.15.4 radios, working in the 2.4 GHz band, applying Offset Quadrature Phase-Shift Keying (O-QPSK) modulation with additional Direct Sequence Spread Spectrum (DSSS). The resulting bit error rate p_b is given by [14]

$$p_b(\gamma) = \frac{8}{15} \cdot \frac{1}{16} \cdot \sum_{i=2}^{16} -1^i \binom{16}{i} e^{\left(20\gamma\left(\frac{1}{i}-1\right)\right)}, \tag{5.1}$$

where γ is the instantaneous Signal-to-Noise-Ratio (SNR) at the receiver. The packet success probability p_s assuming independent bit errors is

$$p_s(\gamma) = (1 - p_b)^L, \tag{5.2}$$

where L is the packet size in bits. The packet error probability p_e is therefore $p_e = 1 - p_s$. Note that p_s depends on the instantaneous γ characterized by the channel dynamics.

5.3.5 Channel Model

The wireless signal strength decays exponentially with distance as described by the *large scale* pathloss channel model. Superimposed on this deterministic value is the random *medium scale* fading model (also known as *shadowing*) and *small scale* multipath fading, as detailed in Chapter 4. We repeat the most important formulations regarding the wireless channel here. Given the transmission power P_t, the mean power at the receiver P_r is therefore

$$P_r(dBm) = P_t(dBm) - PL(d_0) - 10\alpha \log_{10} d - X_\sigma, \tag{5.3}$$

where $PL(d_0)$ is the pathloss at reference distance d_0, α is the pathloss exponent, d is the link distance from the transmitter and $X_\sigma \sim N(0, \sigma)$ is a normal random variable (on dB scale). On a linear scale, normal distribution becomes lognormal such that X_σ models the random component of a wireless signal. Given the average receiver thermal noise P_n in dBm, the mean SNR at the receiver (when fading effects are averaged out) is $\mu(dB) = P_r - P_n$. Recall that the instantaneous SNR at the receiver that varies in space and time is denoted as γ. For a given μ, the instantaneous γ expressed on a linear scale is lognormally distributed conditioned on μ and with standard deviation σ, both expressed in dBs, the probability density function (pdf) of which is

$$p_\gamma(\gamma|\mu) = \frac{10}{\ln 10\sqrt{2\pi}\sigma\gamma} \exp\left[-\frac{(10\log_{10}\gamma - \mu)^2}{2\sigma^2}\right]. \tag{5.4}$$

We assume that channel hopping in the TSCH scheme alleviates small scale **multipath fading** for packet retransmissions [15]. The shadowing effect resulting from large moving obstacles remains. The channel model considered in Chapter 4 differs from the one adopted in this chapter in that the negative effects of multipath fading are cancelled out because of TSCH. Similar channel model with lognormal shadowing was adopted in [16], but static environment was assumed where γ remains constant for long time intervals.

In dynamic environments, the assumption of γ being constant in time no longer holds. Therefore, temporal channel variations have to be included in the channel model. A comprehensive empirical study of low-power wireless links was presented in [5], whose results are supported and confirmed in survey given in [17]. We take two significant observations from these works:

***Observation 1**: Over short time intervals spanning several hundreds of milliseconds, a link may be either perfect or in outage. Packet successes and errors are temporally correlated.*

In the experiments, Srinivasan *et al.* [5] send packets at the inter-packet interval as short as 10 ms to observe the temporal correlation of successive outcomes on a link. They found that the

outcomes are highly correlated, resulting in consecutive successes followed by consecutive errors. When the inter-packet interval is increased, the number of medium-quality links increases. Medium-quality links are defined in [5] as links with success ratios $0.1 < pdr < 0.9$ (where pdr stands for packet delivery rate). These links switch between perfect and outage states, rather than having a constant γ that corresponds to the fixed success probability $0.1 < p_s < 0.9$. In other words, medium success rate on a link is not the result of a corresponding constant packet success probability $p_s(\gamma)$, but rather the consequence of frequent oscillations between the nearly perfect and outage states that, when averaged, result in a medium-quality link. Channel realisation γ is correlated on time scales of several hundreds milliseconds. This is an important conclusion that should be considered in the packet retransmission process.

Observation 2*: It is possible to distinguish two regions in the surroundings of the transmitting node, denoted connected and transitional region. Links in the connected region are more stable than links in the transitional region.*

The connected region by definition contains mostly high-quality links. The *pdr* of a stable link changes only slowly (if at all) over time. The observation suggests that high-quality links within the connected region tend to be stable. Medium-quality links are found mostly in the transitional region [17] and they are unstable as described in *Observation 1*.

Based on these empirical observations, that are revisited in [17], and essentially adopting a block-fading channel, we make the following assumptions:

- The realization of the channel fading, both comprising small scale fading and shadowing, is drawn from distribution in Eq. (5.4).
- The system is duty-cycled such that for every original packet a new realization of γ according to lognormal distribution is encountered.
- In case of a transmission error, the packet is retransmitted up to N_{max} number of attempts (truncated-ARQ) where each retransmission encounters again the same value of γ on the same link.

The last assumption is based on the fact that packet retransmissions are sufficiently close in time to experience the correlated channel state described in [5]. New packets however are generated at a rate at which channel correlation disappears. Therefore, independent channel realisations are assumed for new packets.

5.3.6 Energy Model

From the exemplary radio transceiver data sheets, e.g. [18], we distinguish two basic radio power modes (voltage $V_{DD} = 3\ V$), with the associated current consumptions:

1. *sleep*, $I_s \approx 0$,
2. *awake* (also, *on*), that further exhibits two sub-modes
   - *active*, either transmitting or actively receiving $I_{tx} \approx I_{rx} = I_a = 20\ mA$,
   - *idle (listen)*, waiting for signal $I_{id} = 2\ mA$.

The same basic energy model was used in Chapter 4, with one refinement added in this chapter. While in the previous chapter there was no distinction between a device in active receiving mode or in idle listen mode (there were both regarded as 'transceiver in receive mode'), here we make this distinction.

We assume that the output transmission power is set to $P_t = 0\ dBm$. The energy is calculated as the product of the power consumption of a mode and the time spent in that power mode (power $P_x = V_{DD} \cdot I_x$, energy $E_x = P_x \cdot T$, where x can stand for sleep s, transmitting tx, actively receiving rx or idle listen id). Power modes change within a slot according to TSCH algorithm. Before a transmission, Clear Channel Assessment (CCA) is performed. There is no random backoff and no contention (recall that slots are dedicated). CCA is introduced for coexistence with other systems (e.g. IEEE 802.11 network) with whom the same physical space is shared. Therefore, a device performing CCA in TSCH mode listens to the wireless channel for a fixed time interval to determine whether it is free. If yes, a packet transmission follows, if not, a transmission is delayed until the next slot. An idle radio power mode is activated when there is no data transmission resulting in the idle listen slot of duration T_{id}, if a device is performing clear channel assessment for the time duration T_{cca} and between the end of data transmission and before the beginning of acknowledgement (ACK) for T_{ad} (ACK delay). Since the energy consumption in the sleep state can be neglected, we do not include it in our model. To calculate the time duration of active power modes, packet lengths (in bits) are divided with the data bit rate, $T_{data} = L/R_b$, $T_{ack} = L_{ack}/R_b$. Finally, we can define three basic energy consumption components associated with the MAC layer described in Section 5.3.2:

$$\begin{aligned} E_{data} &= T_{cca} \cdot P_{id} + T_{data} \cdot (P_{tx} + P_{rx}), \\ E_{ack} &= T_{ad} \cdot P_{id} + T_{ack} \cdot (P_{tx} + P_{rx}), \\ E_{idle} &= T_{id} \cdot P_{id}. \end{aligned} \tag{5.5}$$

Note that the energy components include the energy spent both at a transmitter and a receiver.

5.4 Energy Analysis for Low-power Links

5.4.1 Average Number of Transmissions per Packet

If the upper bound on the allowed number of transmission attempts per packet N_{max} was not set, huge amounts of energy would be wasted in periods of channel outage because the packet would be continuously retransmitted without success until the channel became available again. This is why the truncated-ARQ is applied to discard a packet if it was transmitted N_{max} times and still not successfully delivered. While truncated-ARQ can save significant amounts of energy, it produces a certain packet loss on a link, that can be measured with the outage probability parameter.

Taking the channel model described in Section 5.3.5, the average number of transmissions for one realization of γ is then

$$\begin{aligned} N_{tx}(\gamma) = 1 \cdot (1 - p_e(\gamma)) + 2 \cdot p_e(\gamma)(1 - p_e(\gamma)) \\ +3 \cdot p_e(\gamma)^2(1 - p_e(\gamma)) + ... \\ +N_{max}p_e(\gamma)^{N_{max}-1}(1 - p_e(\gamma)) + N_{max}p_e(\gamma)^{N_{max}}. \end{aligned} \tag{5.6}$$

Recall that γ remains constant for all retransmissions. The last member of the sum denotes the packets that were received erroneously N_{max} times and discarded. After some simple algebra we get

$$N_{tx}(\gamma) = \sum_{n=1}^{N_{max}} p_e(\gamma)^{n-1} = \sum_{n=1}^{N_{max}} (1 - p_s(\gamma))^{n-1}. \tag{5.7}$$

The average number of transmission attempts per packet, over all γ realizations, is then

$$\overline{N}_{tx}(\mu) = \int_0^\infty N_{tx}(\gamma)p_\gamma(\gamma|\mu)d\gamma. \tag{5.8}$$

Note that because the integrand in Eq. (5.7) is applied instead of $p_s(\gamma)$ (the latter is usually studied), γ is kept constant for all the retransmissions to reflect the empirically observed link temporal correlation. No approximation for high SNR values can be applied since the lower limit of integration is zero. Therefore we solve the integral in Eq. (5.8) numerically.

5.4.2 Outage Probability

We define the outage probability p_{out} as the probability that a packet is discarded after N_{max} failed transmission attempts. To calculate p_{out}, we use the average number of errors associated to a realization of γ

$$N_{err}(\gamma) = \sum_{n=0}^{\infty} n \cdot (p_e(\gamma))^n \cdot (1 - p_e(\gamma)) = \frac{p_e(\gamma)}{1 - p_e(\gamma)}. \tag{5.9}$$

A link is in outage if the current value of γ is such that the associated average number of errors is $N_{err} \geq N_{max}$. Taking the inverse function of Eq. (5.9), we can find the threshold γ_{th} such that $\gamma_{th} = N_{err}^{-1}(N_{max})$. Therefore, if the current realization of γ satisfies $\gamma \leq \gamma_{th}$, the link is said to be in outage. If γ is lognormally distributed, there is a non-zero outage probability for every device involved in communication regardless of the value of μ. The outage probability can be computed as [4]

$$p_{out} = \int_0^{\gamma_{th}} p_\gamma(\gamma|\mu)d\gamma = Q\left(\frac{\mu - 10\log_{10}(\gamma_{th}(N_{max}))}{\sigma}\right), \tag{5.10}$$

where $Q(\cdot)$ is the tail integral of a unit Gaussian probability density function.

5.4.3 Energy Consumption Analysis

The mean energy spent both at the transmitter and the receiver to exchange a packet over a link, that is, per time slot, is

$$E_{link} = \overline{N}_{tx} \cdot E_{data} + (1 - p_{out}) \cdot E_{ack} + (N_{max} - \overline{N}_{tx}) \cdot E_{idle}, \tag{5.11}$$

where $\overline{N}_{tx}$ and p_{out} are defined in Eq. (5.8) and Eq. (5.10) respectively and the energy components are defined in Eq. (5.5). In order to avoid buffering packets coming from the upper layer in the transmit queue, possible retransmissions need to be considered when the time frame is designed. Therefore some slots result in idle slots when there are no retransmissions and they are represented by the last component in Eq. (5.11). Both $\overline{N}_{tx}$ and p_{out} depend on the mean SNR μ whose relation to the link distance can be derived from Eq. (5.3).

For a fixed distance to the destination, a device may opt for a direct, multi-hop or CDC-ARQ transmission. In case of a multi-hop transmission, we refer to the multi-hop path made of consecutive, equidistant links. A path begins with the source device, continues over $k-1$ relays and finally ends at the destination. The total mean energy spent to transmit a packet over a multi-hop path is

$$E_{tot} = \sum_{n=0}^{k-1}(1 - p_{out})^k \cdot E_{link}, \tag{5.12}$$

because only those packets that were delivered to a relay are forwarded over the next link and p_{out} is the outage probability of each individual link. For a direct transmission when $k = 1$, Eq. (5.12) gives $E_{tot} = E_{link}$. However, to single out the efficient part of the total consumed energy, we are interested in the energy spent per *delivered* packet, because if the packet does not reach the destination, the energy spent in a transmission attempt is wasted. The unit of effective energy consumption is thus *Joule per delivered packet*. The probability of discarding a packet on a multi-hop path is

$$p_{out}^t = 1 - (1 - p_{out})^k. \tag{5.13}$$

Therefore, we calculate the effective mean energy per delivered packet on a multi-hop path as

$$E_{eff} = \frac{E_{tot}}{1 - p_{out}^t}. \tag{5.14}$$

In a direct transmission when $k = 1$, $E_{eff} = E_{link}/(1 - p_{out})$.

Finally, CDC-ARQ represents a combination of the two, as it alternates between the medium-range link and the multi-hop transmission depending on channel conditions. Recall that a transmission is first attempted over a direct link. If it results in error, the packet is immediately redirected because the probability of error for the subsequent attempts on the same link is high. If however the attempt over the direct link results in success, the time slots on a backup path remain idle. Therefore, the mean energy spent in a CDC-ARQ scheme for $k = 2$ backup multi-hop path is

$$\begin{aligned} E_{carq} = p_{out}^c \cdot (E_{data} + E_{tot}(k = 2)) + (1 - p_{out}^c) \cdot \\ \cdot (E_{data} + E_{ack} + kN_{max}E_{idle} + (N_{max} - 1)E_{idle}), \end{aligned} \tag{5.15}$$

where p_{out}^c is the probability of redirecting to a multi-hop path because of a direct link outage. The probability p_{out}^c corresponds to $N_{err} = 1$ (error on a direct link) and can be calculated from Eq. (5.10) for the given link distance by replacing $\gamma_{th} = N_{err}^{-1}(1)$. When the packet is redirected, we need to include the energy spent for the initial attempt that resulted in error. Otherwise, only the energy of the successful transmission with ACK is consumed plus the idle slots on a backup path. The effective mean energy per delivered packet is then

$$E_{eff}^c(k = 2) = \frac{E_{carq}}{1 - p_{out}^c \cdot p_{out}^t(k = 2)}, \tag{5.16}$$

where E_{eff}^c denotes the energy of the cooperative forwarding scheme as opposed to the energy of the fixed forwarding scheme E_{eff}.

Although the expressions for the network energy consumption in CDC-ARQ scheme for $k > 2$ are tractable, they can be quite complex because of multiple medium-range links that can be formed. That is why we chose to validate the model in the simulation with the simplest case of $k = 2$, which, in its turn, also validates the implementation in the simulator. Then we proceed with the evaluation in the simulator only for $k > 2$. This step is in line with the general tendency to validate the developed ns-3 code and thus support the trustworthiness of the simulation output. In addition, a quick access to complex scenarios justifies the use of a simulator.

For better readability, Table 5.1 summarises the notation used throughout the chapter.

Table 5.1: Notation

Notation	Meaning
k	number of hops on a multi-hop path
d	link distance in meters
γ	instantaneous SNR
$p_s(\gamma)$	packet success probability
$p_e(\gamma)$	packet error probability
μ	mean SNR
σ	shadowing standard deviation
N_{max}	maximum number of tx attempts per packet
$\overline{N}_{tx}(\mu)$	average number of tx per packet
$N_{err}(\gamma)$	number of tx errors
L	packet size
p_{out}	outage probability when $N_{max} = 4$
p^c_{out}	outage probability when $N_{err} = 1$
E_{data}	energy consumed during data transmission
E_{eff}	effective mean energy per delivered packet

5.5 Performance Analysis

5.5.1 Implementation in ns-3 simulator

ns-3 is an open-source, discrete-event network simulator written in C++. An overview of ns-3 features relevant for this thesis is given in Chapter 2, Section 2.3.

The functionality required for this study has been implemented by modifying a model for the IEEE 802.15.4 standard, whose name is *lr-wpan* and whose source code can be downloaded from [19]. The MAC implementation available in the initial *lr-wpan* model supports the non-beacon, mesh mode with all devices in the default *idle listen* state of the radio transceiver. This model has been significantly extended to include the duty-cycling operation of the devices, to support the energy consumption measurements and to enable the path diversity necessary for the CDC-ARQ scheme. Firstly, duty-cycling has been implemented with TDMA as explained in Section 5.3.2. Contention during the CCA phase has been disabled and replaced with the simple CCA without random backoff as specified in [3]. Next, the existing log-distance path loss channel model has been extended with a realistic shadowing model described in Section 5.3.5, defined with a standard deviation σ and a channel correlation in time. The implementation follows the Decorator software design pattern as described in Section 2.3.1. The CDC-ARQ functionality has been implemented by introducing dedicated tags in the packet header.

Table 5.2: Simulation Parameters

Parameter	Value	Parameter	Value
P_t	$0\ dBm$	N_{max}	4
σ	$4\ dB$	L	$27\ bytes$
R_b	$250\ kbits/s$	freq. band	$2.4\ GHz$

Finally, the energy consumption module has been extended to subscribe to the changes in the state of a PHY radio transceiver in order to obtain the energy consumption directly from the device (i.e. from the simulated radio). This is implemented with the Observer design pattern presented in Section 2.3.2. The energy module is not aware of the wireless channel nor the MAC layer scheme, therefore the two cannot interfere with the energy reading. Because of this design choice, an independent comparison with the theoretical model is provided.

5.5.2 Simulation Parameters

The default values of simulation parameters are given in Table 5.2. The maximum number of transmission attempts N_{max} is recommended in the standard, as well as the data bit rate that corresponds to the chosen frequency band; the modulation considered is O-QPSK with additional (DSSS), whose bit error rate is given in Eq. (5.1). The default header is generated in the simulation as specified in the standard [3].

5.5.3 Results

Link Metrics

The first step in the validation of the energy model is to show that the presented metrics, namely $\overline{N}_{tx}$ paired with p_{out} characterise a low-power wireless link reliably. To that aim, we observe a low-power link for various distances when the output transmission power P_t is fixed. Figure 5.3 shows the Average Number of Transmissions per Packet in a truncated-ARQ scheme over a low-power, shadowed wireless link. As the distance increases, more and more packets get discarded and $\overline{N}_{tx}$ approaches the maximum allowed number of attempts per packet. If the scheme was not truncated but indefinite retransmissions until successful delivery were permitted, in the considered shadowed environment the function $\overline{N}_{tx}$ would not be bounded. The unbounded function $\overline{N}_{tx}$ would tend to infinity which makes the analysis intractable. In general, system is designed such that outage states are brought to minimum because they destabilise the system. That is why the upper limit N_{max} had to be imposed on the number of transmission attempts. Not only does it limit the influence of outage states, but it also preserves

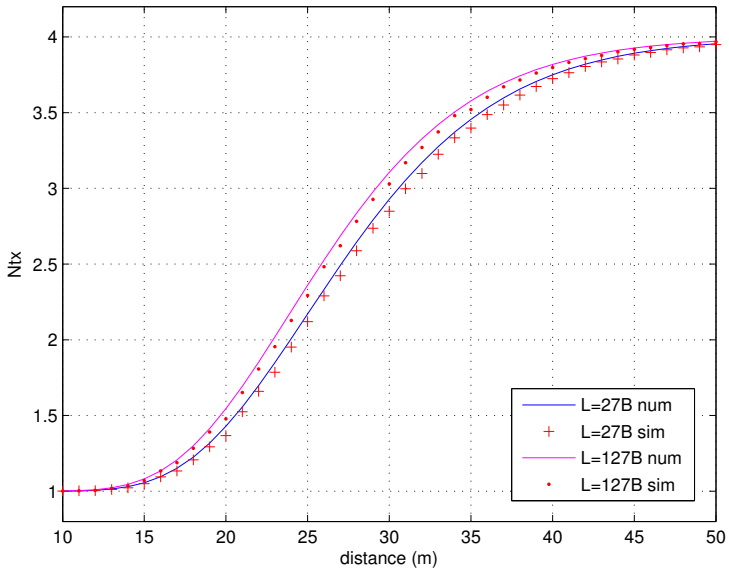

Figure 5.3: Average Number of Transmissions per Packet as a function of link distance; payload of minimum $L = 27\ bytes$ and maximum length $L = 127\ bytes$; truncated-ARQ, $N_{max} = 4$

energy and system resources, for the cost of some discarded packets. However, the probability of discarding a packet can be controlled either with careful system design or with CDC-ARQ. Figure 5.3 shows $\overline{N}_{tx}$ for the minimum and maximum packet lengths allowed by the standard ($27\ bytes \leq L \leq 127\ bytes$). It can be seen that the packet size does not influence this metric significantly. The average number of transmissions is an important parameter in estimating the energy consumption since the energy is directly proportional to its value, as Eq. (5.11) shows. Note from Figure 5.3 that the results obtained in Matlab for the numerical solution of Eq. (5.8) match well with the simulation results obtained in ns-3.

The (un)reliability of the scheme can be estimated with the number of packets that get discarded after N_{max} attempts. The outage probability p_{out} that complements the $\overline{N}_{tx}$ metric is shown in Figure 5.4 for several values of the standard deviation of shadowing σ. A value of the outage probability depicted in Figure 5.4 for a given link distance corresponds to a value of $\overline{N}_{tx}$ in Figure 5.3 for the same distance. For example, when $\overline{N}_{tx} = 2$ for $L = 27\ bytes$, the $p_{out} = 0.3$ for $\sigma = 4\ dB$, i.e. 30% of packets are discarded on average over this link. With the increase in σ, the range of link distances with medium packet loss probabilities increases. In another words, without shadowing the graph would resemble the step function that produces the unrealistic circle coverage area with the perfect reliability within the circle and the absolute outage outside of it. The inclusion of shadowing effects makes every link unreliable, with the predictable (average) degree of unreliability p_{out}. The numerical estimation of p_{out} in Eq. (5.10) obtained in Matlab agrees well with the number of discarded packets in ns-3 simulation. A slight disagreement is the consequence of the missed ACKs not considered in the theoretical

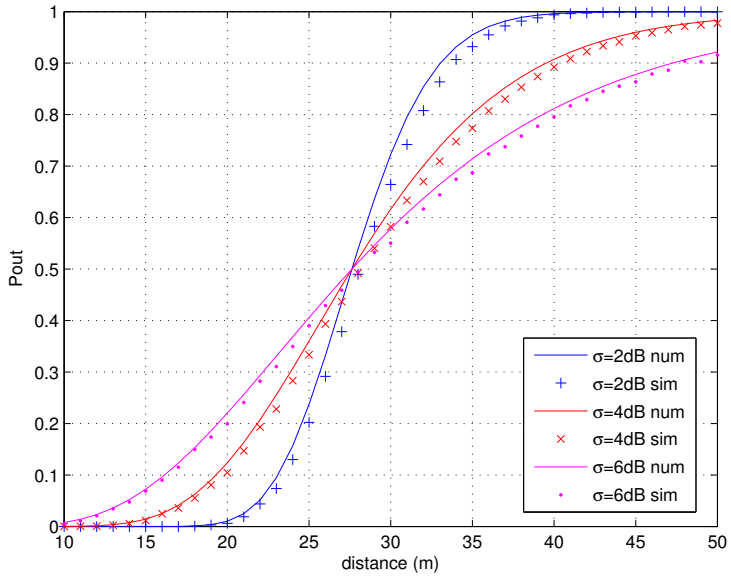

Figure 5.4: Outage probability as a function of link distance for different shadowing σ; output transmission power is set to $0\ dBm$

model that cause retransmissions in the simulation. It has been determined by simulation that successfully delivered data packets whose ACK is not received do not exceed 5% of all the transmitted packets. The probability of unsuccessful ACK transmission approaches 5% for medium link outage probabilities, but it decreases to values below 2% for low or high outage probabilities. It can be seen in Figure 5.4 that the slight disagreement is highest precisely for the medium outage probabilities. In addition, observe that a smaller σ yields smaller outage probability for $p_{out} < 0.5$, but provides worse delivery rates for $p_{out} > 0.5$. Nevertheless, in all studied cases, the direct transmission scheme is inefficient for larger distances and implies the use of either multi-hop transmission or a CDC-ARQ technique to avoid significant packet loss. We next determine for what distance range one of the three techniques is the most appropriate.

Energy Consumption Optimisation

In the second step, energy consumption is measured in the simulation to verify the model derived in Section 5.4. While the first step focused on an isolated link, here we study various multi-node scenarios. Results show how to optimise system's energy consumption in a multi-node scenario. Given the reliability constraints, bounds for optimal link distances are shown to indicate the design choice between direct, multi-hop or CDC-ARQ forwarding. For the strict reliability requirement, CDC-ARQ proves to be the most efficient forwarding strategy.

The mean consumed energy per delivered packet of the direct and multi-hop transmission is compared in Figure 5.5 for $k = 1$, $k = 2$ and $k = 3$ (the model for E_{eff} in Eq. (5.14) is valid

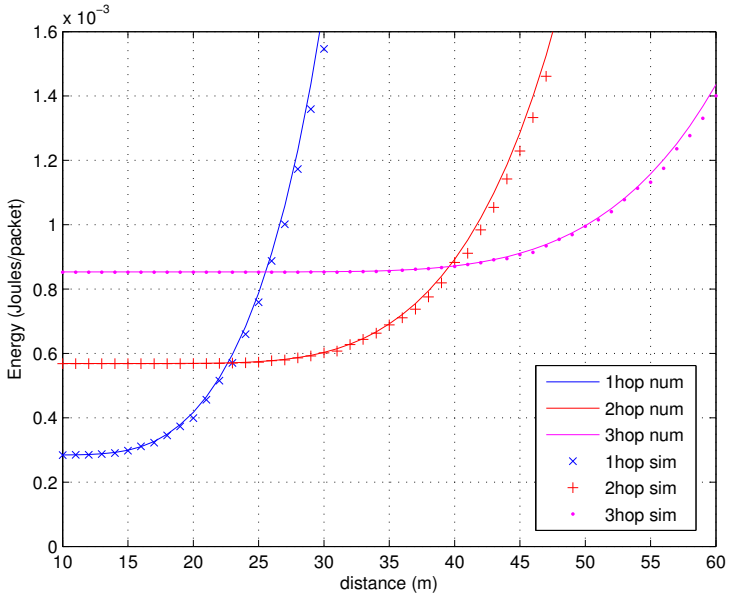

Figure 5.5: Total mean energy spent per delivered packet for direct, 2-hop and 3-hop transmission over the total source-to-destination distance

for any k). For $k > 1$ the distance on the graph denotes the total distance traversed from source to destination via relays such that the individual link distance is k times smaller than the total distance. For distances $d < 23\ m$ there is no need for the multi-hop transmission because the direct link provides good service while consuming less energy. For $23\ m < d < 40\ m$ the optimal setting requires the transmission over two hops, that is, over two equidistant links of $d/2$ meters; past that distance over three hops and so on. The threshold distance can be obtained numerically from Eq. (5.14) by substituting the corresponding k or from the simulation as Figure 5.5 shows. The energy consumption significantly increases as the outage probability for the corresponding link distance increases. Namely, packet loss presents a waste of energy resources and has considerable effect on the mean energy consumption. Note in Figure 5.4 that at distances close to the threshold link distances of $d = 23\ m$ ($k = 1$) and $d = 20\ m$ ($k = 2$), even $10 - 30\%$ of packets can be lost. Therefore, the results presented in Figure 5.5 apply to systems with loosened reliability requirements, but are not suitable for reliability-sensitive systems.

For the applications with strict reliability requirements, link distances must be decreased. In the design phase, maximum p_{out} is fixed in Eq. (5.10) to get the maximum link distance that meets the requirement. For example, when the link outage is set to $p_{out} < 1\%$, from Eq. (5.10) we get $d = 14\ m$ as the maximum link distance that still satisfies the outage constraint. Number of hops is next devised depending on the total distance between the source and the destination. In practice this is usually achieved with link estimators that select high-quality and therefore mostly short-range links. The alternative CDC-ARQ technique meets the same reliability requirement with lower energy consumption by including medium-quality links in

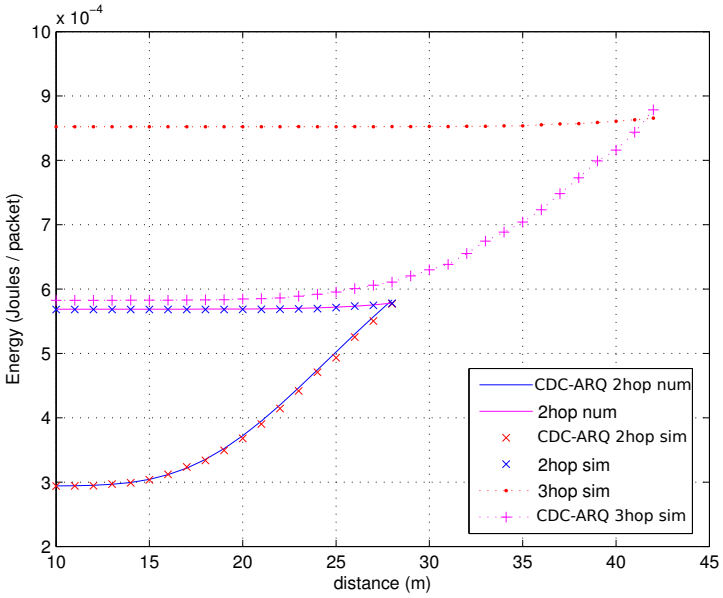

Figure 5.6: Total mean energy spent per delivered packet with the imposed outage constraint $p_{out} < 1\%$; multi-hop and CDC-ARQ forwarding compared

the communication, besides backup high-quality links. To verify this hypothesis, we study the scenario shown in Figure 5.1. In this scenario, there is a two-hop path (4-3-2) that can alternate with a medium quality link (4-2) and a three-hop path (7-6-5-1) that alternates with two medium-quality links (7-5 and 6-1).

Figure 5.6 shows how much energy can be saved by applying CDC-ARQ in comparison to using the fixed multi-hop path exclusively. For total distances $14\ m < d < 28\ m$ without CDC-ARQ on average 570 μJ of energy is spent per packet on a fixed two-hop path. CDC-ARQ that combines a medium-quality link up to 28 m in length with the two-hop path consumes less energy. The energy savings in CDC-ARQ are obtained when channel conditions allow successful transmissions over a medium-quality link and eventually take less hops to reach the destination. Failures on the medium-quality link represent the cost of the CDC-ARQ. As the link distance increases, there will be more failures and consequently more redirections to the two-hop path. It can be observed that the energy consumption increases accordingly until it becomes equal to the fixed multi-hop transmission. At the distance $d = 28\ m$, about the half of packets are transmitted over a medium-quality link and the other half is redirected. This is a threshold point. Results obtained in simulation agree with the model in Eq. (5.14) and Eq. (5.16).

For source-to-destination distances $28\ m < d < 42\ m$, three short-range links are necessary to satisfy the outage constraint. Their mean energy consumption is 850 μJ per delivered packet. When medium-quality links participate in the communication, the energy consumption can again be significantly decreased as Figure 5.6 shows. Three-hop scenario was verified in simu-

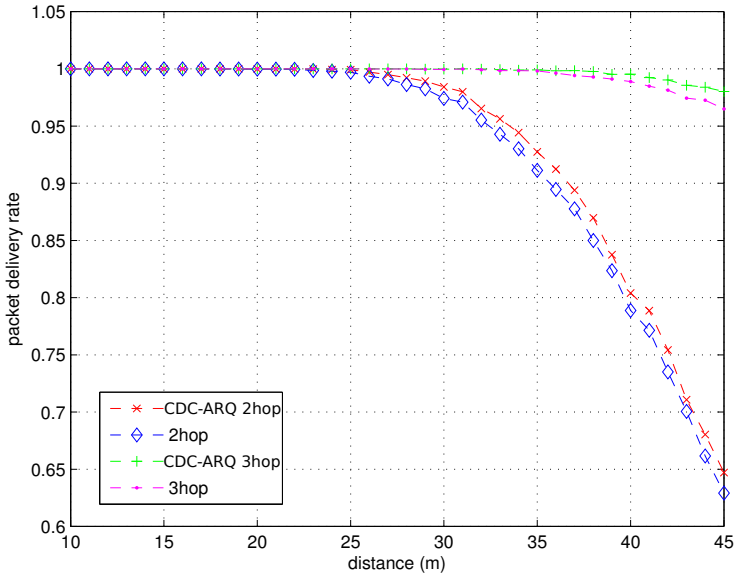

Figure 5.7: Total packet delivery rate for the given source-to-destination distance

lation only given its analytical complexity. In conclusion, when the reliability demands require multi-hop transmission over short-range links, CDC-ARQ should be applied to decrease the mean energy consumption per delivered packet.

Although the data packet size L does not influence $\overline{N}_{tx}$ significantly, with the larger L, E_{data} in Eq. (5.5) increases. Consequently, the total energy spent to deliver a packet is larger, e.g. $E_{eff} = 1.24\ mJ$ when $L = 127\ bytes, k = 2, p_{out} < 0.01$ compared to $E_{eff} = 570\ \mu J$ when $L = 27\ bytes$. However, apart from the absolute value, the characteristics of energy consumption behaviour for the permitted values of L ($27\ bytes < L < 127\ bytes$) closely resemble the ones already commented and shown in Figures 5.5 and 5.6.

Packet Delivery Rate

Finally, in order to demonstrate that the presented results satisfy the outage constraint set in advance, the total packet delivery rate for the given source-to-destination distance is measured in the simulation and the results are shown in Figure 5.7. Just as the model predicts, when $k = 2$ and for the total distances up to $d = 28\ m$, the number of discarded packets is limited to less than 1%. The same is confirmed for $k = 3$ and total distances up to $d = 42\ m$. The delivery rate decreases for distances greater than the threshold distance obtained from the model such that the reliability requirement cannot be met any more. It can be observed in Figure 5.7 that CDC-ARQ performs slightly better than the fixed transmission over the multi-hop path.

5.6 Chapter Summary and Conclusions

In this chapter, we elaborate on a metric adequate for low-power wireless links denoted Average Number of Transmissions per Packet. The metric considers shadow fading and truncated-ARQ. Based on this metric, we were able to calculate the energy consumption of devices compatible with IEEE 802.15.4e that is suitable for duty-cycled, low-power, energy-efficient M2M networks. The energy model presented in this work was validated in the ns-3 network simulator in the realistic simulation environment that mimics the functioning of an actual device. Based on the energy model, we determined the optimal operating regions of direct, multi-hop and CDC-ARQ forwarding, as well as the implications of using each. All these results provide useful guidelines on the design of an energy-efficient network, for systems with either loose or strict reliability requirements.

This chapter concludes the study of wireless networks for the Home and Building Automation use case presented in this thesis. Recall from Introduction in Chapter 1 that the main challenge associated to this use case is to improve the energy efficiency of the communication protocols. In the previous chapters including this one (Chapters 3, 4 and 5), we have examined various low-power technologies that are most likely to be deployed at the consumer and proposed the improvements and possible optimisations. In the next chapter, the applications using these technologies are addressed. There are two types of applications in the M2M system: those installed at the consumer's gateway and those collecting and processing data from many gateways and devices. We therefore expand our study to the entire end-to-end M2M system beyond the consumer. Precisely, the standardised middleware is presented that facilitates data exchange over many different communication technologies.

Bibliography

[1] M. Palattella, N. Accettura, X. Vilajosana, T. Watteyne, L. Grieco, G. Boggia, and M. Dohler, "Standardized Protocol Stack for the Internet of (Important) Things," *IEEE Communications Surveys and Tutorials*, vol. 15, no. 3, pp. 1389–1406, 2012.

[2] L. Zhang, R. Ferrero, E. R. Sanchez, and M. Rebaudengo, "Performance analysis of reliable flooding in duty-cycle wireless sensor networks," *Transactions on Emerging Telecommunications Technologies*, 2012.

[3] *IEEE 802.15.4e Standard: Low Rate Wireless Personal Area Networks (LR-WPANs) Amendment 1: MAC sublayer*, IEEE Std., April 2012.

[4] P. Mary, M. Dohler, J.-M. Gorce, G. Villemaud, and M. Arndt, "M-ary symbol error outage over Nakagami-m fading channels in shadowing environments," *IEEE Transactions on Communications*, vol. 57, no. 10, pp. 2876–2879, October 2009.

[5] K. Srinivasan, P. Dutta, A. Tavakoli, and P. Levis, "An Empirical Study of Low-Power Wireless," *ACM Transactions on Sensor Networks*, vol. 6, no. 2, pp. 1–49, March 2010.

[6] M. Dianati, X. Ling, K. Naik, and X. Shen, "Performance analysis of the node cooperative ARQ scheme for wireless ad-hoc networks," in *IEEE Global Telecommunications Conference (GLOBECOM)*, vol. 5, December 2005, pp. 3062–3067.

[7] (2012) network simulator 3. [Online]. Available: http://www.nsnam.org/

[8] J. Deng, Y. S. Han, P.-N. Chen, and P. Varshney, "Optimal Transmission Range for Wireless Ad Hoc Networks based on Energy Efficiency," *IEEE Transactions on Communications*, vol. 55, no. 9, pp. 1772–1782, September 2007.

[9] K. Vardhe, C. Zhou, and D. Reynolds, "Energy Efficiency Analysis of Multistage Cooperation in Sensor Networks," in *IEEE Global Telecommunications Conference (GLOBECOM 2010)*, December 2010, pp. 1–5.

[10] G. de Oliveira Brante, M. Kakitani, and R. Souza, "Energy Efficiency Analysis of Some Cooperative and Non-Cooperative Transmission Schemes in Wireless Sensor Networks," *IEEE Transactions on Communications*, vol. 59, no. 10, pp. 2671 –2677, October 2011.

[11] M. H. Alizai, O. Landsiedel, J. A. B. Link, S. Gotz, and K. Wehrle, "Bursty traffic over bursty links," in *Proceedings of the 7th ACM Conference on Embedded Networked Sensor Systems*, ser. SenSys, 2009, pp. 71–84.

[12] D. Lai, A. Manjeshwar, F. Herrmann, E. Uysal-Biyikoglu, and A. Keshavarzian, "Measurement and characterization of link quality metrics in energy constrained wireless sensor networks," in *IEEE Global Telecommunications Conference, GLOBECOM*, vol. 1, 2003, pp. 446–452.

[13] T. Iwao, K. Yamada, M. Yura, Y. Nakaya, A. Cardenas, S. Lee, and R. Masuoka, "Dynamic data forwarding in wireless mesh networks," in *IEEE International Conference on Smart Grid Communications (SmartGridComm)*, 2010, pp. 385–390.

[14] *IEEE 802.15.4 Standard: Low Rate Wireless Personal Area Networks (LR-WPANs)*, IEEE Std., September 2011.

[15] L. Doherty, W. Lindsay, and J. Simon, "Channel-Specific Wireless Sensor Network Path Data," in *International Conference on Computer Communications and Networks (ICCCN)*, August 2007, pp. 89–94.

[16] M. Z. Zamalloa and B. Krishnamachari, "An Analysis of Unreliability and Asymmetry in Low-Power Wireless Links," *ACM Transactions on Sensor Networks*, vol. 3, no. 2, June 2007.

[17] N. Baccour, A. Koubaa, L. Motolla, M. Zuniga, H. Youssef, C. Boano, and M. Alves, "Radio Link Quality Estimation in Wireless Sensor Networks: a Survey," *ACM Transactions on Sensor Networks*, vol. 8, no. 4, November 2012.

[18] (2010) CC2430 datasheet. [Online]. Available: http://www.ti.com/product/CC2430

[19] (2011) Low-rate, wireless personal area network (LR-WPAN) ns-3 model. [Online]. Available: http://code.nsnam.org/tomh/ns-3-lr-wpan/

Chapter 6

A Real-Time M2M Middleware Platform

In this chapter, we expand the study of M2M systems beyond the wireless area network device domain. The focus changes from the communication protocols for wireless area networks studied in the previous chapters to the application middleware that facilitates data exchange in these networks. The wireless technologies studied previously are installed at the consumer, but the middleware expands in the end-to-end M2M system beyond the consumer. More specifically, the middleware is used by M2M applications at both ends: *(i)* M2M gateway application that manages the devices in the locally installed area network and *(ii)* M2M network application that collects and processes data from many devices and gateways connected through the access network. The communication requirements of these applications are the main focus of this chapter. The responsiveness of middleware to those requirements is analysed, some pitfalls are identified and solutions are proposed.

Due to a wide success of Internet and web protocols (primarily Hyper Text Transfer Protocol (HTTP) for data exchange) it is reasonable to choose web services as the base technology for this middleware. As explained in the Introduction of this thesis in Chapter 1, we focus on Smart Grid use cases. Precisely, Home and Building Automation and Wide Area Measurement System (WAMS) are examined. Applications for Home and Building Automation use case, e.g. Demand Response and others, have modest communication requirements that can be entirely met with the classic web services using HTTP. Therefore, these applications are fully supported by the currently existing middleware platforms. However, a research challenge has

been identified for the Wide Area Measurement System (WAMS) use case and the applications therein. This challenge is presented and addressed next.

In this chapter, we analyse distributed computing technologies that meet the stringent communications requirements of various Smart Grid applications. We show that the solutions and practices developed for Machine-To-Machine (M2M) communications, ETSI M2M middleware in particular, can be successfully applied to future Smart Grid networks. In order to provide for the critical event-driven, real-time communication required by some applications, an upgrade to ETSI M2M is devised and analysed.

6.1 Introduction

Historically, Smart Grid applications have relied on the Supervisory Control and Data Acquisition (SCADA) systems to transfer commands and updates over large distances. In the past decades, SCADA was deployed throughout the electric power grid to combat the large scale blackouts and monitor the state of the power grid. These systems have evolved little over the years. With SCADA, a substation collects local measurements and delivers them to the application in the control centre, managed by human operators. Communication links between the individual substations and the control centre form a star topology, and the collected data is stored in a centralised database. The data rates on links are low, up to a few kilobits per second, and the latency is in the range of several seconds or more. In short, the currently used communications system in the electric power grid is heavily outdated. Modern power applications and devices cannot execute protection and control operations because of SCADA communication constraints [1].

One of these modern devices is the Phasor Measurement Unit (PMU). PMUs can measure bus voltages, currents, frequency etc. at the rates of several times per power cycle. They synchronise with the Global Positioning System (GPS) clocks in order to timestamp their measurements. PMUs deployed over a wide area provide a global time-synchronised snapshot of the power grid state, which contributes to the real-time situational awareness that cannot be achieved with SCADA. With this information, the scope of control applications widens, compared to the local control performed today within a substation. This in turn allows for global protective actions to be performed even before the power grid becomes unstable. However, in order to benefit from a wide area measurement system, an enhanced communication system is needed to deliver the measurements to the networked control applications [2]. The system consists of two major parts: communication infrastructure and middleware [3]. The currently developed technical solutions for such middleware, as well as their shortcomings, are addressed in this chapter.

A common, grid-wide, universal middleware for distributed networked operations facilitates

real-time interactions between the devices and applications. The shared middleware also simplifies application development on a variety of platforms, operating systems, networking technologies etc. One notable example is GridStat [4], a publish-subscribe middleware implemented with the Common Object Request Broker Architecture (CORBA). A competitor to CORBA for implementing a distributed system, one that is becoming increasingly predominant, is the web service technology. RESTful web services are particularly favoured over other solutions, primarily because of their simplicity while providing the full functionality that other solutions can offer. We make a case for the web services to constitute the basis of the Smart Grid communication framework, and then we analyse ETSI M2M web service middleware [5] in the context of the Smart Grid. ETSI M2M document on the Smart Grid [6] outlines some adequate use cases and their requirements, without providing the technical solutions to realise them. Therefore, we first devise a working architecture that relies on the ETSI M2M components mapped to the Smart Grid. Then we analyse the application layer protocols used in web services while focusing on real-time performance.

6.1.1 Contribution

An application middleware proposed in this chapter addresses one major disadvantage of the request-response (client-server) web model using HTTP: the lack of support for real-time communications. For instance, delivering a stream of PMU updates to the client application is cumbersome and does not cater for the strict latency requirement. Although various workarounds have been devised, e.g. [7], a client-server web model was not initially designed to support real-time events. We address this problem with two upgrades and specify when to use each of them. To the best of our knowledge, this is the first attempt of considering the entire set of Smart Grid requirements, including real-time communications, with one ubiquitous communication middleware based on web service technology.

In Section 6.2, we briefly summarise the essential communication requirements for the Smart Grid and define the traffic patterns of example grid applications. In Section 6.3, we adapt the ETSI M2M architecture to the Smart Grid scenario, identifying key components, their location and interconnections. Finally, the upgrade of the middleware to address the real-time communication requirement, is presented in Section 6.4.

6.2 Smart Grid Communication Requirements

Many recent studies, e.g. [4], [8] identify three principal Smart Grid communication requirements:

- Quality of Service (QoS)

- Flexibility
- Security

6.2.1 Quality of Service

Regarding QoS, a major constraint is put on data *latency*. Four categories with different latency requirements are identified depending on the network application: protection, control, monitoring or reporting. Some concrete values for the maximum response times are [6]:

- protection $1 - 10\ ms$ (real-time)
- control $100\ ms$ (real-time)
- monitoring $1\ s$ (near real-time)
- reporting, billing, post-incidental analysis $>\ 1\ h$ (slow)

In addition to the latency constraints, a certain data availability that is guaranteed by the network is expected, e.g. $> 99.99\%$ for critical data updates [4].

6.2.2 Flexibility

A communication system for Smart Grids needs to support a variety of data update rates, latencies, heterogeneous underlying networks, operating systems etc. In addition, [4] stresses the need for an *open* interface, one that is easily extendable and allows for application interoperability across multiple vendors. In this respect, web services are more flexible than the CORBA middleware.

Flexibility also applies to the middleware design: data updates should be easily available to any legitimate participant at any location, at a predefined rate, which cannot be easily achieved with SCADA. Not all updates that a device is generating, but only the requested ones, need to go to the right application at the right rate and latency. Therefore, a certain *filtering* functionality is needed.

6.2.3 Security

A critical infrastructure such as the power grid has to be highly secure. Security covers the authentication schemes in order to deny access to unauthorised parties, and the proven techniques for data confidentiality and data integrity. In addition, the privacy concern should be addressed to prevent any possible misuses.

Table 6.1: Communication requirements for three example Smart Grid applications

Application (subscriber)	Oscillation Monitoring	State Estimation	Demand Response
purpose	control	monitoring	peak shaving
latency	$< 100\ ms$	$< 1\ s$	seconds to minutes
category	real-time	near real-time	slow
device (publisher)	PMU directly	substation or PMU	gateway for smart appliances
rate	30 updates/s	5 updates/s	4 updates/min
scope	selected PMUs	all PMUs	all gateways
# publishers	< 100	hundreds	millions
location	transmission	distribution	consumer

6.2.4 Power Grid Data Traffic Patterns

We have analysed data requirements of three example Smart Grid applications in order to deduce a traffic pattern of the power grid measurement updates. Applications such as Oscillation Monitoring and State Estimation heavily depend on WAMS, while Demand Response is chosen as a representative Smart Grid application that relies on the wireless technologies studied in the previous chapters of this thesis. Devices, e.g. PMUs or smart meters and appliances, take measurements and publish data for the interested applications to subscribe to. The special (and very different) requirements of each application are given in Table 6.1. We assume that the Oscillation Monitoring application will be used for control, which explains the strict latency constraint. This application monitors oscillations, primarily within the transmission grid, that can bring the power grid to an unstable state. State Estimation is increasingly calculated for the distribution grid to supplement the one in the transmission grid, so that the complete overview of the power grid state is available. In this case, requirements are somewhat loosened compared to the Oscillation Monitoring, but the number of devices is higher. Finally, we consider Demand Response application that processes consumption data coming from smart appliances. In this case, neither the latency constraint, nor the update rate is critical compared to the other two applications.

6.3 M2M Communications in Smart Grid

A wide area real-time situational awareness is impossible to achieve and coordinate if it depends on a number of human operators. One of the visions of the Smart Grid concept is to minimise the human involvement, or even to exclude the human from the control loop entirely. Towards this end, the Smart Grid can capitalise on the technologies for M2M communication systems that are being developed and deployed [8]. To enable distributed computing between remote applications and devices, a middleware platform is needed. The prevailing M2M middleware will likely be implemented with the web service technology to provide the required interoperability and scalability.

6.3.1 RESTful Web Services

Representational State Transfer (REST) offers software architecture guidelines for implementing a web service [9]. Instead of exposing the methods, a RESTful web service exposes internal *data*, organised into data units called resources. Resources define the functionality of the service exclusively through the specific data that they expose. Resources are accessed and modified using the methods of the web application layer protocol, in most cases this is HTTP (or Constrained Application Protocol (CoAP) for resource-constrained devices). There are four essential methods for data manipulation: Create, Retrieve, Update and Delete (CRUD methods for short), and the web application layer protocol has to support them (as HTTP and CoAP do). In this way the web application layer becomes part of the service, and not just a wrapper around it. A resource is referenced with a globally unique Uniform Resource Identifier (URI link) and any RESTful resource is manipulated with the same set of CRUD methods.

A web service is hosted on a server to be accessed by clients. A client accesses the service by sending a HTTP request to the specific resource on the server and the result is delivered in a HTTP response. The communication is always initiated by the client and realised by the exchange of HTTP messages that contain a representation of the addressed resource, which is a serializable document that holds info on the resource's state. Every HTTP message begins with a HTTP method (in a request) or a response code (in a response), followed by a header and (optionally) a message body. HTTP is an application layer protocol that operates over a TCP/IP connection.

6.3.2 Mapping of ETSI M2M to the Smart Grid

ETSI M2M architecture relies on RESTful web services. The architecture was introduced in Chapter 2, Section 2.4. Essentially, ETSI standardised the resource structure that is hosted on the servers. In addition, between the network interfaces and the application, ETSI M2M

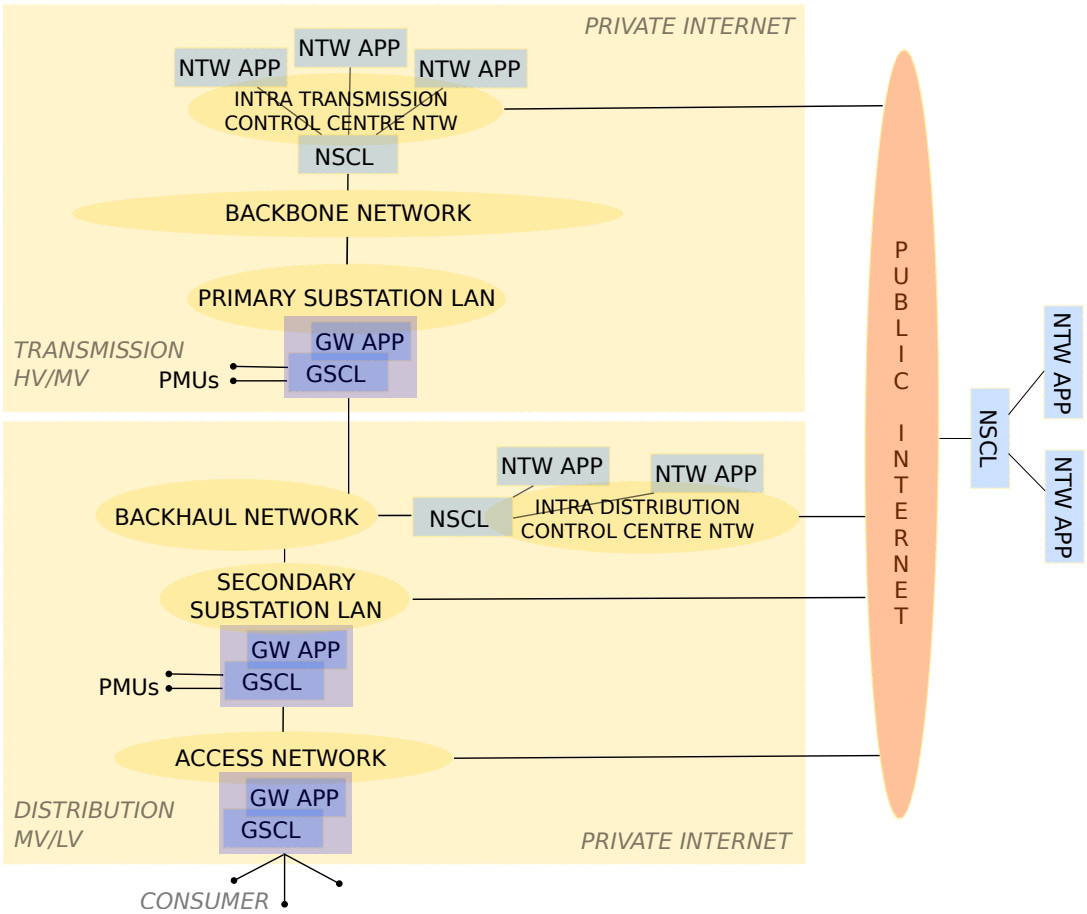

Figure 6.1: A mapping of ETSI M2M components to the Smart Grid

introduces a middleware layer denoted *Service Capability Layer* (xSCL) to support the service logic, where x can stand for Network, Gateway or Device (therefore, we have NSCL, GSCL and DSCL modules). The purpose of xSCL is to hide the specific underlying network from the application and allow for the common interface to be used across all application types. For example, xSCL is responsible for establishing a transport session for the data transfer, taking care of all security aspects, checking if a device is online, executing remote software updates, etc. ETSI M2M is implemented in the Fraunhofer FOKUS testbed [10] and in InterDigital Communications prototype [11].

The ETSI M2M architecture is distributed rather than centralised. This is achieved with GSCL at the gateway, which is a lightweight web server meant to serve as a network proxy. In effect, GSCL offloads the processing load from the NSCL, which is a fully fledged web server. Figure 6.1 shows our mapping of ETSI M2M to the Smart Grid.

The basic energy layer infrastructure of the power grid is organised into the transmission and the distribution grid. The transmission grid consists of high voltage lines which transmit electric power from the place where it is generated (hydro or coal plants) closer to the place where it is consumed (either by industrial or residential consumers). Before entering the distribution

grid, power is stepped down to medium voltage in the primary substations. The primary substations mark the end of the transmission and the beginning of distribution grid. The distribution grid consists of medium voltage lines leading to the secondary substations, where the power is stepped down again to low voltage that is serviced to a consumer [12].

As Figure 6.1 shows, NSCLs are located in the control centre, in the transmission and/or distribution grid. PMUs and the consumer devices such as smart meters connect to the corresponding gateway (GSCL) either at the substation or at the consumer premises, respectively. Network applications are clients who subscribe to the resources at NSCL, published by the PMUs and other devices. According to Table 6.1, Oscillation Monitor is a network application in the transmission control centre, State Estimation is located in the distribution control centre and Demand Response communications can go over the secure public Internet, given the relaxed QoS requirements. All critical measurement updates are exchanged on the private Internet.

ETSI M2M middleware supports the communication requirements given in Table 6.1. Adjustable update rates are supported by the filtering functionality of NSCL and GSCL. Any publishing device can create its data resource that is announced to the applications through the middleware. In addition, because of the distributed architecture (GSCL in the substation or at the consumer, NSCL in the control centres), the solution is scalable. Flexibility is enabled with the standardised, generic resource structure that can be easily extended and modified to suit the specific application needs. Interoperability is provided with the web service technology, available to any participant using the web protocols (HTTP or CoAP). Security is inherently supported in xSCLs.

Regarding vertical requirements of each application in Table 6.1, Demand Response is fully supported by the original ETSI M2M specification in [5]. Conversely, real-time communication requirements of Oscillation Monitoring and State Estimation pose a challenge for the current architecture. Detailed analysis of how the real-time communication requirements are addressed with the upgrades proposed in this chapter for ETSI M2M, is given in the next Section.

6.4 Real-time Communication with REST

Although the subscription mechanism is supported by ETSI M2M, the solution to enable it presented in [5] only specifies HTTP long polling techniques. With long polling, instead of an immediate response, a client's HTTP request (poll) is held until a response is available at the server. Like this, the server can deliver an update as soon as it arrives because it has an open connection to the client provided by the long poll request. In the case of frequent updates, each response is immediately followed by a new poll, which (nearly) achieves real-time performance.

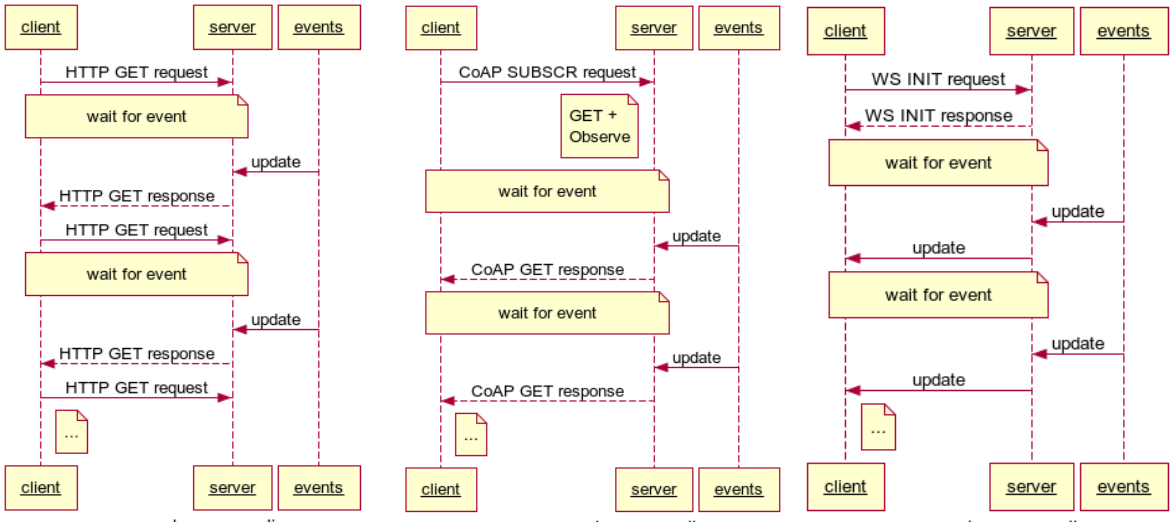

Figure 6.2: Sequence diagram for long polling (left), CoAP (middle) and Websocket messaging (right)

However, the long polling technique and the others alike are a workaround for the fact that HTTP clients are not designed to accept real-time updates. Given that there are applications whose main functionality critically depends on the real-time update delivery, we have considered two alternative solutions:

- CoAP using UDP/IP
- Websocket using TCP/IP

CoAP relies on UDP, which is connectionless, best-effort transport protocol. As such, UDP does not guarantee reliable, ordered delivery; there are no retransmissions of lost packets and thus no additional, unpredictable latency that is characteristic of TCP. Because of low latency, UDP is preferred to TCP for the delivery of PMU updates [3], even at the cost of some dropped packets. In particular, non-confirmable CoAP messages are suitable for PMU updates. CoAP supports the full set of CRUD methods and thus provides the required REST functionality.

With CoAP, the classical CRUD methods in the proposed middleware can be extended with Subscribe and Unsubscribe. Subscribe is a special case of GET request: a client subscribes to a resource thus indicating that it wants to be notified about any update of the resource, as long as the subscription is active. Therefore, Subscribe method extends the GET method by requesting the continuity of data retrievals. This is implemented by enabling the Observe option in the CoAP request header, as specified in [13]. The server sends a CoAP GET response (but without the header overhead) each time an update is available, without having to receive a CoAP GET request first.

On the other hand, some Smart Grid messages (e.g. control commands or alarms) require reliable, real-time delivery. In our solution, reliable message exchange is provided with Websock-

Table 6.2: HTTP long polling vs. CoAP and Websocket

	Header overhead	Network latency	TCP Acknowledgements
HTTP	$\simeq$ 100 bytes	est. 5 ms (RTT)	2 per each update
CoAP	6 bytes	est. 2.5 ms	N/A
WS	6 bytes	est. 2.5 ms	1 per each update
savings	94%	50%	100% (CoAP) 50% (WS)

ets. Websocket is an application layer protocol that enables a bidirectional, full-duplex socket connection over TCP/IP [14]. A Websocket connection is initiated with the special HTTP upgrade request that, if accepted and approved by the server, creates a persistent socket connection that is not released until explicitly requested (by the client or the server). After the HTTP upgrade request and response, the messages that follow do not conform to the HTTP format, but only add minimal headers to the application data. The full HTTP header is redundant because data is exchanged within an ongoing session and not as independent requests/responses. To comply with an event-driven communication scheme, a client application that supports Websockets needs to implement event listeners (onopen, onmessage, onclose). The message flow of long polling, CoAP and Websocket is compared in Figure 6.2.

Upgrading the ETSI M2M subscription mechanism with CoAP and Websockets can bring significant improvements to the real-time performance of the system. CoAP is intended for a stream of measurements generated at a predefined rate, whose timely delivery takes precedence over delivering each and every measurement. In other words, it is better to send new available measurement to the subscribed application than retransmit the old one, and therefore meet the strict latency requirement. Applications that use CoAP to get measurements tolerate certain message loss. Conversely, Websockets are targeted only at protection and control applications that exchange frequent messages exceeding e.g. one update per second, while complying with critical latency requirements and reliable message delivery.

Subscriptions with CoAP or Websocket (WS) complement the standard operations defined in ETSI M2M architecture. The improvements that directly influence the real-time performance are summarised in Table 6.2. The estimates in the table highlight the most important improvements obtained with upgrades presented in this chapter, in comparison to the original long polling solution. Table 6.2 focuses on the impact of the application layer protocol, rather than the influence of underlying network disturbances. In detail, the improvements are the following:

- *Header overhead is reduced.* The values in Table 6.2 assume typical minimal HTTP header per request/response pair (no cookies). CoAP minimal header (4 bytes) is extended with the Observe option (2 bytes) to allow subscriptions [13]. In the Websocket case, only WS frame delimiters account for the header overhead. Since data is exchanged within an ongoing Websocket session, session parameters are exchanged only at the beginning, so that the communication can continue without the full HTTP header overhead attached to each data update.

- *Network latency is halved.* An update is sent as soon as it is available and it takes *one* network trip to deliver it, after which another update can be sent. HTTP request and response pairs take the network *round* trip per each update (Round Trip Time (RTT) in Table 6.2). HTTP application layer thus effectively doubles the latency component originating from the network, as can be seen in Figure 6.2. To estimate the value in Table 6.2, we assumed five hops over 100 km optical fibre each, and no queueing at routers (recall that network imperfections are not considered in the estimate).

- *Acknowledgements are either eliminated, or reduced.* Without Acknowledgements, there is less traffic and thus the network is less prone to congestion problems. HTTP requires that both the request and response are acknowledged, while with Websocket only the message containing updates on the data requested at the beginning of the session is acknowledged. Persistent TCP/IP connections which remain open for multiple messages were assumed in both cases.

Finally, there is a downside to integrating CoAP and Websockets into the architecture. The downside is the added complexity, since three different modes of operation are supported instead of just one: stateless and reliable HTTP, stateless and unreliable but low-latency CoAP and session-oriented, reliable and low-latency Websocket. However, this architecture reflects the diversity of the application requirements, as well as the heterogeneity of the complex communication infrastructure.

With these upgrades, the application requirements presented in Table 6.1 can be adequately met. Oscillation Monitoring and State Estimation subscribe to the PMU updates announced at the corresponding NSCL using CoAP. Control commands resulting from the real-time updates are sent back to the affected power grid components over Websocket sessions. Demand Response message exchange between GSCL at the consumer and the related application registered at NSCL uses the classical HTTP that fully supports all of its requirements.

6.5 Chapter Summary and Conclusions

The devices and applications necessary for the transition from the electric power grid to the Smart Grid already exist. A missing link is the communication system (including the middleware) that provides the connection between the two ends while complying with the set of stringent QoS requirements. We provide arguments for using the distributed ETSI M2M architecture as the basis of this middleware. The integration of the middleware into the Smart Grid network has been devised and the appropriate placement of each component is proposed in the chapter. Notably, the middleware is universally deployed at the transmission, distribution and consumer side and covers a wide set of application requirements.

One particularly challenging communication requirement is the delivery of frequent updates in real-time over wide distances. ETSI M2M RESTful web services can hardly cope with real-time communications without the introduction of system upgrades. We therefore introduce CoAP for time-critical measurements stream and Websockets for time-critical control commands and alarms. These upgrades complement the standard functionality in order to respond to the application requirements that cannot be met otherwise. The thorough analysis of how the resulting heterogeneous solution is able to meet the communication requirements of the diverse Smart Grid applications has been presented in this chapter.

Bibliography

[1] C. Hauser, D. Bakken, and A. Bose, "A failure to communicate: next generation communication requirements, technologies, and architecture for the electric power grid," *IEEE Power and Energy Magazine*, vol. 3, no. 2, pp. 47–55, 2005.

[2] A. Scaglione, Z. Wang, and M. Alizadeh, "New models for networked control in smart grid," in *Smart Grid Communications and Networking*, E. Hossain, Z. Han, and V. Poor, Eds. Cambridge Univ. Press, 2012.

[3] E. Ancillotti, R. Bruno, and M. Conti, "The role of communication systems in smart grids: Architectures, technical solutions and research challenges," *Computer Communications*, vol. 36, no. 17, pp. 1665 – 1697, 2013.

[4] H. Gjermundrod, D. Bakken, C. Hauser, and A. Bose, "GridStat: A Flexible QoS-Managed Data Dissemination Framework for the Power Grid," *IEEE Transactions on Power Delivery*, vol. 24, no. 1, pp. 136–143, 2009.

[5] ETSI M2M TR 102 690, "Machine-to-Machine communications (M2M); Functional architecture," ETSI, Tech. Rep., 2012.

[6] ETSI M2M TR 102 935, "Applicability of M2M architecture to Smart Grid Networks," ETSI, Tech. Rep., 2012.

[7] Known Issues and Best Practices for the Use of Long Polling and Streaming in Bidirectional HTTP. [Online]. Available: http://tools.ietf.org/html/rfc6202

[8] J. Alonso-Zarate, J. Matamoros, D. Gregoratti, and M. Dohler, "Machine-to-machine communications in Smart Grid," in *Smart Grid Communications and Networking*, E. Hossain, Z. Han, and V. Poor, Eds. Cambridge University Press, 2012.

[9] R. T. Fielding, *Architectural Styles and the Design of Network-based Software Architectures*. University of California, Irvine, USA, 2000.

[10] M. Corici, H. Coskun, A. Elmangoush, A. Kurniawan, T. Mao, T. Magedanz, and S. Wahle, "OpenMTC: Prototyping Machine Type communication in carrier grade operator networks," in *IEEE Globecom Workshops*, 2012, pp. 1735–1740.

[11] G. Lu, D. Seed, M. Starsinic, C. Wang, and P. Russell, "Enabling Smart Grid with ETSI M2M standards," in *IEEE Wireless Communications and Networking Conference Workshops*, 2012, pp. 148–153.

[12] U. Feuchtinger, R. Frank, J. Riedl, and K. Eger, "Smart Communications for Smart Grids," Siemens, Tech. Rep., 2012.

[13] Observing Resources in CoAP. [Online]. Available: http://tools.ietf.org/html/draft-ietf-core-observe-13

[14] The WebSocket Protocol. [Online]. Available: http://tools.ietf.org/html/rfc6455

Chapter 7

Conclusions and Future Work

This thesis has focused on energy-efficient wireless communication schemes and real-time middleware for M2M networks. M2M device domain has been considered in Chapters 3, 4 and 5, while M2M applications have been the main topic of Chapter 6. All studied cases are related to Smart Grid applications. Regarding wireless communication schemes, Chapter 3 has examined the energy efficiency of a C-ARQ scheme for non-duty-cycled networks, in contrast to the previous works on C-ARQ that were focused on maximising the throughput. We then turned to duty-cycled schemes in Chapters 4 and 5. Specifically, Chapter 4 has presented a preliminary study of whether C-ARQ can improve the energy efficiency of a duty-cycled scheme by combating shadowing and multipath fading effects in the wireless channel. Building on the positive outcome of this chapter, we have further developed Cooperative and Duty-Cycled (CDC-ARQ) scheme in Chapter 5 and have executed comprehensive performance evaluation. These solutions enable Home and Building Automation whose aim is to optimise the consumption of electrical energy. This one and other Smart Grid-related M2M applications have been studied in Chapter 6. The focus of this chapter has been on the middleware that facilitates real-time distributed computing to allow timely exchange of data. In the continuation, the main findings of this thesis are summarised.

7.1 Conclusions

A C-ARQ scheme that was examined in **Chapter 3** is known as PRCSMA and it defines an exponential backoff algorithm for the spontaneous relays trying to access the wireless channel. The relays employ adaptive data rate to retransmit the packet that the destination failed to receive in the initial transmission attempt from the source. An energy model for PRCSMA was derived and its performance was evaluated. The results show that PRCSMA outperforms non-cooperative ARQ for medium to high packet error rates in the original link. Also, the range of packet error probabilities that correspond to the highest energy efficiency of PRCSMA is found from the model. Another set of results shows that collisions are costly in the cooperation phase and should be avoided by adjusting the contention windows size. In summary, this chapter presented a C-ARQ scheme compatible with widely spread IEEE802.11 MAC protocol that is easy to implement in order to improve the energy efficiency of the communication protocol.

When devices are duty-cycled, there are no spontaneous relays. **Chapter 4** studied whether C-ARQ principles can still be beneficial in duty-cycled networks. In this case, a relay has to be woken up in order to participate in the cooperation. We found that when the current channel realization in the original link is unfavourable and likely to be in outage, gains of C-ARQ outweigh the cost. Energy efficiency improves even if extra energy was consumed at the relay because C-ARQ combats shadowing and multipath fading in the original link. Note that a relay is woken up only when needed, therefore the cost of C-ARQ is assumed only if the original link is severely shadowed. The results presented in this chapter show that C-ARQ is especially suitable for networks with hard reliability constraints because not only does it improve the energy efficiency, but it also reduces the packet loss. We adopted beacon-enabled, IEEE 802.15.4 network as a study case. Cooperation process is regulated by the coordinator that may have an up-to-date channel state information to each of the associated devices. If this is the case, the coordinator can select the relay with optimal channel conditions, resulting in improved performance, as was shown in the chapter.

Chapter 5 generalises the previous results to a multi-hop, duty-cycled network whose MAC is specified in IEEE 802.15.4e standard amendments. There is no coordinator and the transmission slots are scheduled for each sender-receiver pair. In this chapter, CDC-ARQ scheme was designed to regulate the dynamic forwarding in a multi-hop, duty-cycled network depending on channel conditions. Link metrics to reflect the channel conditions and the energy model for devices were derived. Based on the energy model, the optimal operating regions were determined for direct, multi-hop or CDC-ARQ forwarding, as well as the implications of using each. The results provide useful guidelines on the configuration of an energy-efficient network, for systems with either loose or strict reliability requirements. The energy model was validated in the ns-3 network simulator in the realistic simulation environment that mimics the functioning of an actual device.

Finally, **Chapter 6** looks at M2M applications in the Smart Grid. Precisely, it studies the middleware that provides a connection between the two ends: M2M devices studied in the previous chapters and M2M applications at the other end. We provide arguments for using the distributed ETSI M2M architecture as the basis of this middleware. The integration of the middleware into the Smart Grid network was devised and the appropriate placement of each component is proposed. Notably, the middleware is universally deployed at the transmission, distribution and consumer side and covers a wide set of application requirements. One particularly challenging communication requirement is the delivery of frequent updates in real-time over wide distances. ETSI M2M RESTful web services can hardly cope with real-time communications without the introduction of system upgrades. We therefore introduce CoAP for time-critical measurements stream and Websockets for time-critical control commands and alarms. These upgrades complement the standard functionality in order to respond to the application requirements that cannot be met otherwise. The thorough analysis of how the resulting heterogeneous solution is able to meet the communication requirements of the diverse Smart Grid applications was presented in this chapter.

7.2 Future Work

In this section, a number of open research lines inspired by the topics addressed in this thesis is discussed.

- **C-ARQ for power save mode of IEEE 802.11.** A C-ARQ scheme compatible with IEEE 802.11, PRCSMA, whose energy efficiency was studied in this thesis is based on devices in active mode that never switch off their radio transceivers. IEEE 802.11 standard was extended to support power save mode that specifies sleeping cycles for devices. It would be interesting to combine principles of PRCSMA with strategies of waking up the relays in channel outage events and thus design a C-ARQ scheme for power save mode.

- **Introduce energy harvesting in CDC-ARQ.** The devices that harvest energy from the environment (e.g. solar energy, vibrations, electromagnetic energy) and thus function without battery replacement (theoretically forever) is a very active research area. Still, because the devices are low-cost, the amounts of harvested energy are small and require energy-efficient communication protocols regardless of the continuous battery recharge. The principles of CDC-ARQ still apply, but the energy harvesting opens new possibilities for various enhancements. For example, a device that is currently getting energy from the environment might advertise itself as a relay and therefore share this extra energy with other devices. This would improve the packet delivery rate of all the neighbouring devices, using the energy that is available sporadically.

- **Refine the battery and channel models.** The storage capability and battery quality degrades in time. More realistic battery models could provide better insights on the performance of C-ARQ schemes presented in this thesis. For example, the device and network lifetime could be measured with precision. Also, another criteria may be introduced when choosing a relay (aside from the current channel quality) that checks the energy currently available at the device. Energy and battery models in ns-3 provide a solid basis for this task. Along this line, more accurate results can also be achieved by implementing the channel hopping applied in IEEE 802.15.4e in ns-3.

- **Check how the upgrades to ETSI M2M middleware perform in a real network.** In this thesis, qualitative analysis of the real-time behaviour of web services was presented. For the practical adoption of the middleware and its upgrades, measurements in real networks are necessary. Packet queueing at routers and other network disturbances could affect the real-time performance of the middleware significantly and these conditions should be examined in order to find a solution that meets the strict latency requirements.